ALMA (© NAOJ)

MAKE NEW STANDARDS.
東海国立大学機構

GIFU UNIVERSITY

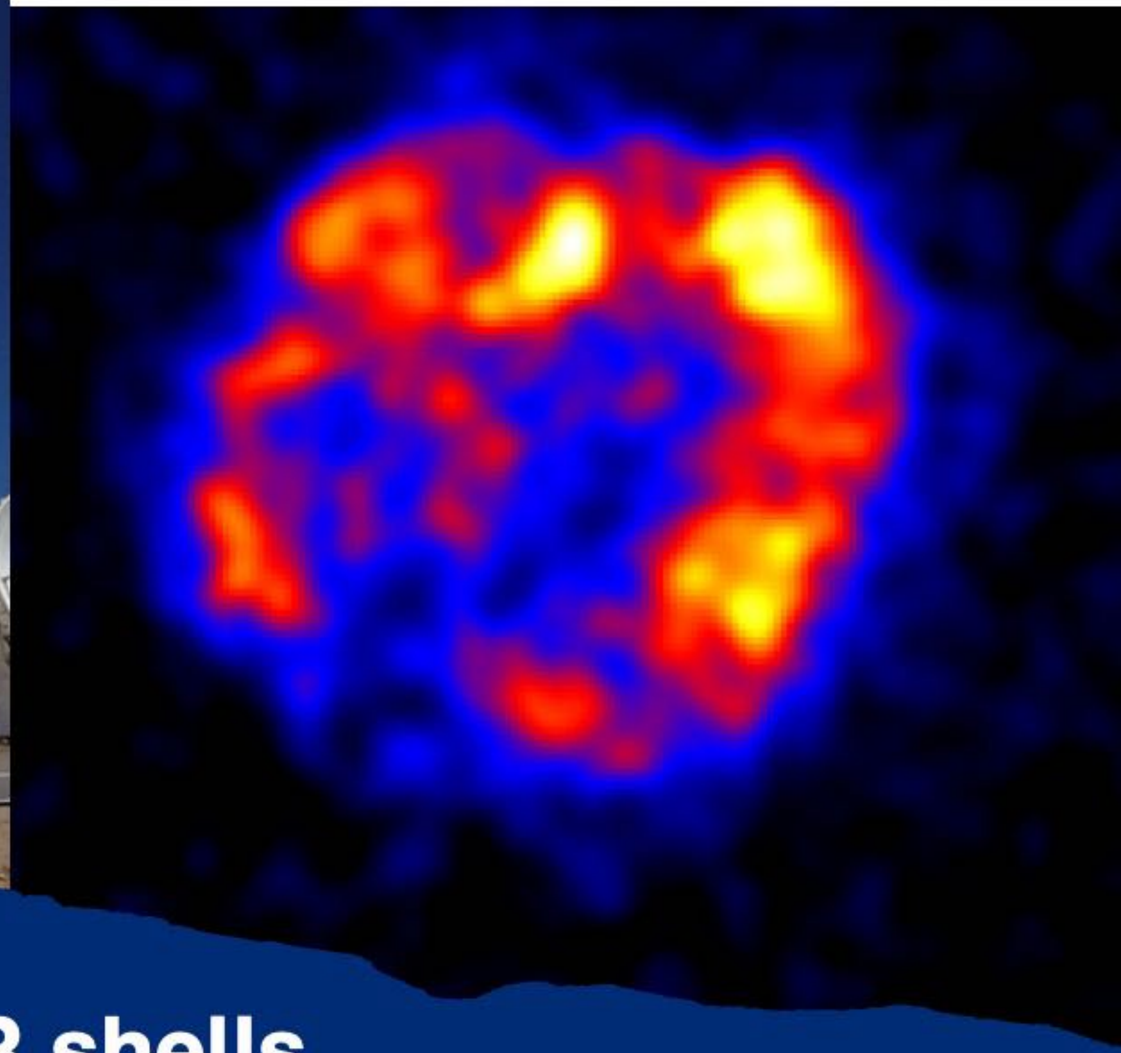

ALMA CO Observations of shocked filaments in young SNR shells

Hidetoshi SANO (Gifu University)

CDY Seminar: Cosmic Rays and Gamma Rays
2023, April 19, 22:00–23:00 (JST) via Zoom

Why supernova remnants?

- Shockwaves, injection of heavy elements, and cosmic-ray production
  → SNRs hold a key to understanding the ISM and galaxy evolution (+ star formation)
- Bright in multi-wavelength from radio to gamma-rays
  → Multi-wavelength studies can reveal physical processes from various aspects

Radio (21 cm, 3 mm)	Infrared (22 μm)	Optical (656.28 nm)	X-rays (1 nm)	Gamma-rays (1 am)
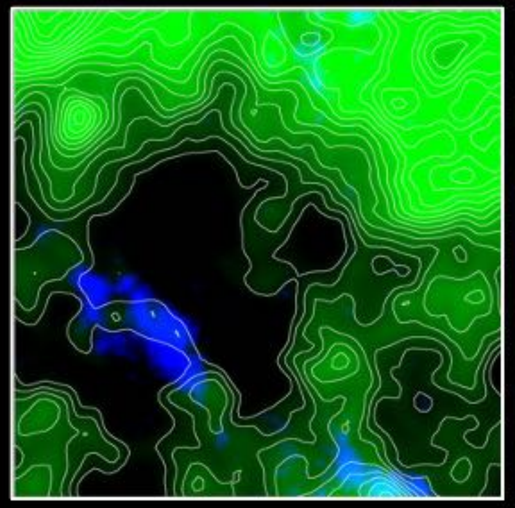	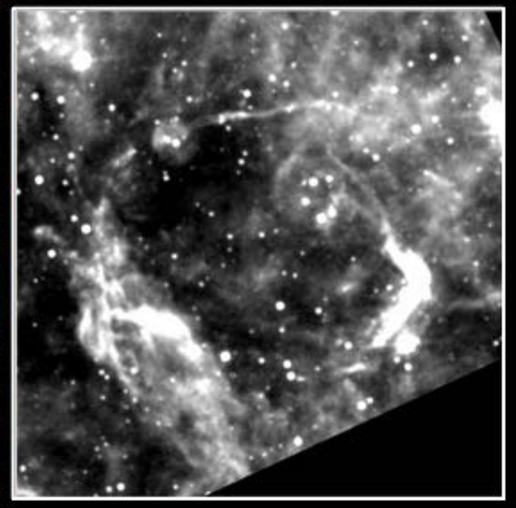	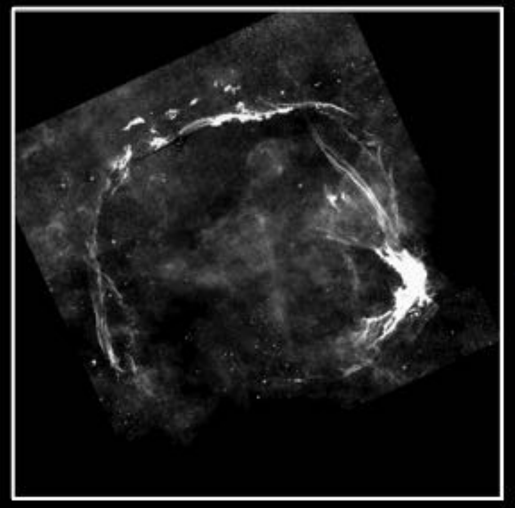		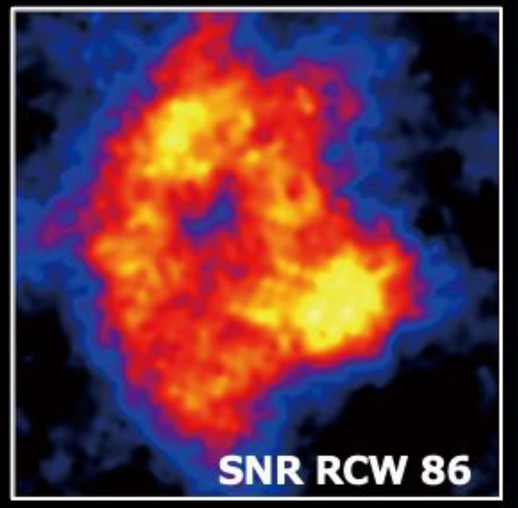
Atomic hydrogen Molecular hydrogen	Stars (embedded within dust) Interstellar dust	Stars Plasma (~10^4 K)	Plasma (~10^7 K) Heavy elements Cosmic-ray electrons	Radioisotope Cosmic-ray electrons & protons
		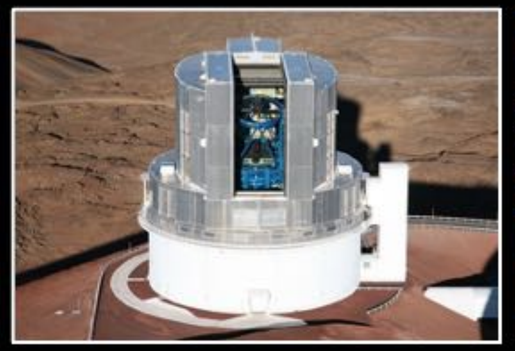		
Radio Astronomy	Infrared Astronomy	Optical Astronomy	X-ray Astronomy	Gamma-ray Astronomy

collaborate collaborate collaborate

We newly established a strong collaboration

Why supernova remnants?

- Shockwaves, injection of heavy elements, and cosmic-ray production
  → SNRs hold a key to understanding the ISM and galaxy evolution (+ star formation)
- Bright in multi-wavelength from radio to gamma-rays
  → Multi-wavelength studies can reveal physical processes from various aspects

Physical processes in a supernova remnant

Inhomogeneous & clumpy distributions of the clouds are important!!

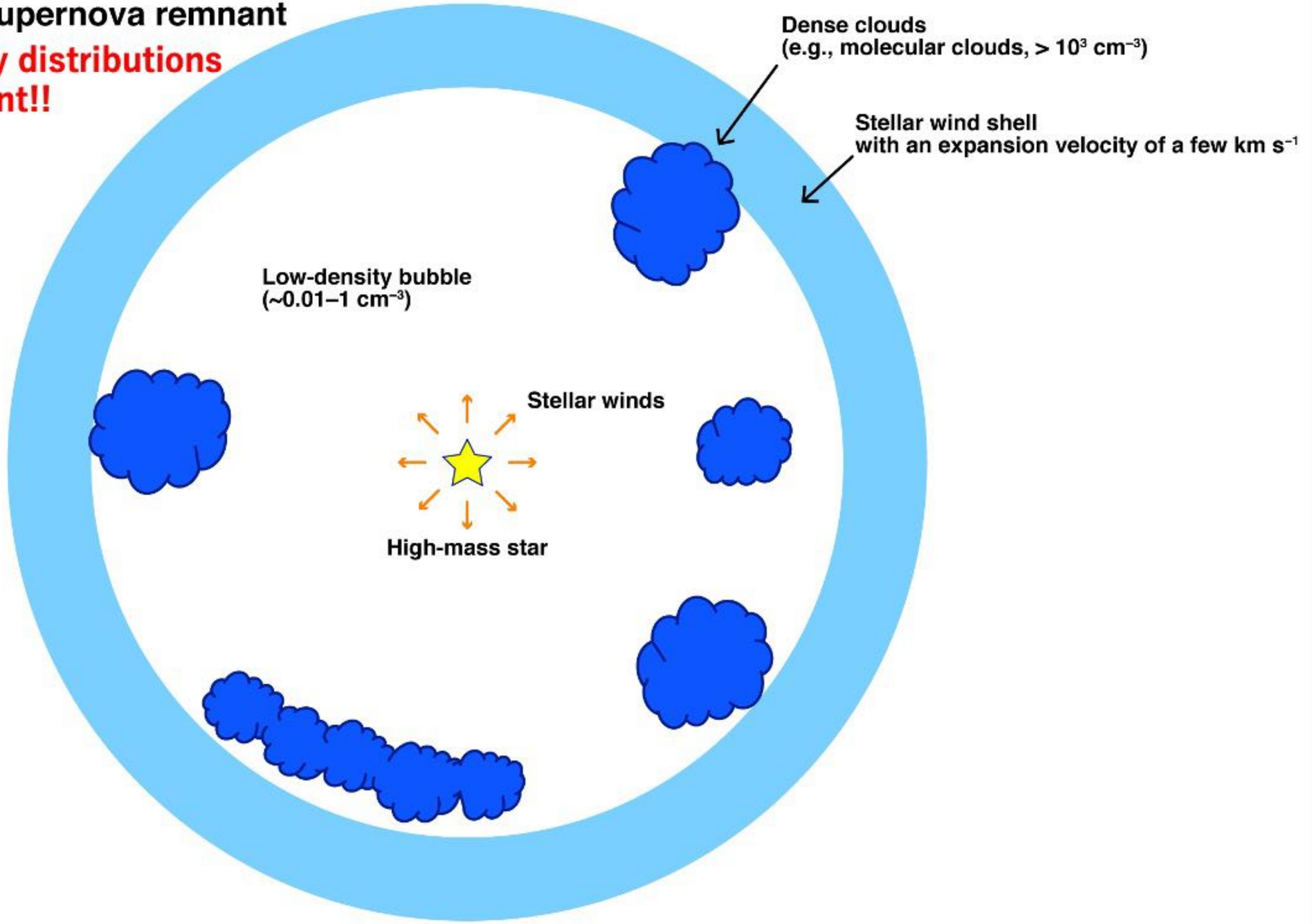

Physical processes in a supernova remnant

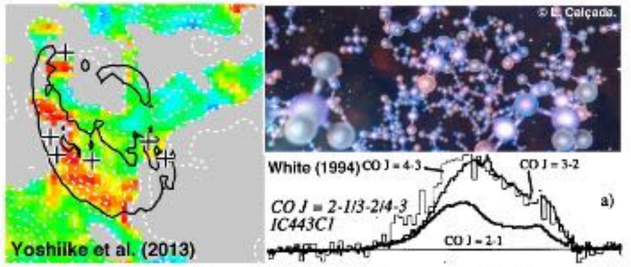

Partially heating of gas/dust with line broadening
+ chemical evolution of the ISM
+ CI chemistry in the vicinity of SNRs
+ Recombining plasma production

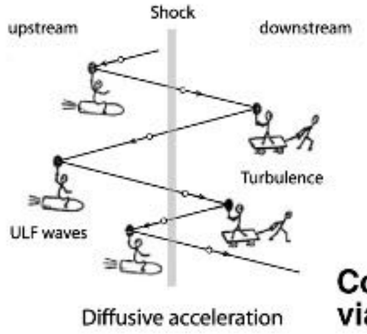

Cosmic-ray acceleration via DSA

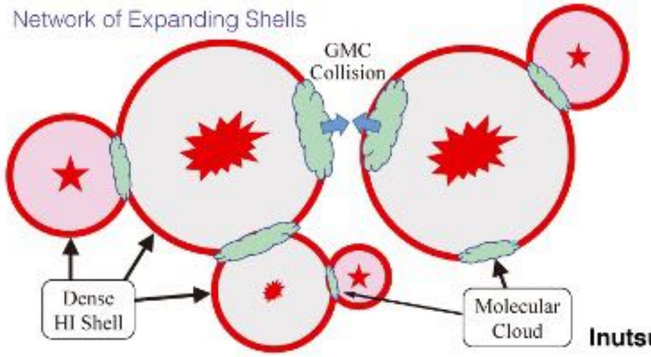

Inutsuka et al. (2015)

Molecular filament formation by multiple shock compressions

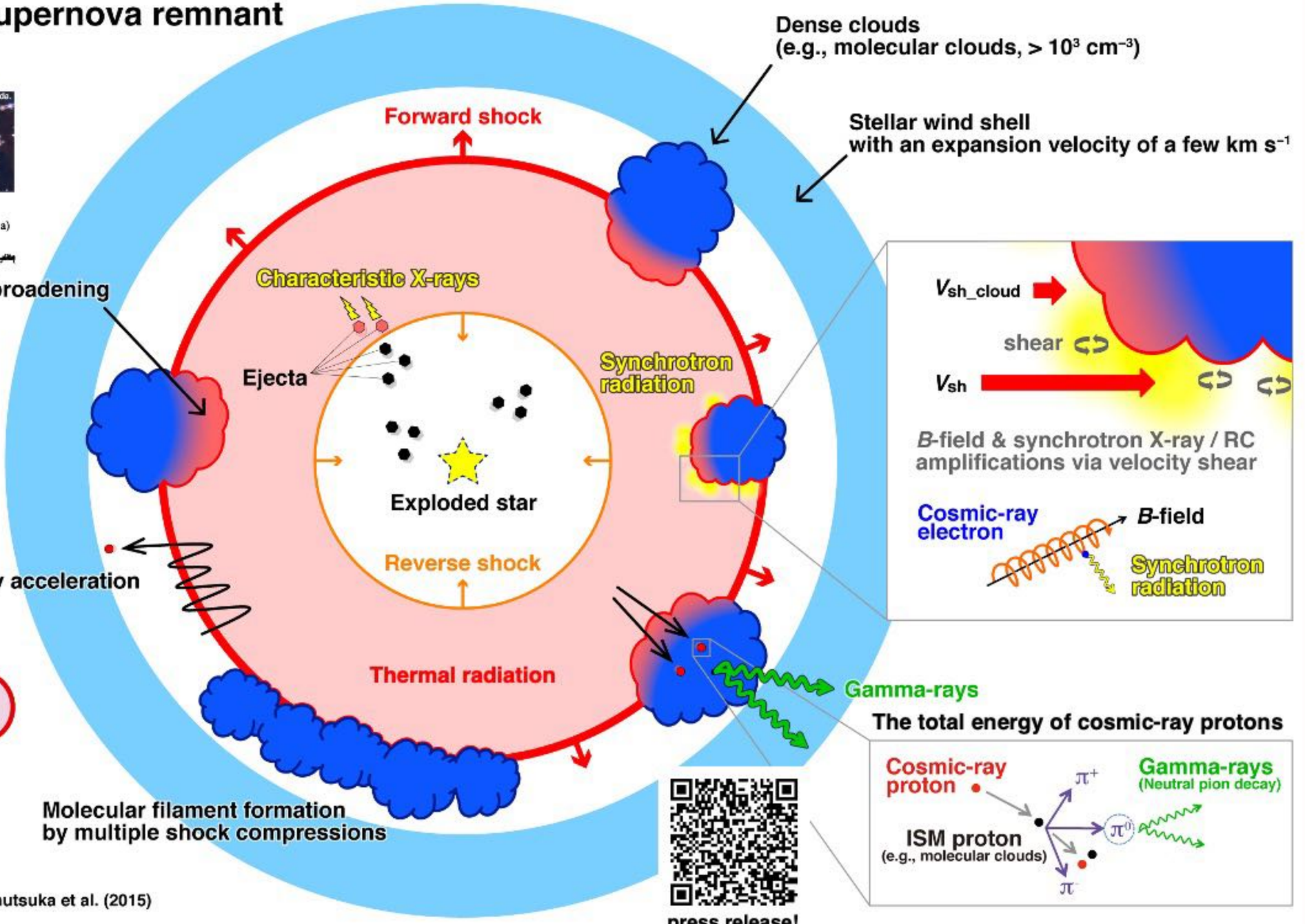

press release!

Physical processes in a supernova remnant

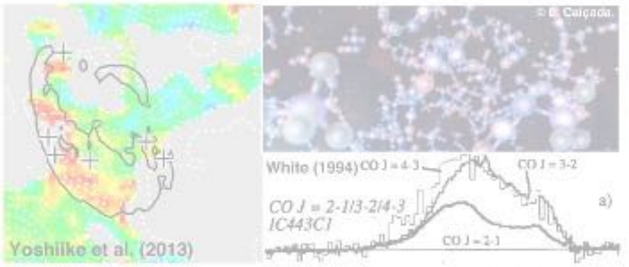

Partially heating of gas/dust with line broadening
+ chemical evolution of the ISM
+ C
+

Interstellar gas associated with supernova remnants are essential in understanding the low- and high-energy physical processes in the interstellar medium

Diffusive acceleration via DSA

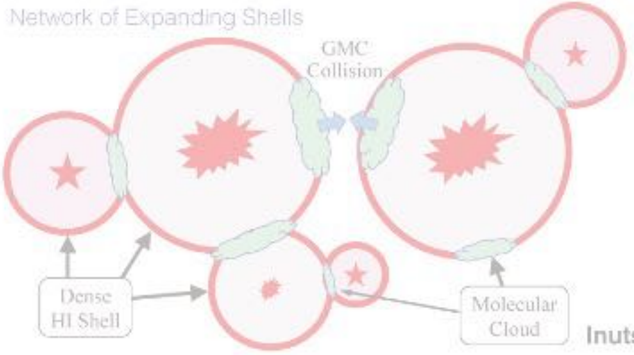

Inutsuka et al. (2015)

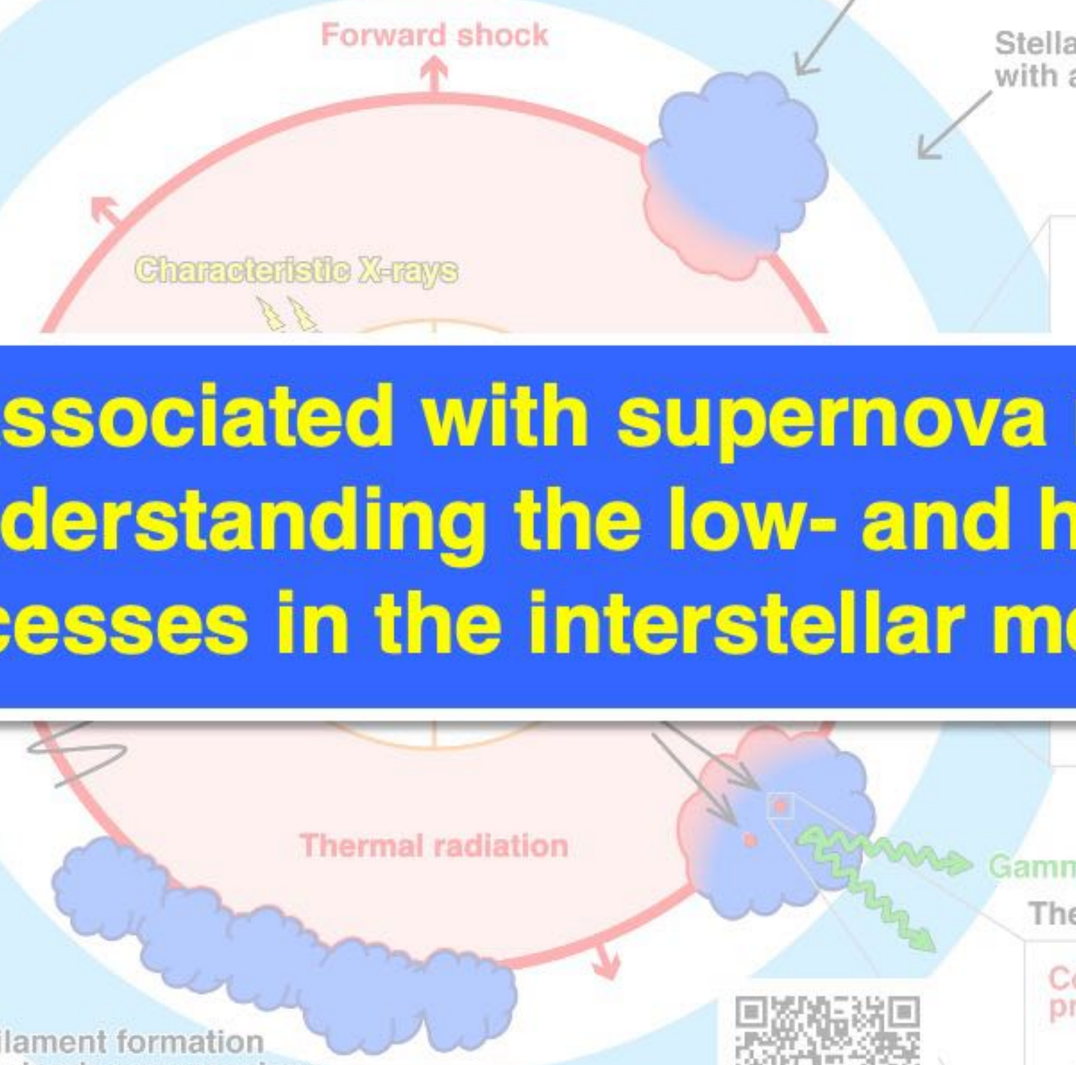

Molecular filament formation
by multiple shock compressions

press release!

The total energy of cosmic-ray protons

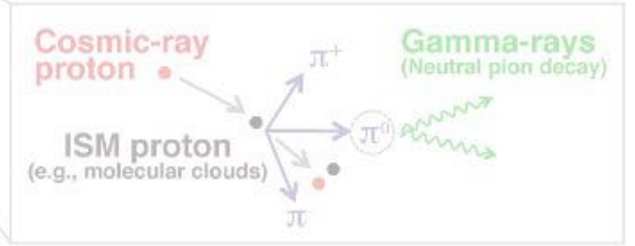

① Pursuit of the origin of Galactic cosmic-rays + ALMA results

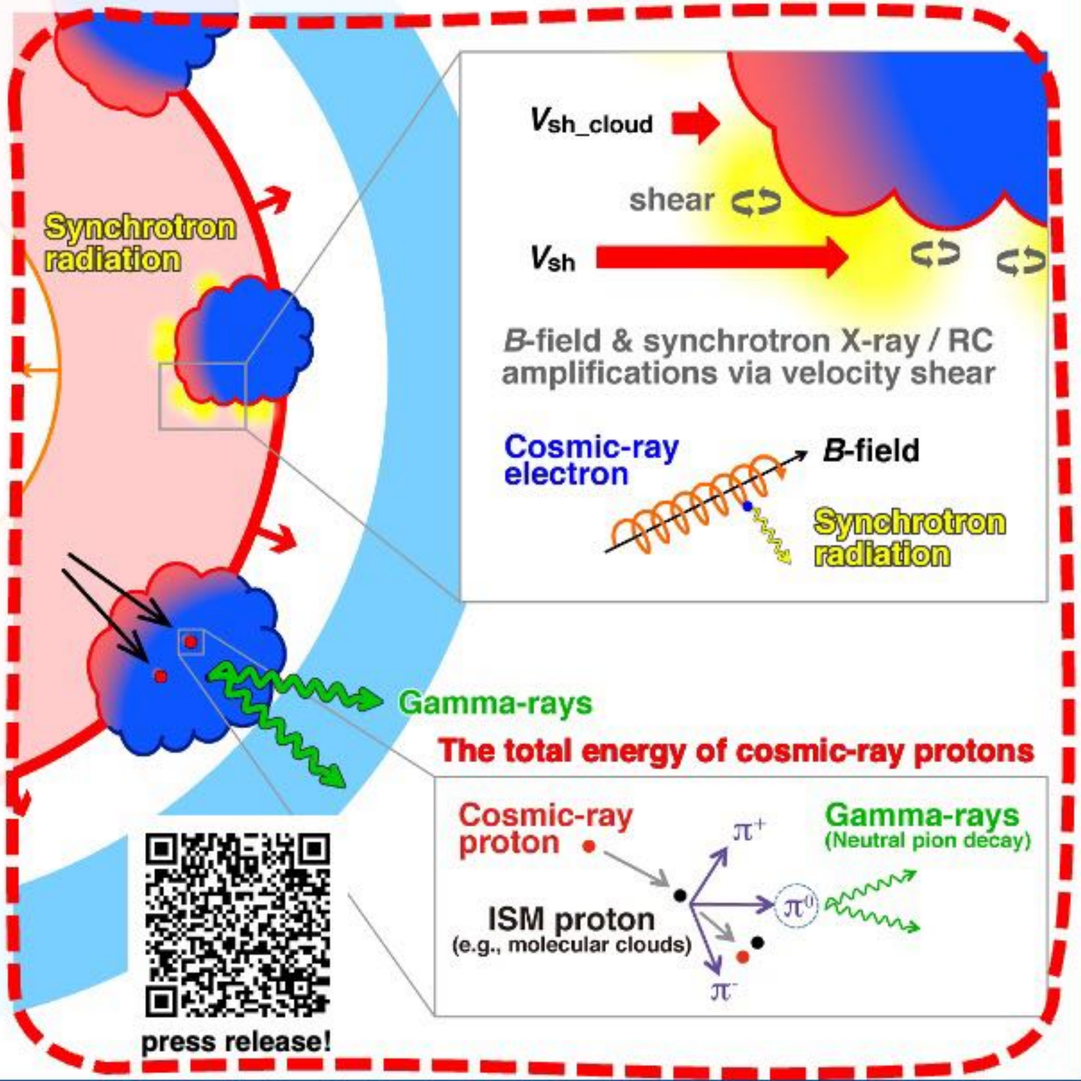

② The latest ALMA results of shocked filaments in SNRs

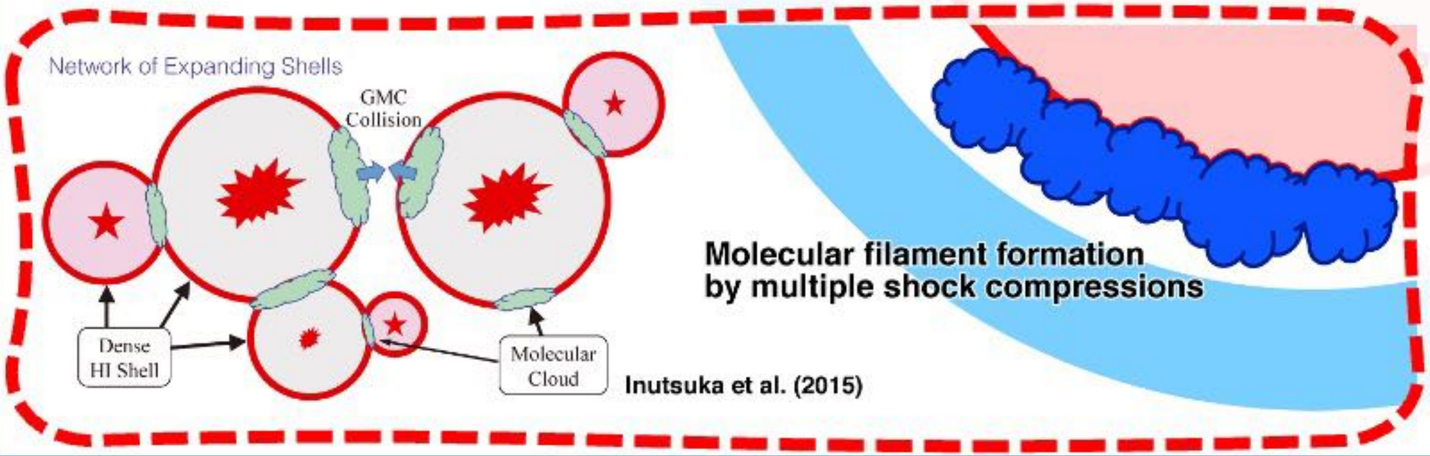

Origin of Galactic cosmic-rays (CRs)

The origin & acceleration mechanism of Galactic cosmic-ray protons had been debated since their discovery in 1912 (100-year problem)...

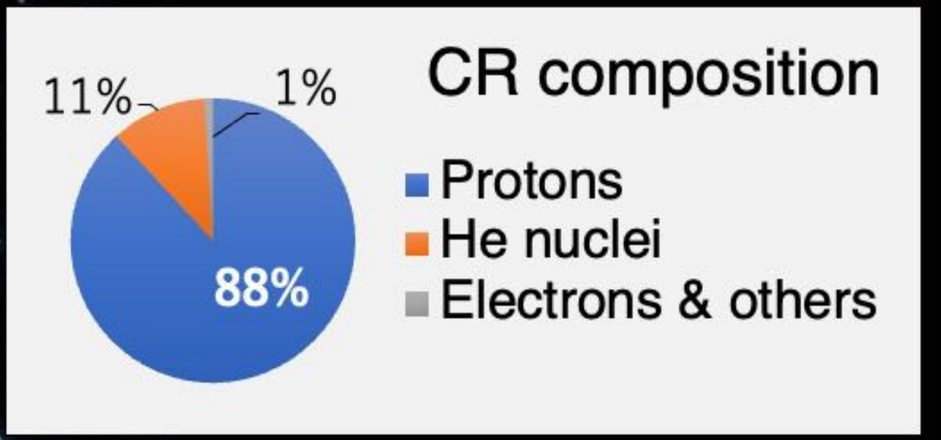

Components in the local universe	Energy density [eV cm^{-3}]
CMB	0.27
Star light	0.54
Magnetic field	0.89
Turbulence	0.22
Cosmic-rays	1.39

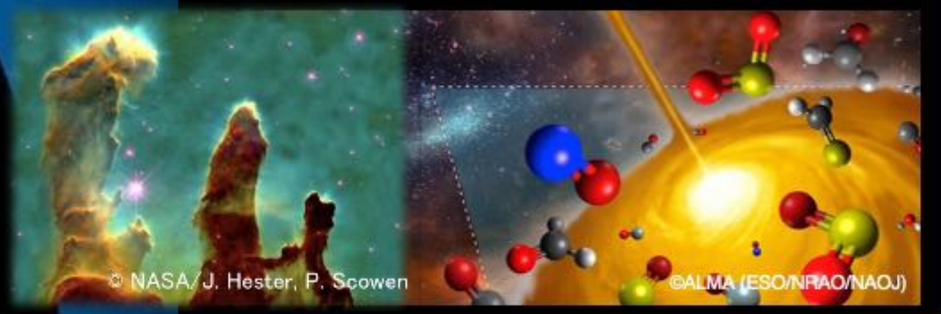

Observed CR spectra and their origin

$$dN(E) \propto E^{-p} dE$$

N: number of particles with kinetic energy *E*
p: spectral index

***dN(E)/dE* ∝ *E*$^{-2.7}$**
(less than *Knee*)

➡ Shock acceleration in the Galactic SNRs

***dN(E)/dE* ∝ *E*$^{-3.0}$**
(grater than *Ankle*)

➡ Extragalactic objects (AGN, starburst gal., GRB?)

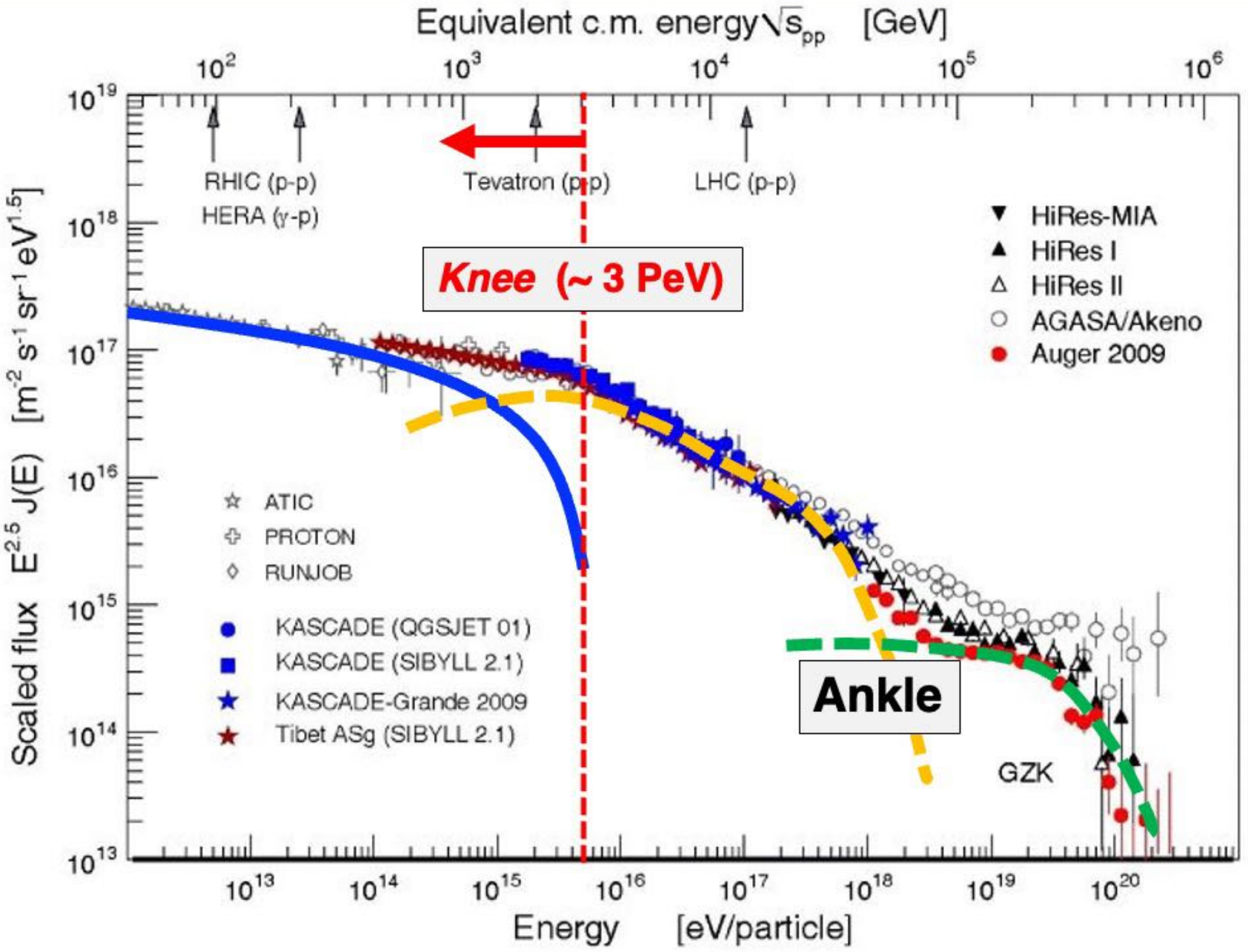

Diffusive shock acceleration (DSA) in supernova shocks

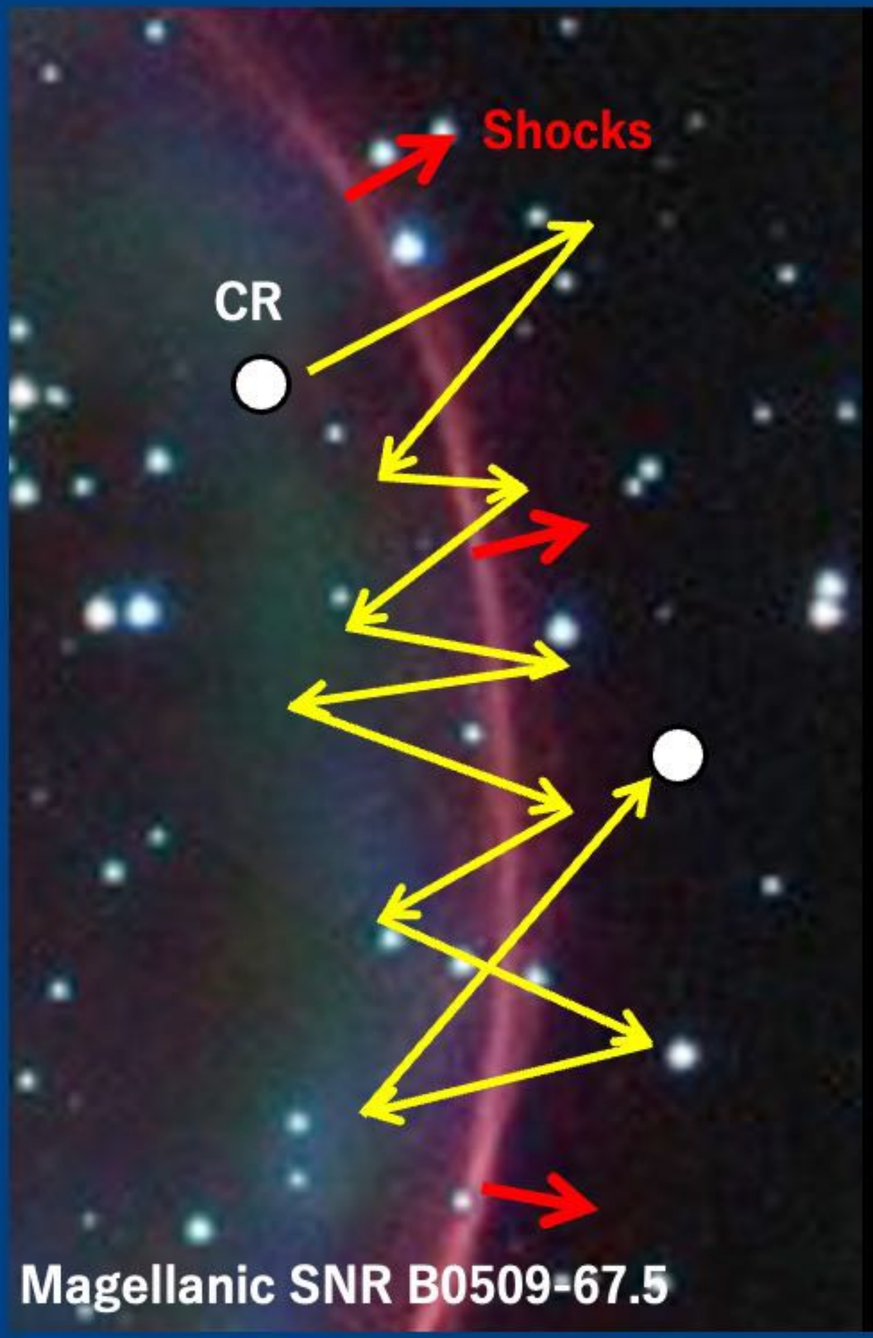

$$\rho_1 v_1 = \rho_2 v_2 \quad \text{(Mass conservation)}$$

$$P_1 + \rho_1 v_1^2 = P_2 + \rho_2 v_2^2 \quad \text{(Momentum conservation)}$$

$$\rho_1 v_1 \left(\frac{v_1^2}{2} + \frac{P_1}{\rho_1} + u_1 \right) = \rho_2 v_2 \left(\frac{v_2^2}{2} + \frac{P_2}{\rho_2} + u_2 \right), \quad \text{(Energy conservation)}$$

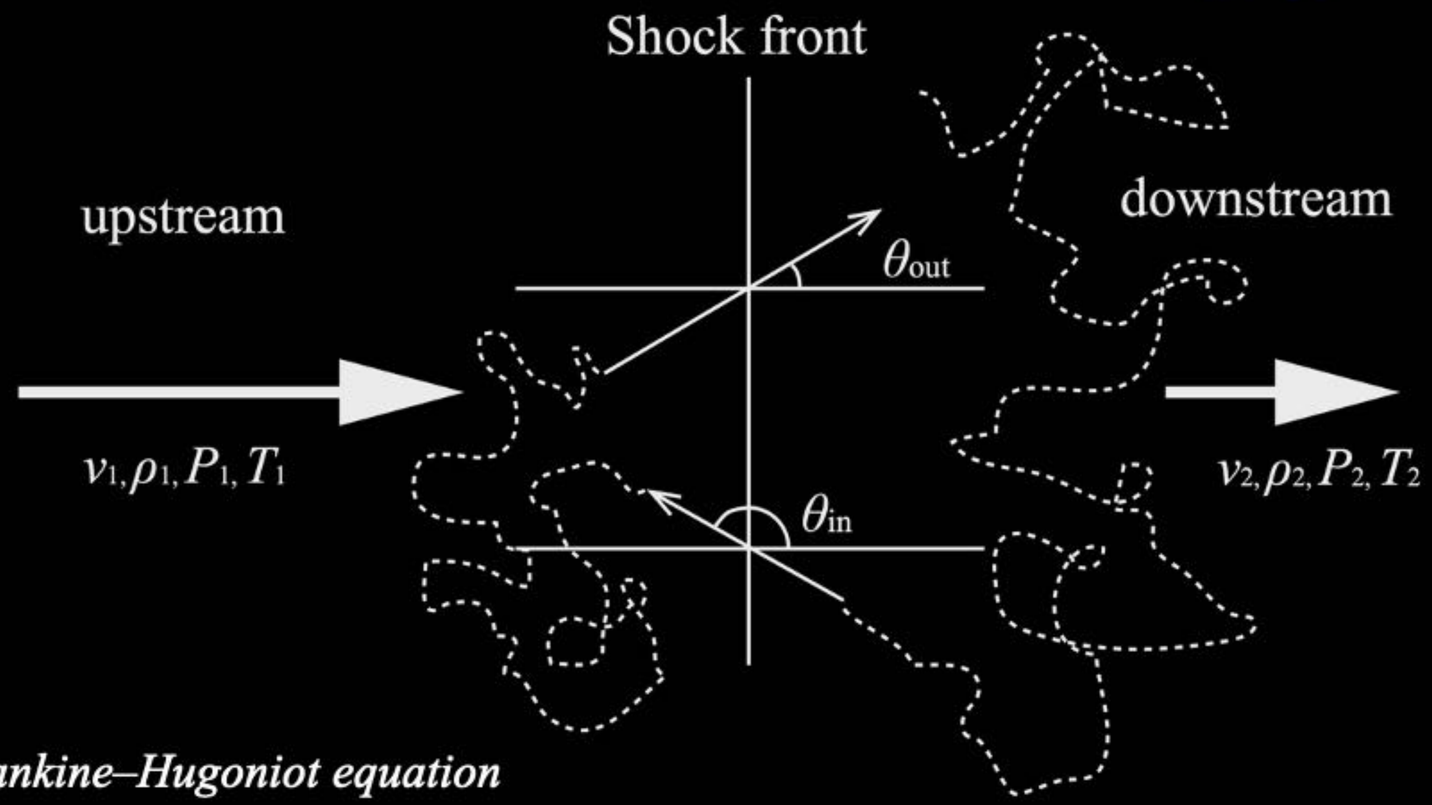

Rankine–Hugoniot equation

Diffusive shock acceleration (DSA) in supernova shocks

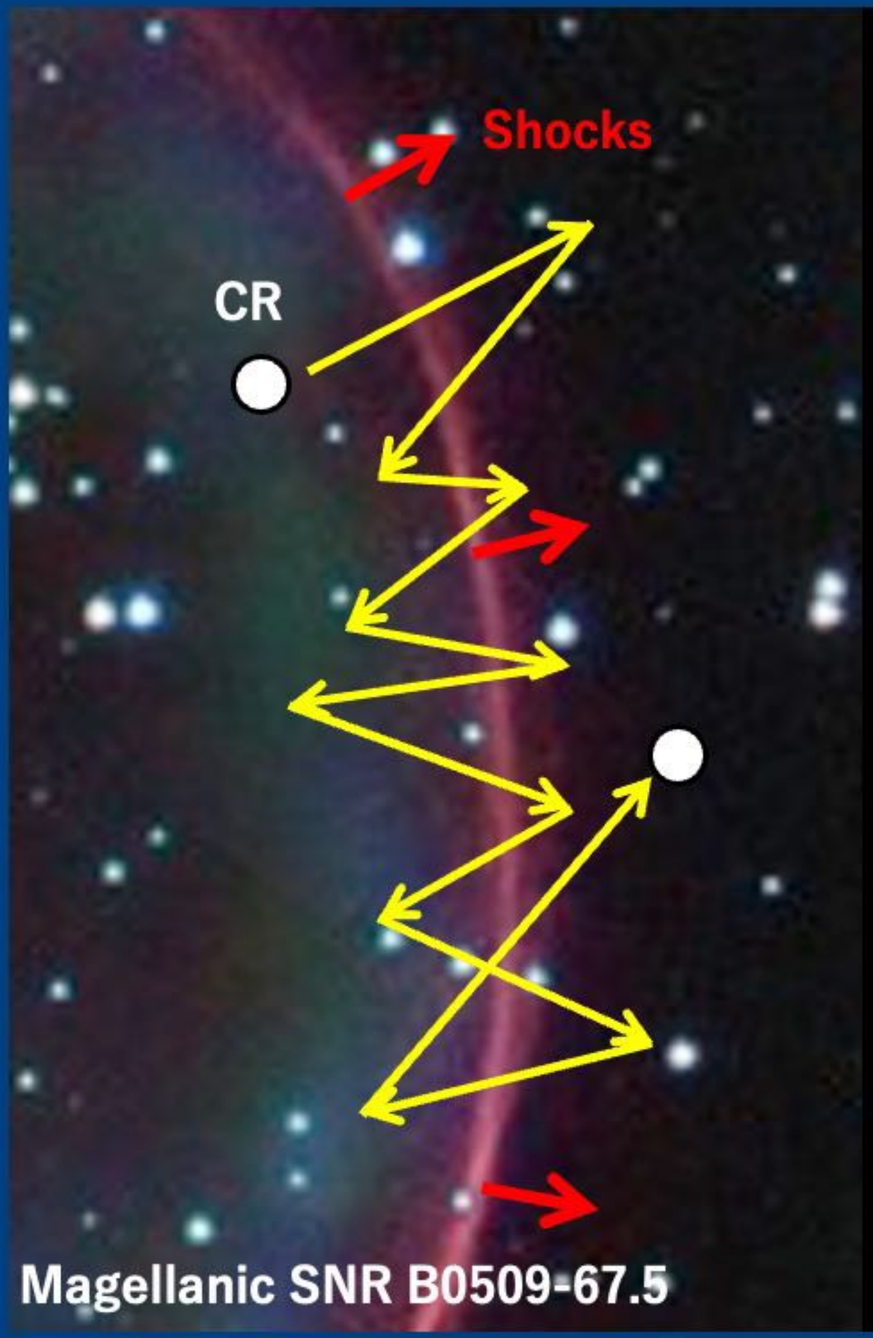

Averaged energy gain E_n

$$E_n = E_0\left(1+\frac{4(v_1-v_2)}{3c}\right)^n$$

Escape probability P_{escape}

$$P_{\rm escape} = \frac{4v_2}{c}\times\left(1-\frac{4v_2}{c}\right)^n$$

Energy spectrum of accelerated particles dN/dE

$$\frac{dN}{dE} \propto E^{-\frac{3v_2}{v_1-v_2}-1} = E^{-\alpha}$$

Maximum energy of accelerated particles E_{max}

$$E_{\rm max} \sim 100\times\eta^{-1}\,Z_{\rm e}\left(\frac{v_{\rm s}}{5000\ {\rm km\ s^{-1}}}\right)\left(\frac{B}{10\ \mu{\rm G}}\right)\left(\frac{R}{10\ {\rm pc}}\right)\ {\rm TeV}.$$

η : gyro-factor $(B / \delta B)^2$

Z_e: charge of accelerated particle

Realistic energy balance is required

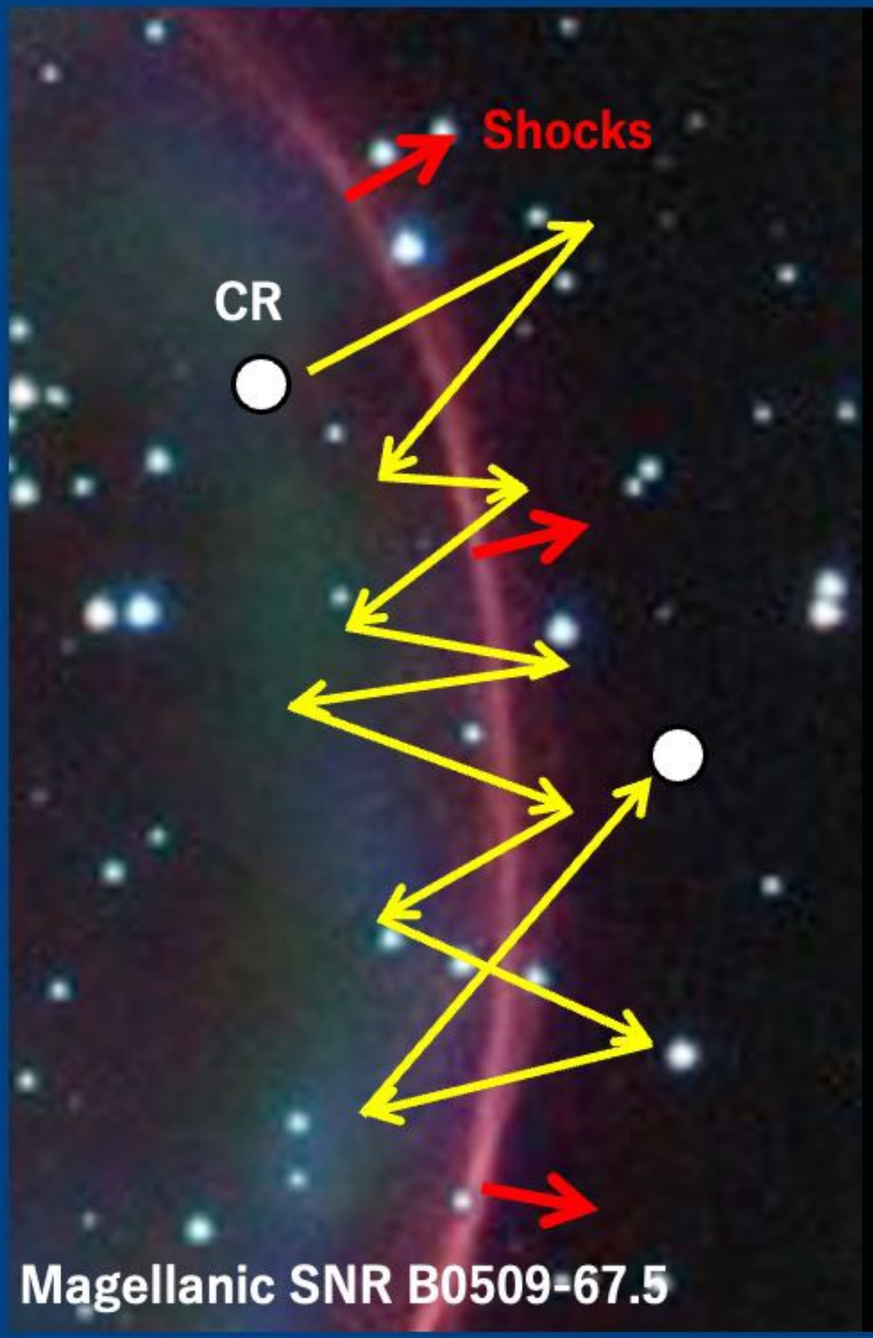

Injection rate of cosmic-rays L_{CR}

$$L_{CR} = \frac{V\,\varepsilon_{CR}}{\tau_{esc}} \sim 10^{41}\ \mathrm{erg\ s^{-1}},$$

V : Volume of the Galaxy ($= \pi R^2 h \sim 4 \times 10^{66}$ cm^3, $R \sim$15 kpc, $h \sim$200 pc)
ε_{CR}: Energy density of CRs ($= 1.39$ eV cm$^{-3} = 2.2 \times 10^{-12}$ erg cm^{-3})
τ_{esc}: Escape time scale ($\sim 3 \times 10^6$ yr, e.g., Gabich 2013)

Total power of supernova explosion P_{SNR}

$$P_{SNR} = \frac{E}{f_S}$$

E_{SN} : Typical rele
f_{SN}: Frequency of SNe (3 SN

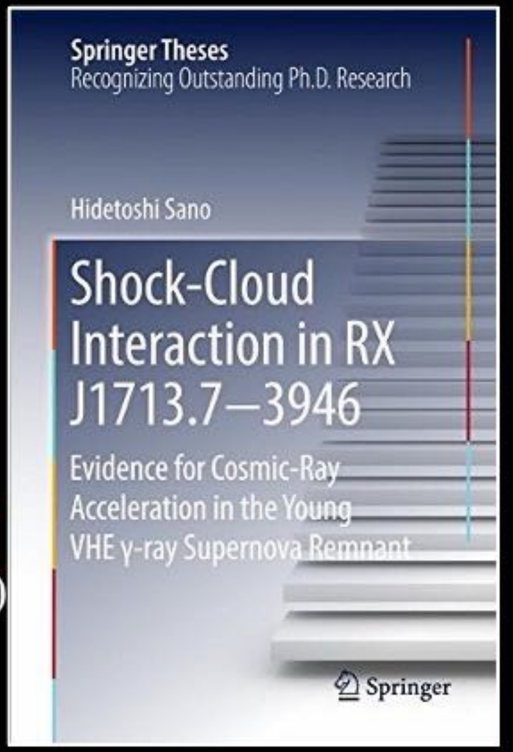

Direct CR observations cannot reveal the acceleration site...

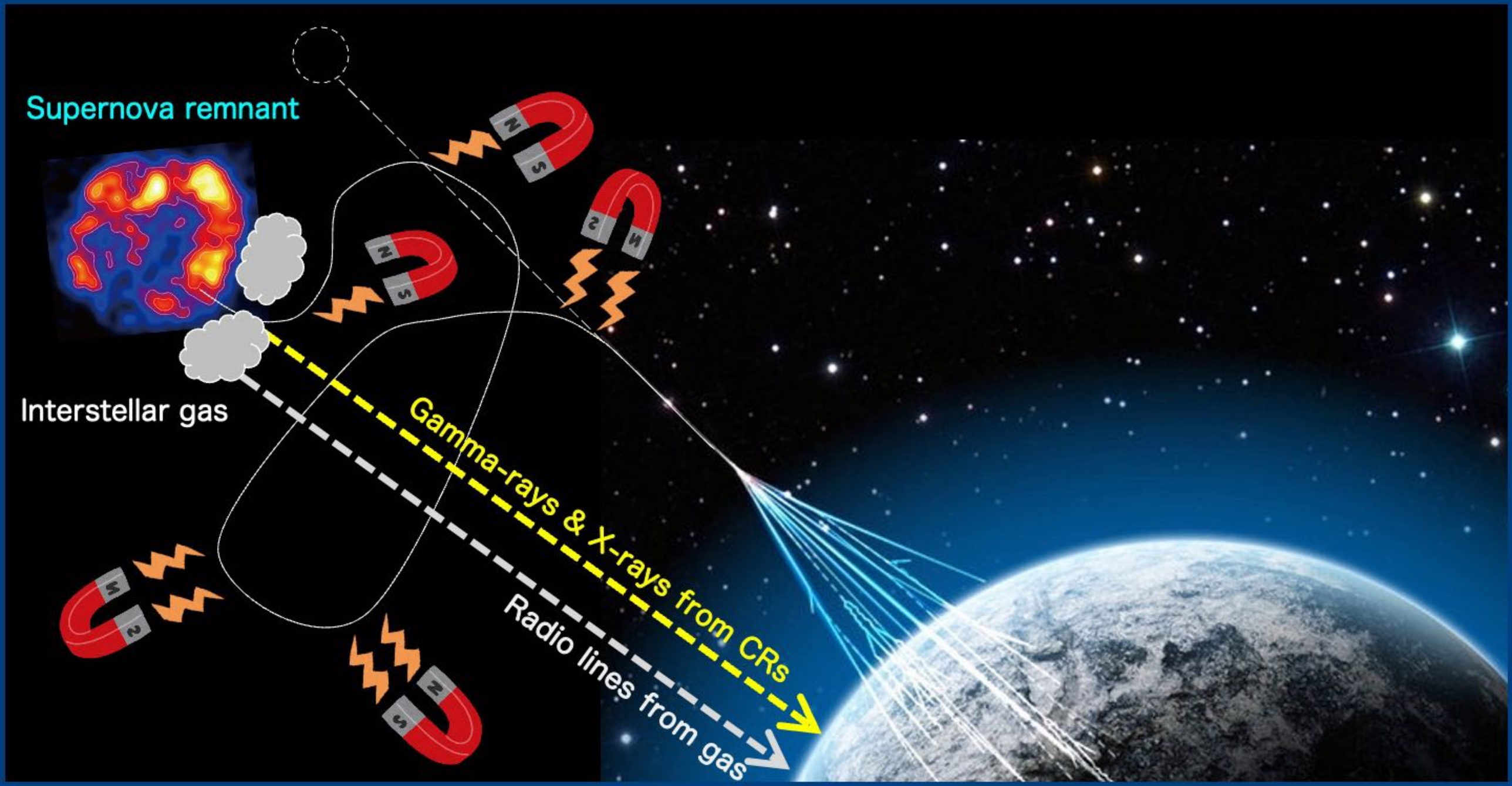

Gamma-ray supernova remnants as CR accelerators

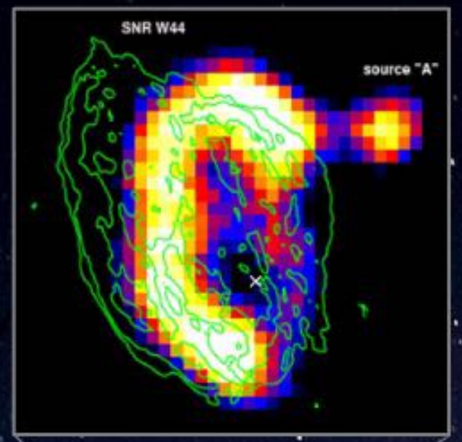

GeV gamma-ray
from SNR W44

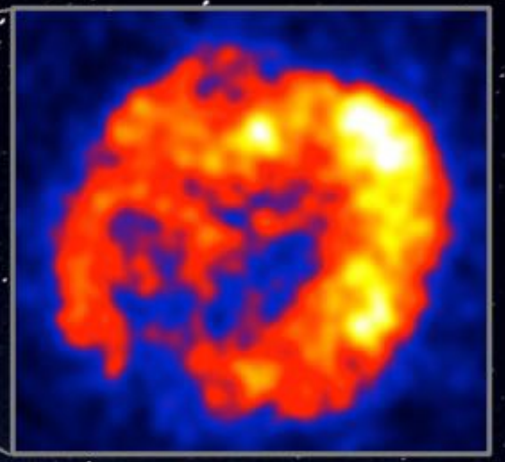

TeV Gamma-rays from
SNR RX J1713.7-3946

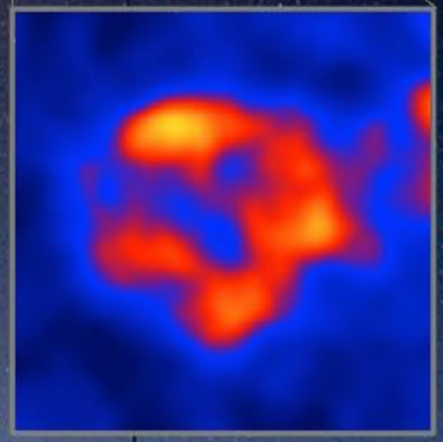

TeV Gamma-rays from
SNR HESS J1731–347

RX J1713.7-3946 (H.E.S.S. Collaboration et al. 2018a)
HESS J1731–347 (H.E.S.S. Collaboration et al. 2011)
W44 (Giuliani et al. 2011)

Hadronic vs Leptonic Gamma-rays

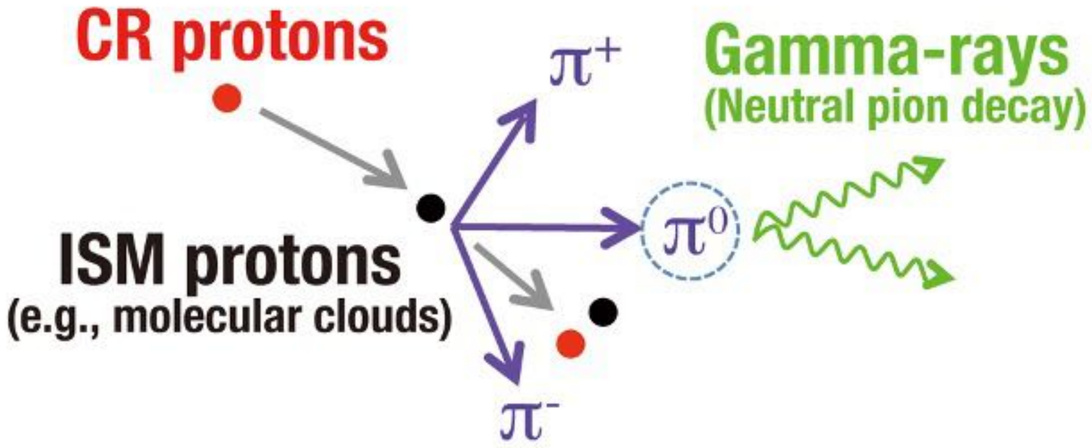

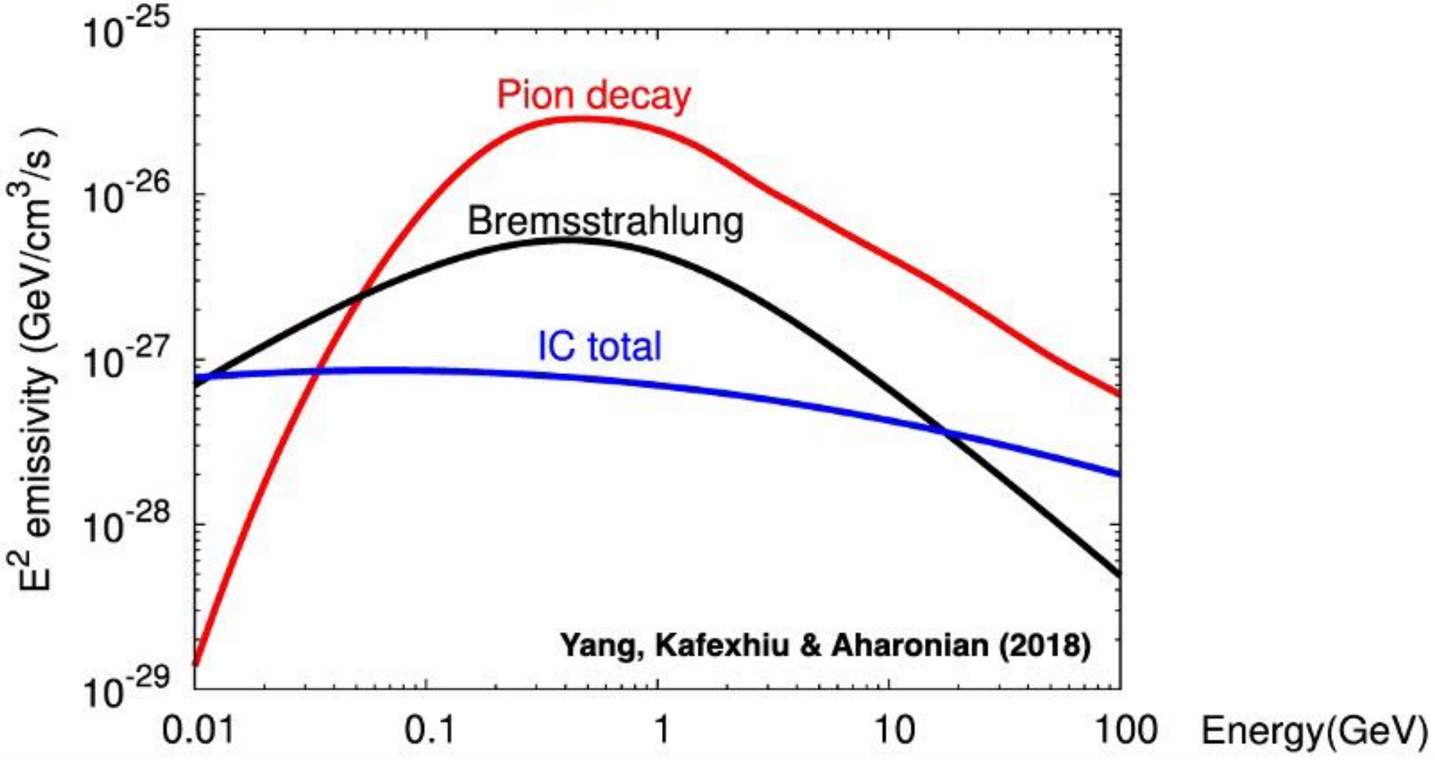

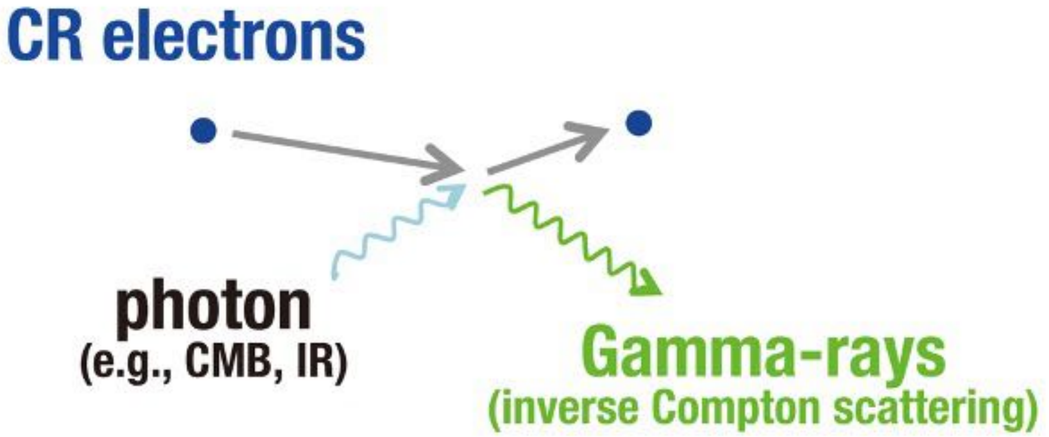

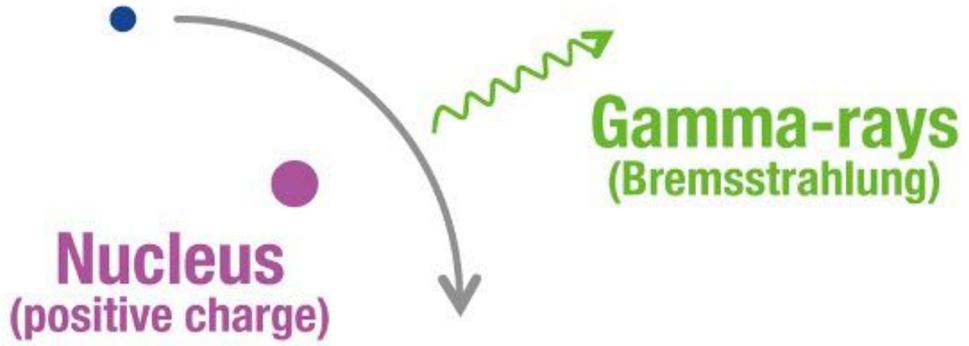

Low-energy gamma-rays are distinguishable

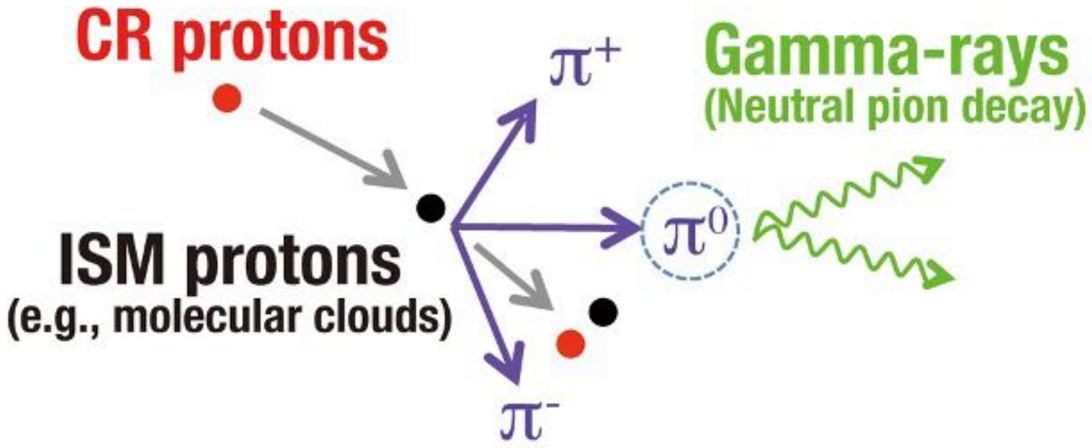

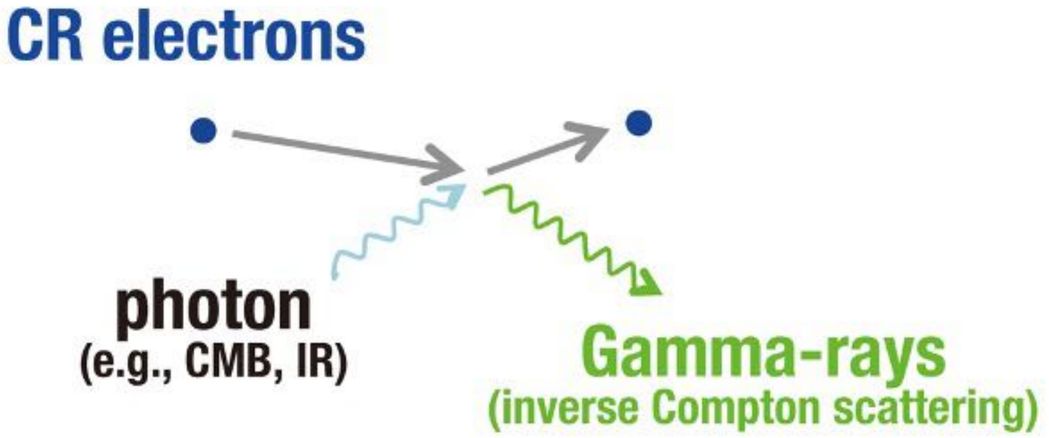

Giuliani et al. (2011), W44

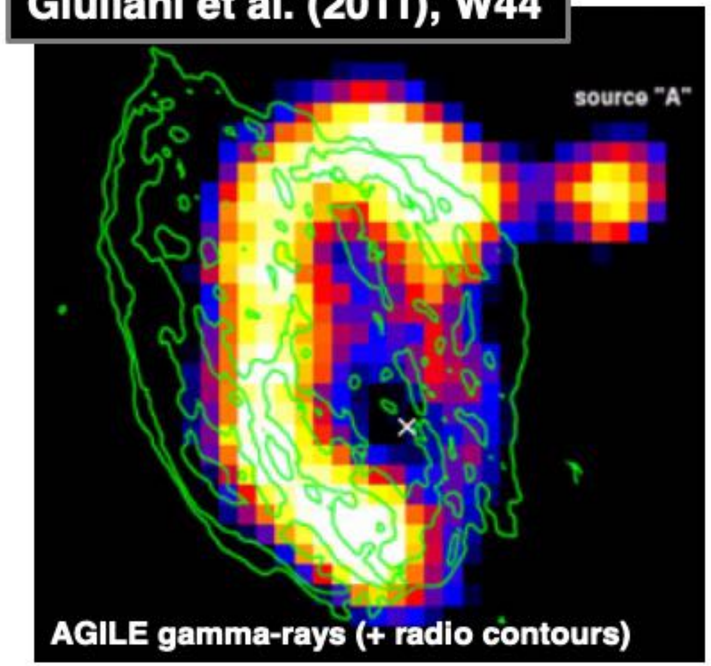

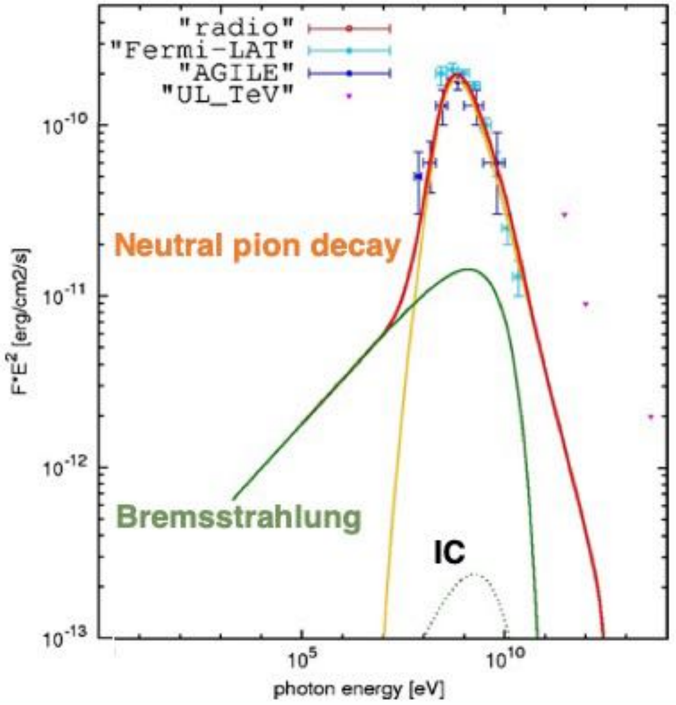

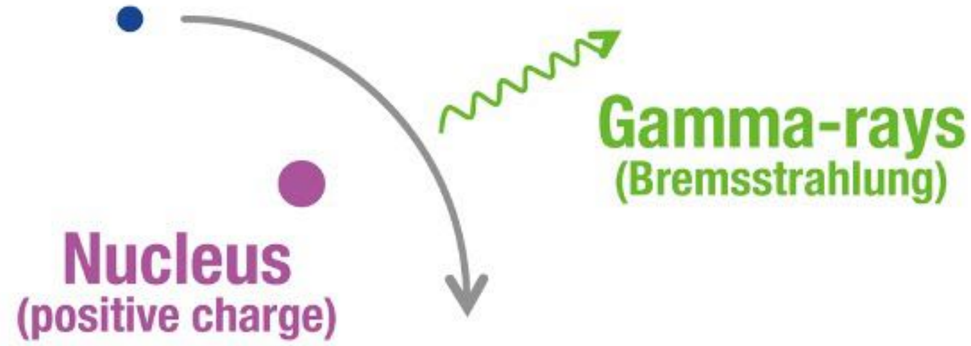

Subsequent Fermi observations confirmed the pion-decay bump (W44 & IC 443, Ackermann et al. 2013, Science, 339, 807)

Young TeV bright SNRs are responsible for PeV CR acceleration!?

W44 (~30,000 yrs)

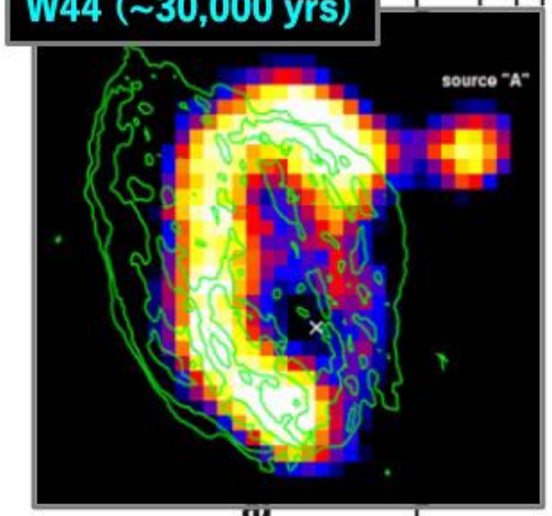

RX J1713.7 – 3946 (~1600 yrs)

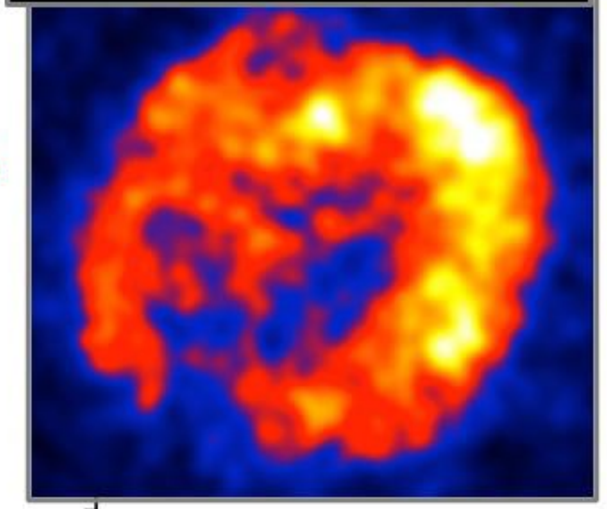

Tycho's SNR (449 yrs)

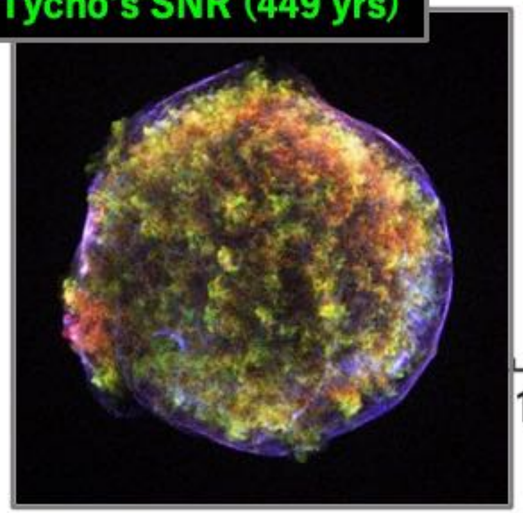

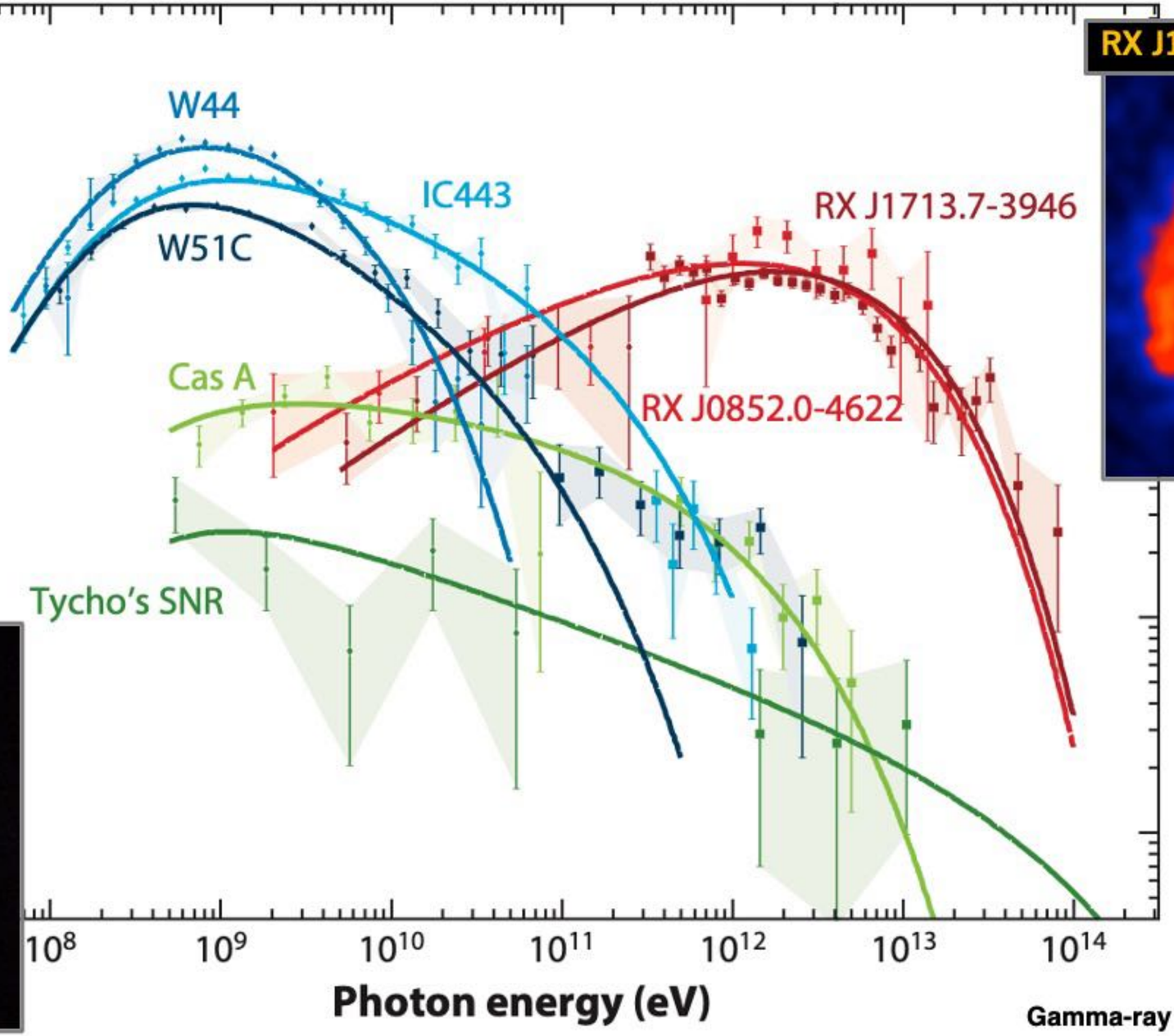

Gamma-ray spectra from SNRs (Funk 2015)

Hadronic vs Leptonic Gamma-rays in young TeV bright SNRs

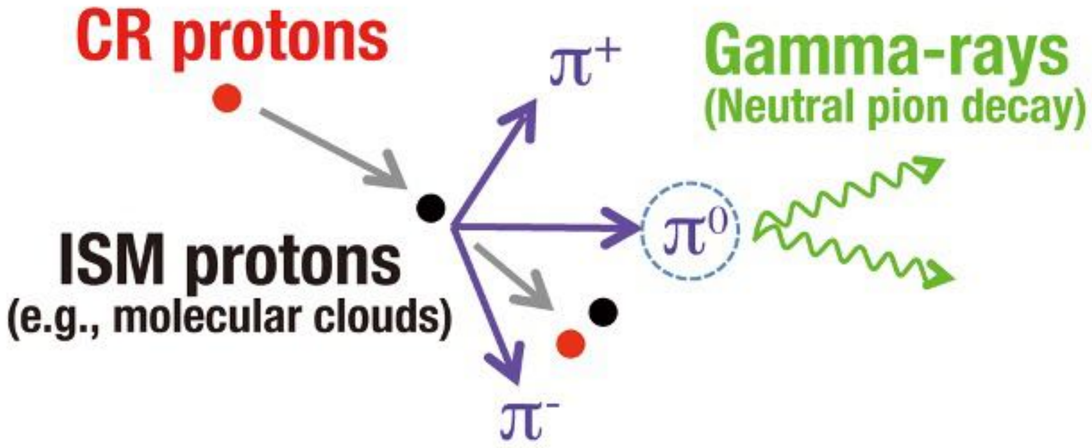

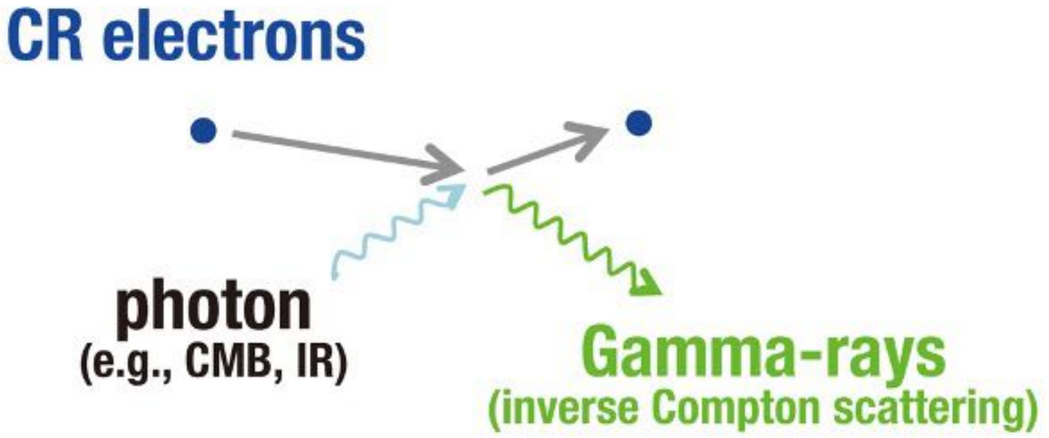

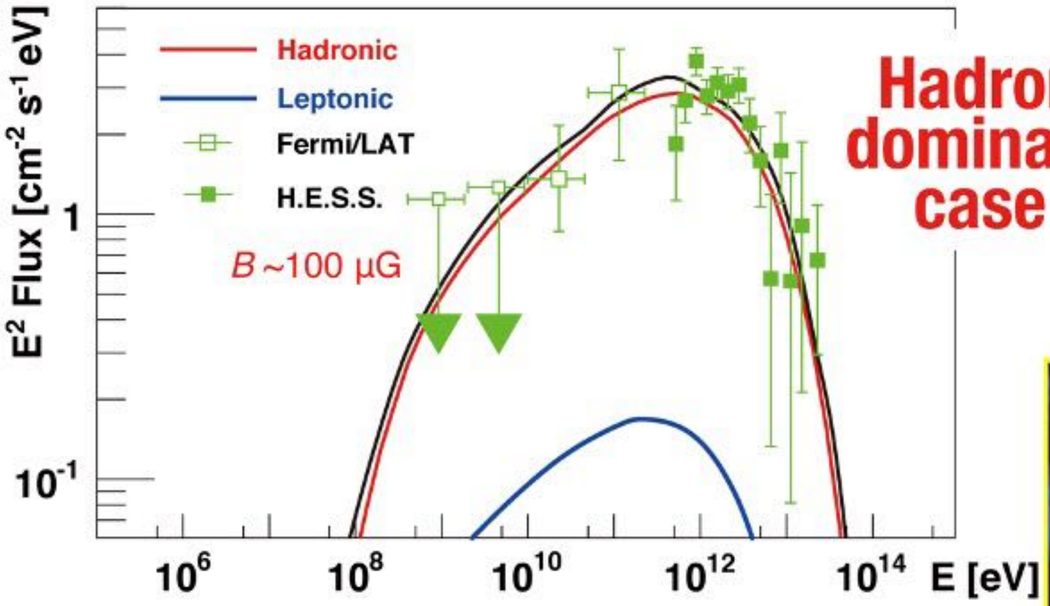

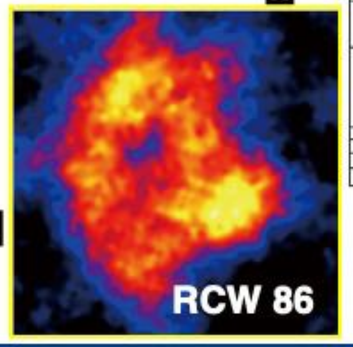

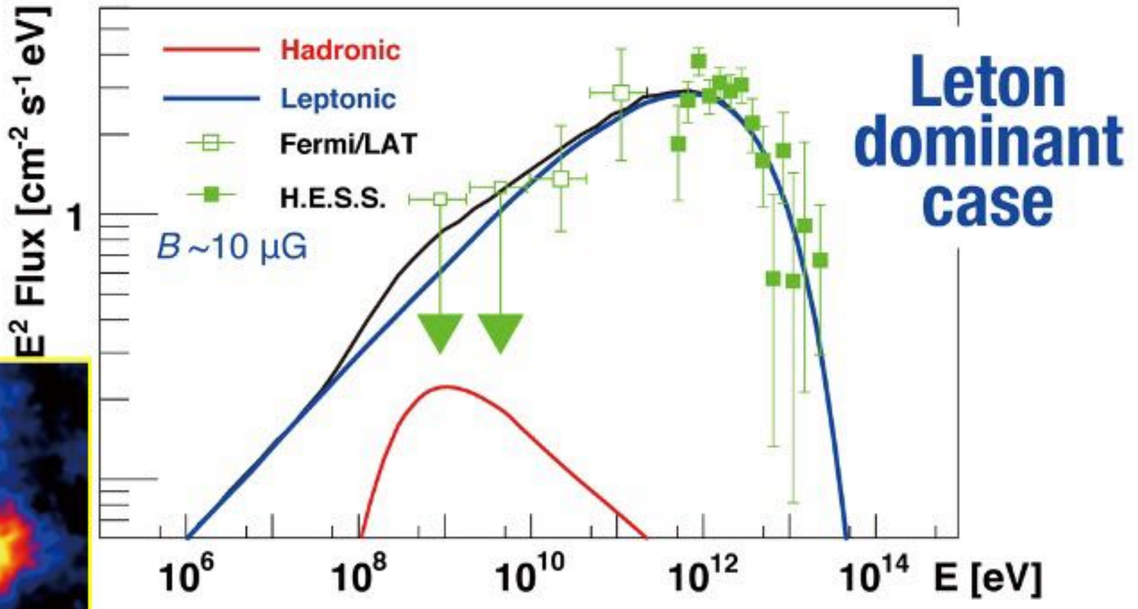

Gamma-ray spectra from RCW 86 (H.E.S.S. Collaboration et al. 2018b)

Hadronic vs Leptonic Gamma-rays in young TeV bright SNRs

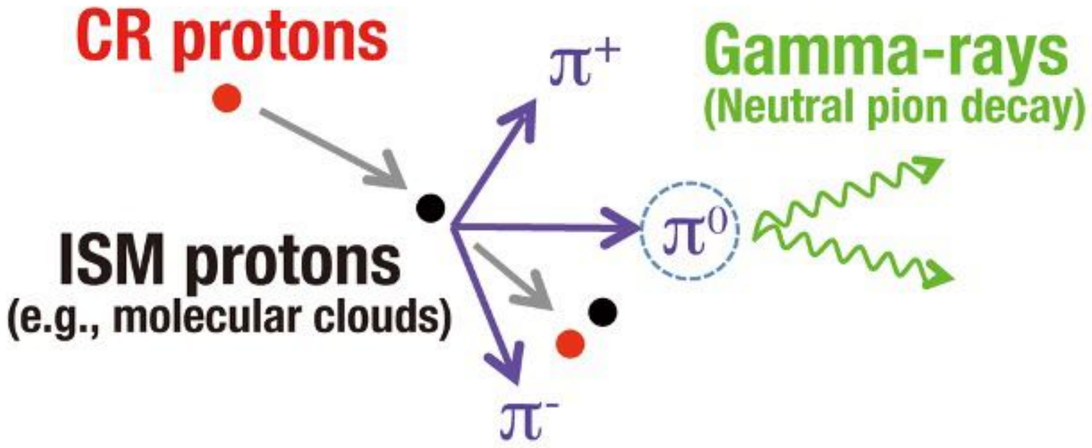

$$F \propto \frac{W_p n}{d^2}$$

W_p: total energy in accelerated protons
n: gas density
d: distance to the SNR

Gamma-ray flux ∝ ISM proton density

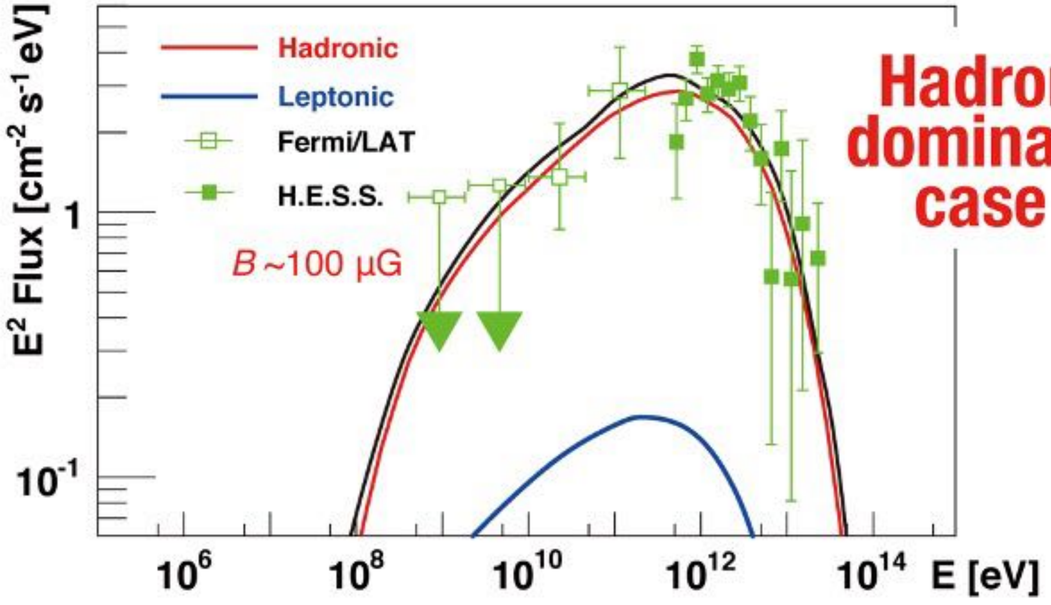

Gamma-ray spectra from RCW 86 (H.E.S.S. Collaboration et al. 2018b)

Molecular Hydrogen H_2

- traced by CO 2.6 mm line emission
- Density > 1000 cm^{-3}, T_k ~10 K

Atomic Hydrogen HI

- traced by HI 21 cm line emission
- Density ~ 1–100 cm^{-3}, T_k ~ 40–100 K

Spatial correlation between the ISM & Gamma-rays (2012–)

RX J1713.7–3946

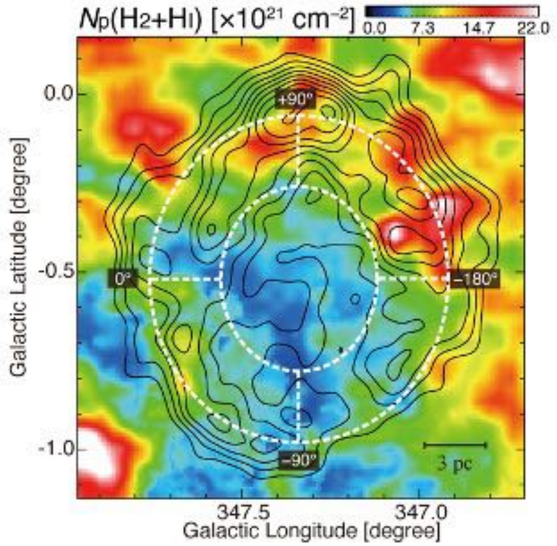

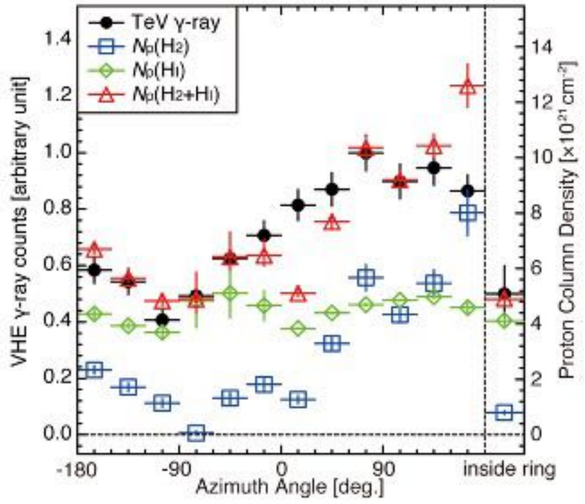

Vela Jr.

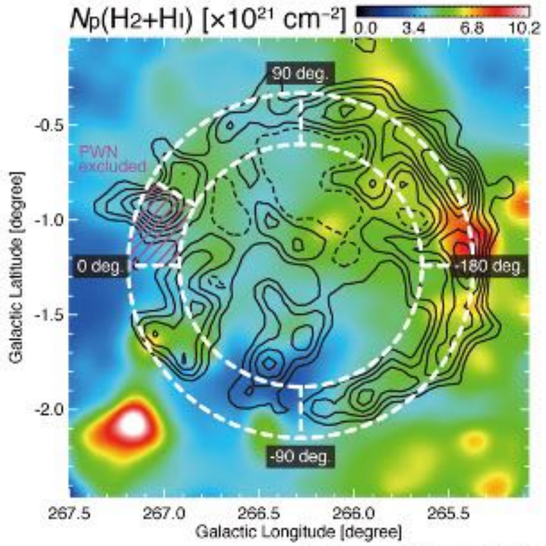

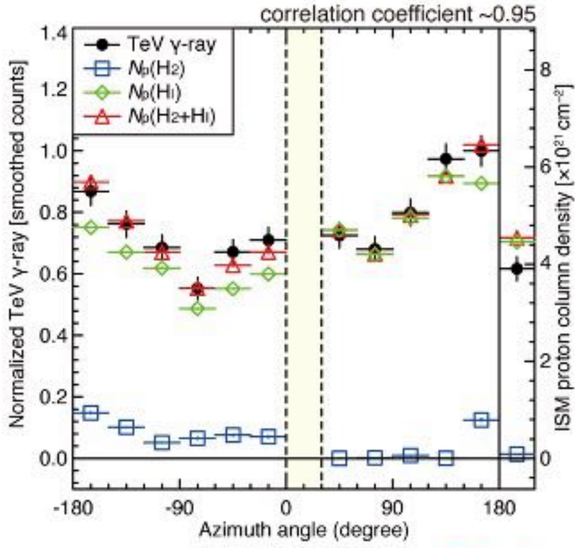

RCW 86

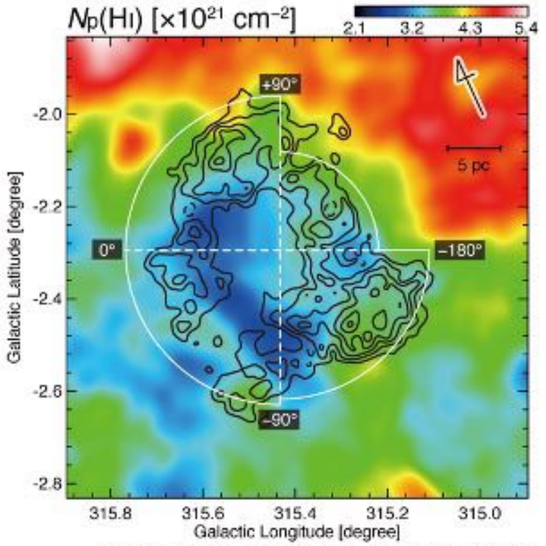

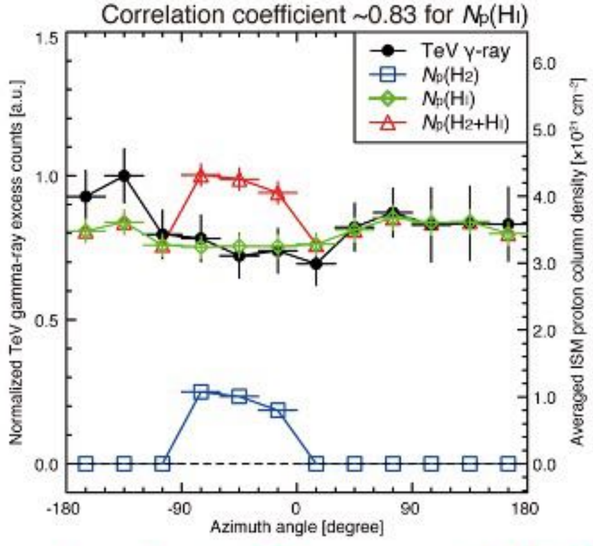

HESS J1731–347

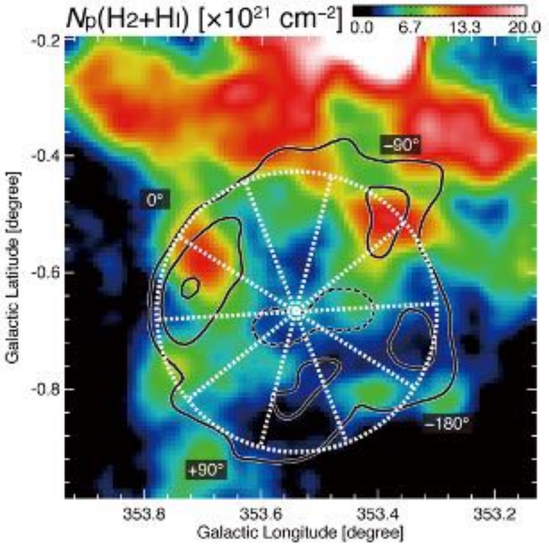

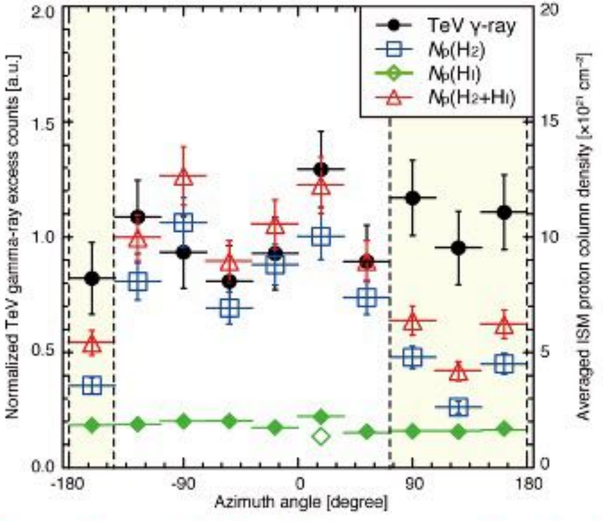

Image: ISM protons $N_p(H_2 + H_I)$, Contours: H.E.S.S. TeV gamma-rays

Total energy of accelerated CR protons ~10^{48}–10^{49} erg (compatible with a conventional value)

Fukui et al. 2012 ApJ, 746, 82; Fukui et al. 2017, ApJ, 850, 71; Sano et al. 2019, ApJ, 876, 37; Fukuda et al. 2014, ApJ, 788, 94

Quantifying hadronic and leptonic gamma-rays (2021)

Gamma-ray Excess N_g = **Interstellar Gas Density N_p** + **Synchrotron X-rays N_x**

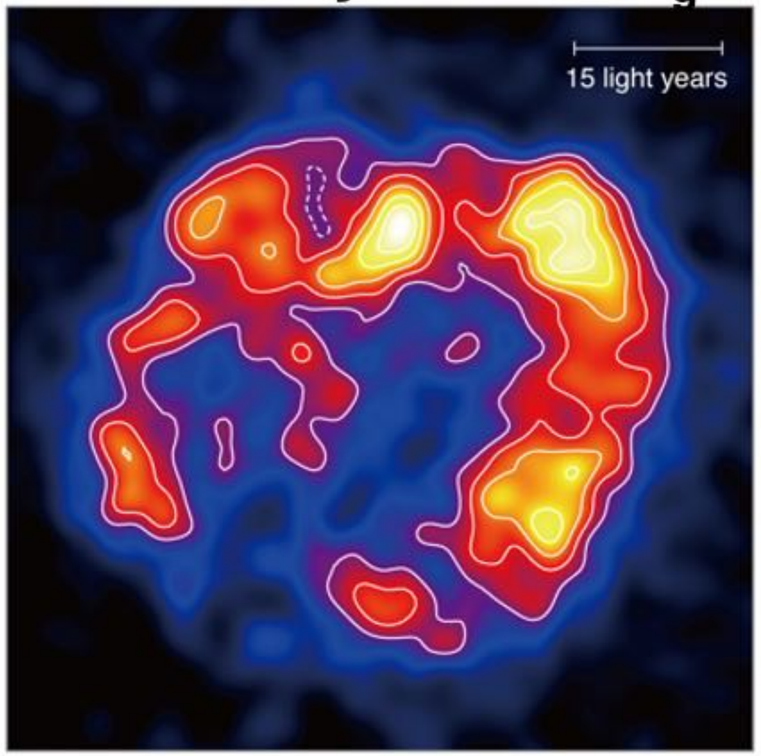

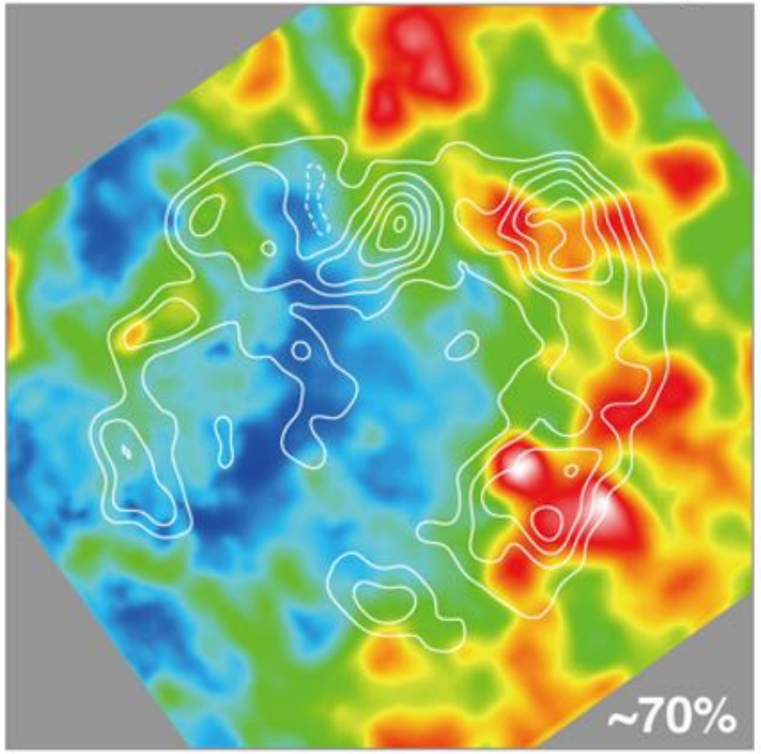

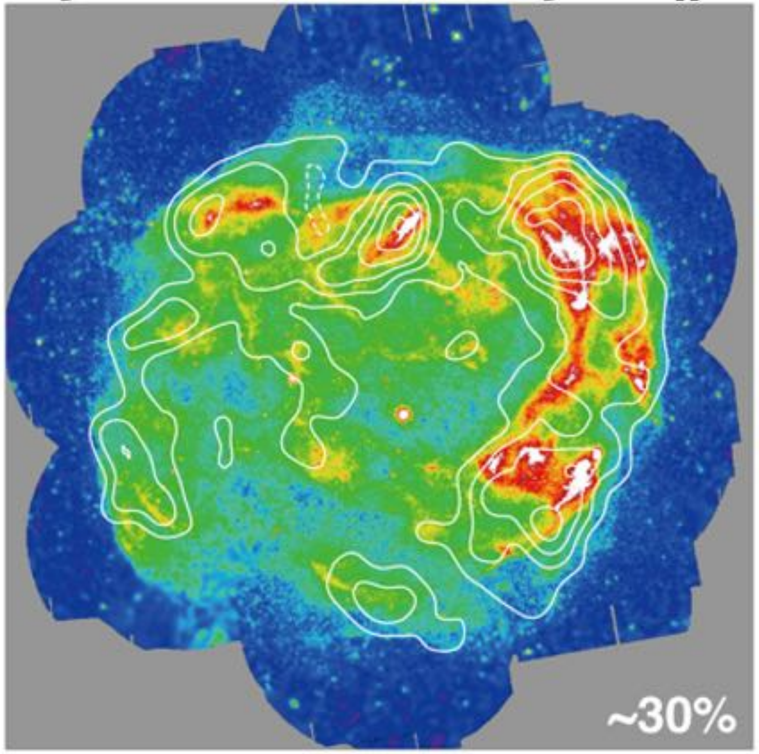

Fukui, Sano et al. 2021, ApJ, 915, 84

$$N_g = N_{g\_hadronic} + N_{g\_leptonic}$$

$$N_{g\_hadronic} = K_1 \, n_{CR\ proton} \, N_p$$

$$N_{g\_leptonic} = K_2 \, n_{CR\ electron} \, n_{CMB} = (K_2 \, n_{CMB} / K_3 \, B^2) \, N_x$$

$n_{CR\ proton}$: CR proton density　　n_{CMB} : density of CMB photons　　K_1, K_2, K_3 : constant

$n_{CR\ electron}$: CR electron density　　B : magnetic field

Quantifying hadronic and leptonic gamma-rays (2021)

Gamma-ray Excess N_g

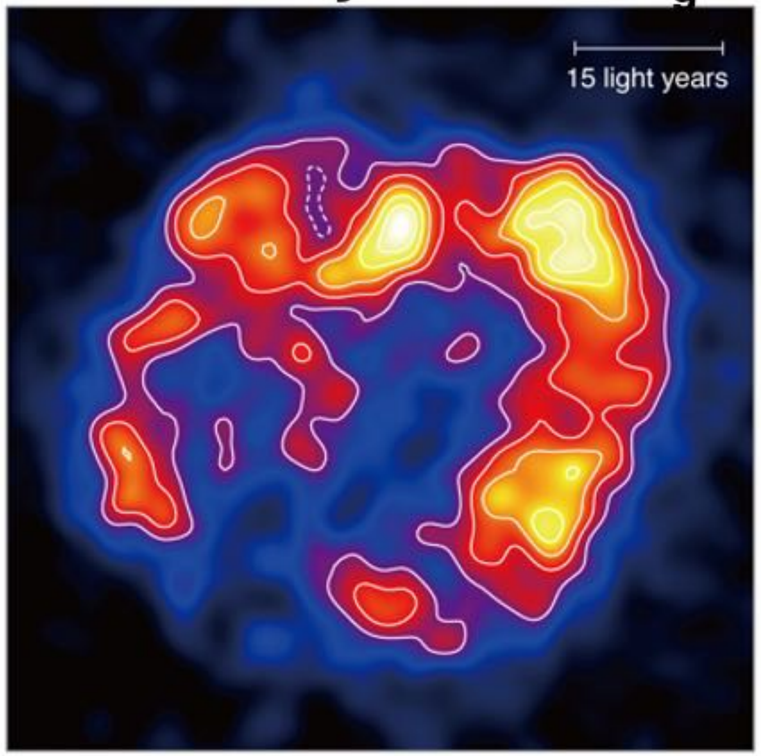

$N_{g\_hadronic} : N_{g\_leptonic} = 7 : 3$

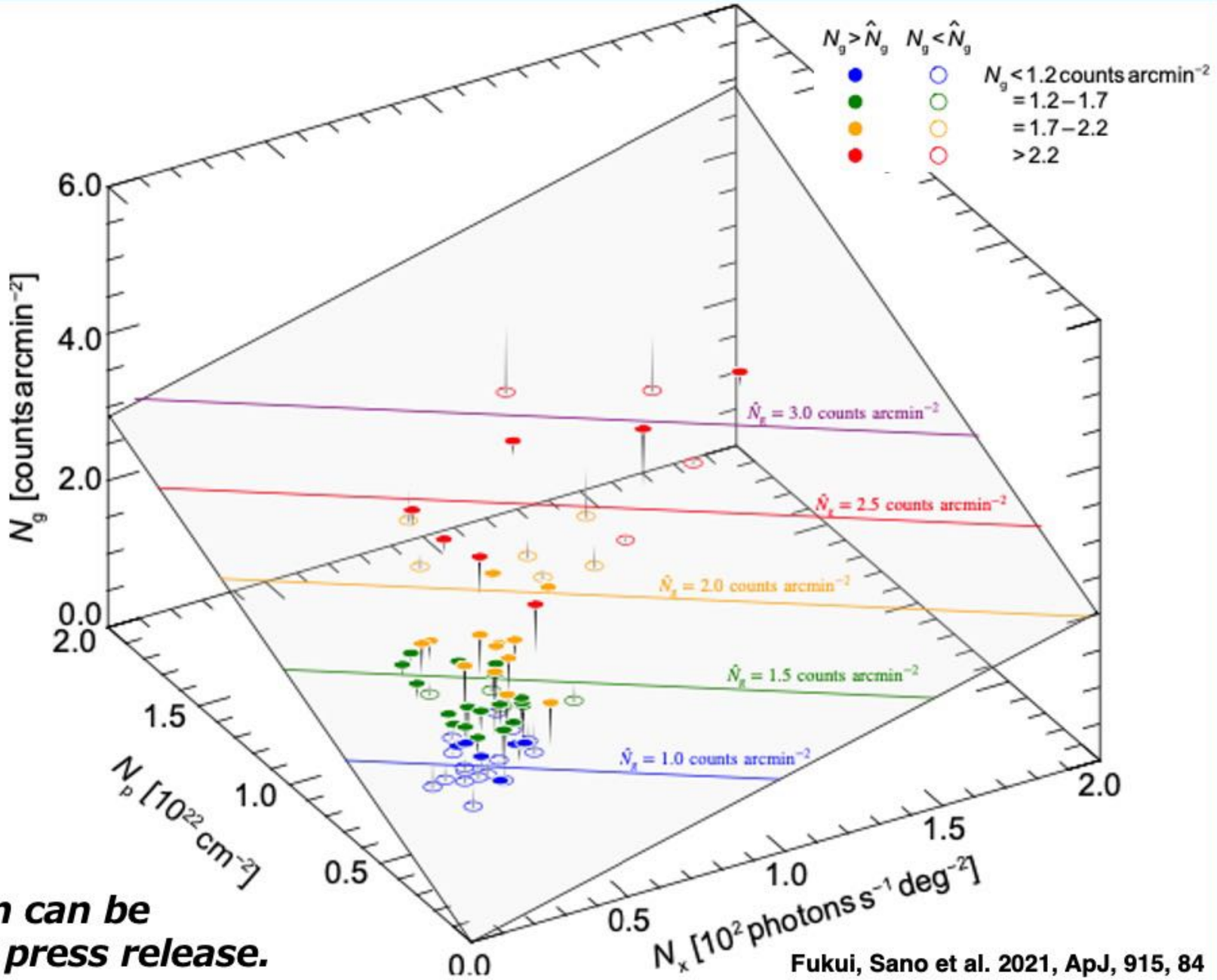

Fukui, Sano et al. 2021, ApJ, 915, 84

More detailed information can be found in the web page of press release.

Total energy of accelerated cosmic-ray protons W_p (2021–)

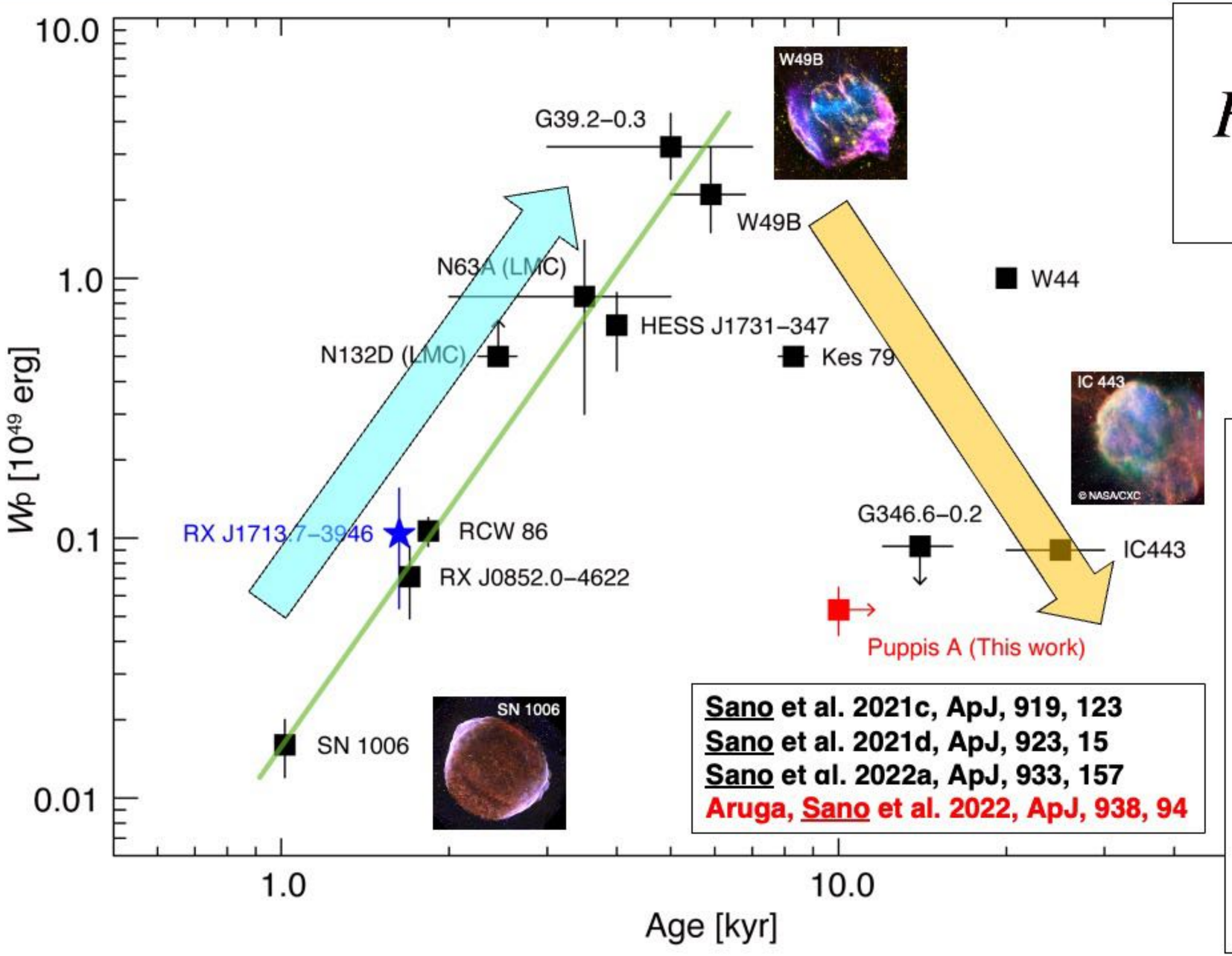

$$F \propto \frac{W_p n}{d^2}$$

(W_p: total energy in accelerated protons; n: gas density; d: distance to the SNR)

- **Conventional (theoretical) values**
  W_p ~10^{49}–10^{50} erg
- **Observational values (this work)**
  W_p ~10^{47} to more than 10^{49} erg

Young SNRs (age < 6000 yr)
Increasing W_p as a function of age
➡ time dependent evolution!?

Old SNRs (age > 8000 yr)
Steady Decreasing of W_p
➡ time dependent diffusion of CRs

SNR RX J1713.7−3946

RX J1713.7–3946 (G347.3–0.5)

- Shell-type SNR discovered by *ROSAT*
  (Pfeffermann & Aschenbach 1996)
- Distance / Diameters : ~1 kpc / ~18 pc (~1°)
  (e.g., Fukui et al. 2003; Cassam-Chenaï et al. 2004; Leike et al. 2021)
- Age : ~1600 yr (SN 393)
  (Wang et al. 1997; Fukui et al. 2003; Tsuji & Uchiyama 2016)
- **Associated with molecular/atomic clouds**
  ➡ shock-cloud interaction with *B* amplification
  (e.g., Fukui et al. 2003, 2012, 2021; Moriguchi et al. 2005; Inoue et al. 2009, 2012; Sano et al. 2010, 2013, 2015, 2020; Maxted et al. 2012, 2013)
- TeV / GeV Gamma-rays
  ➡ Steep *νFν* spectrum + Hadron dominant
  (e.g., Muraishi et al. 2000; Aharonian et al. 2004, 2006, 2007; Zirakashvili & Aharonian 2010; Abdo et al. 2011; Inoue et al. 2012; Gabici & Aharonian 2014; H.E.S.S. Collaboration 2018; Celli et al. 2019; Inoue 2019; Fukui et al. 2021)
- **Synchrotron X-rays ➡ Time variation**
  (e.g., Koyama et al. 1997; Slane et al. 1999; Hiraga et al. 2005; Uchiyama et al. 2007; Takahashi et al. 2008; Tanaka et al. 2008, 2020; Acero et al. 2009; Sano et al. 2015; Okuno et al. 2018; Tsuji et al. 2019; Kuznetsova et al. 2019; Higurashi et al. 2020)

SNR RX J1713.7−3946: X-ray enhancement around the clouds

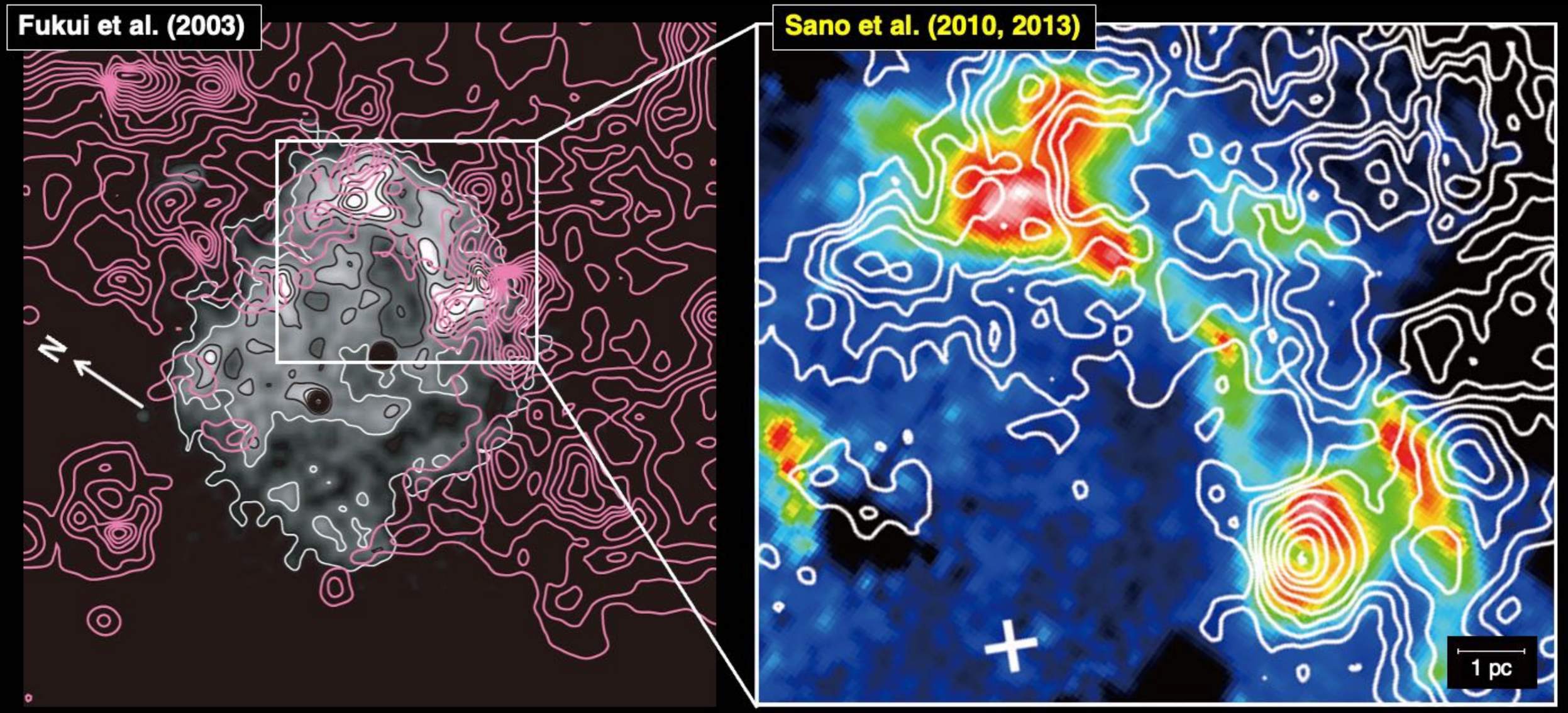

Image: *ROSAT* X-rays
Contours: NANTEN ^{12}CO(J = 1–0)

Image: Suzaku X-rays (E: 5–10 keV)
Contours: NANTEN2 ^{12}CO(J = 2–1)

SNR RX J1713.7−3946: Spatial variation of photon indies

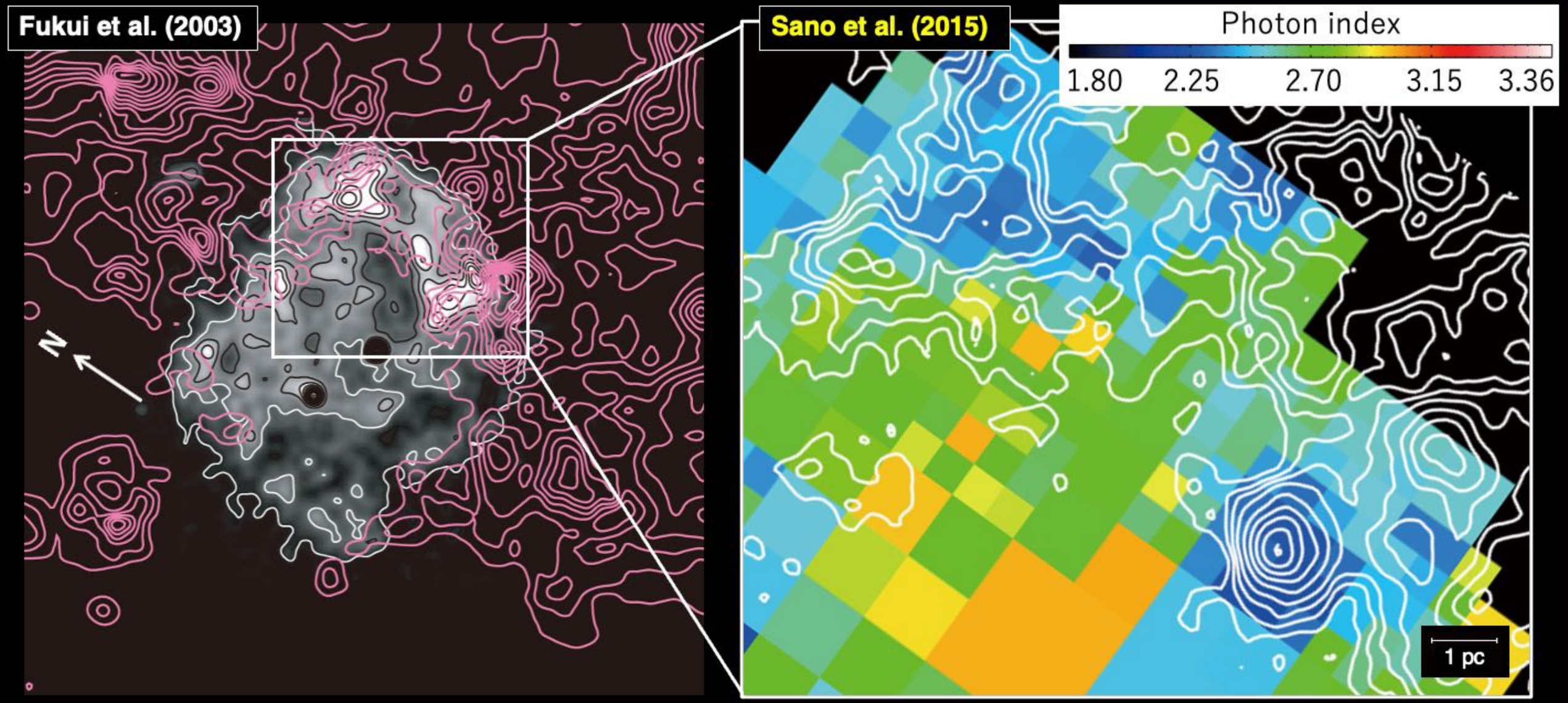

Image: *ROSAT* X-rays
Contours: NANTEN ^{12}CO(J = 1–0)

Image: Synchrotron X-ray photon index
Contours: NANTEN2 ^{12}CO(J = 2–1)

SNR RX J1713.7−3946: Shock interactions with clumpy clouds

Fukui et al. (2003)

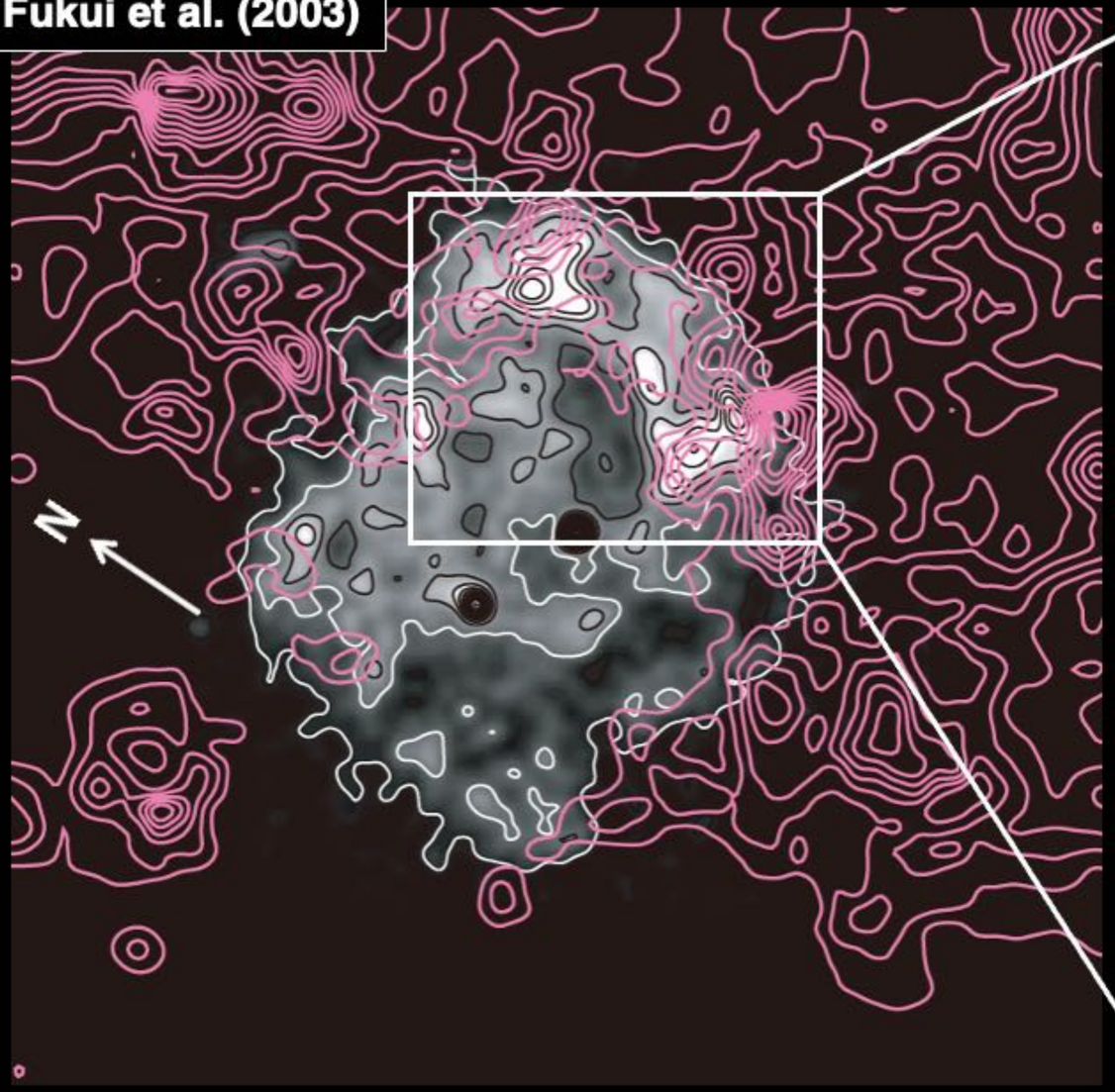

Image: *ROSAT* X-rays
Contours: NANTEN ^{12}CO(J = 1–0)

T. Inoue et al. (2012)

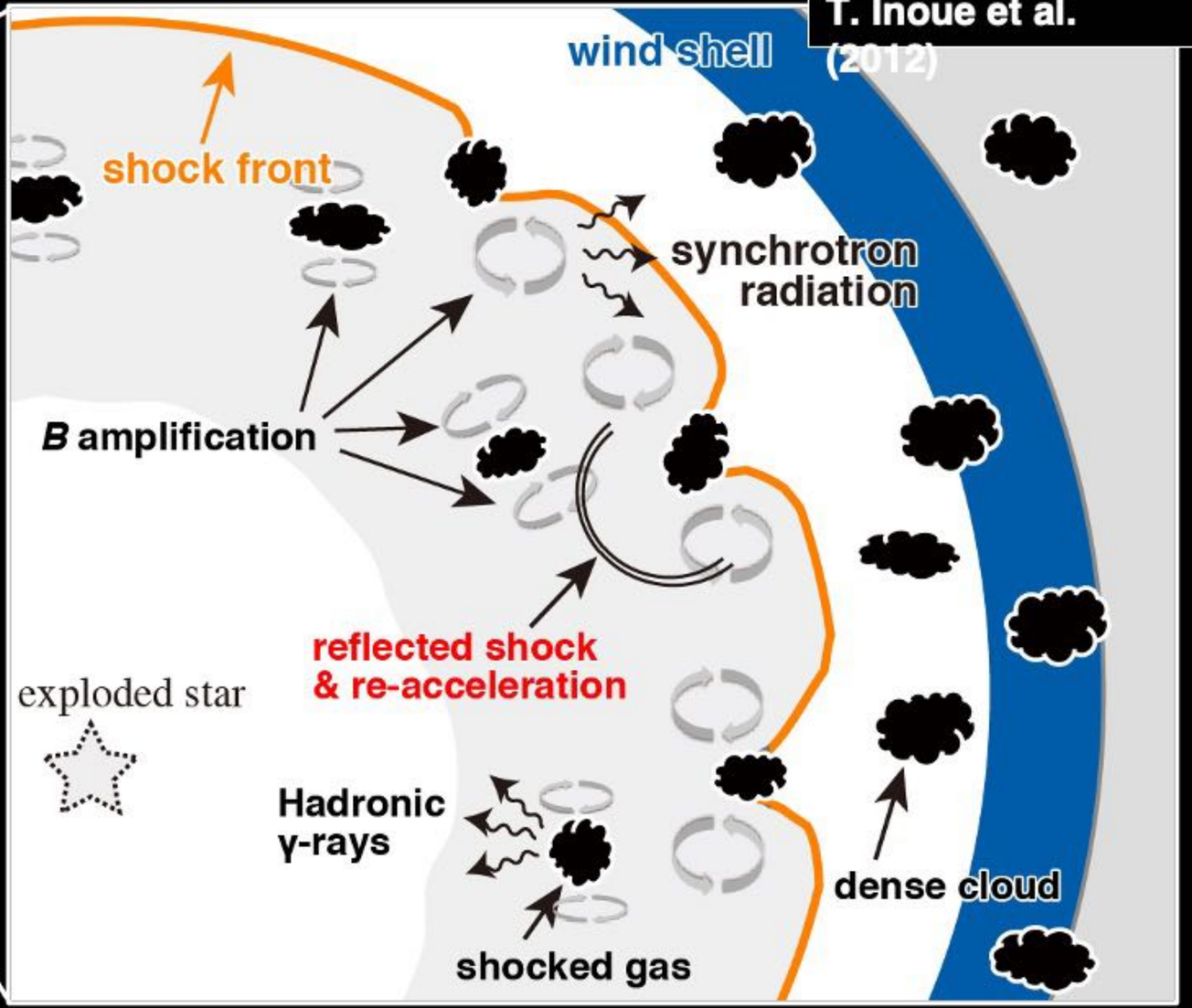

Schematic image of shock-cloud interaction
Cloud density: ~10^3 cm^{-3}, Intercloud density: ~0.01 cm^{-3}

SNR RX J1713.7−3946: Time variability of X-ray hot spots

Fukui et al. (2003)

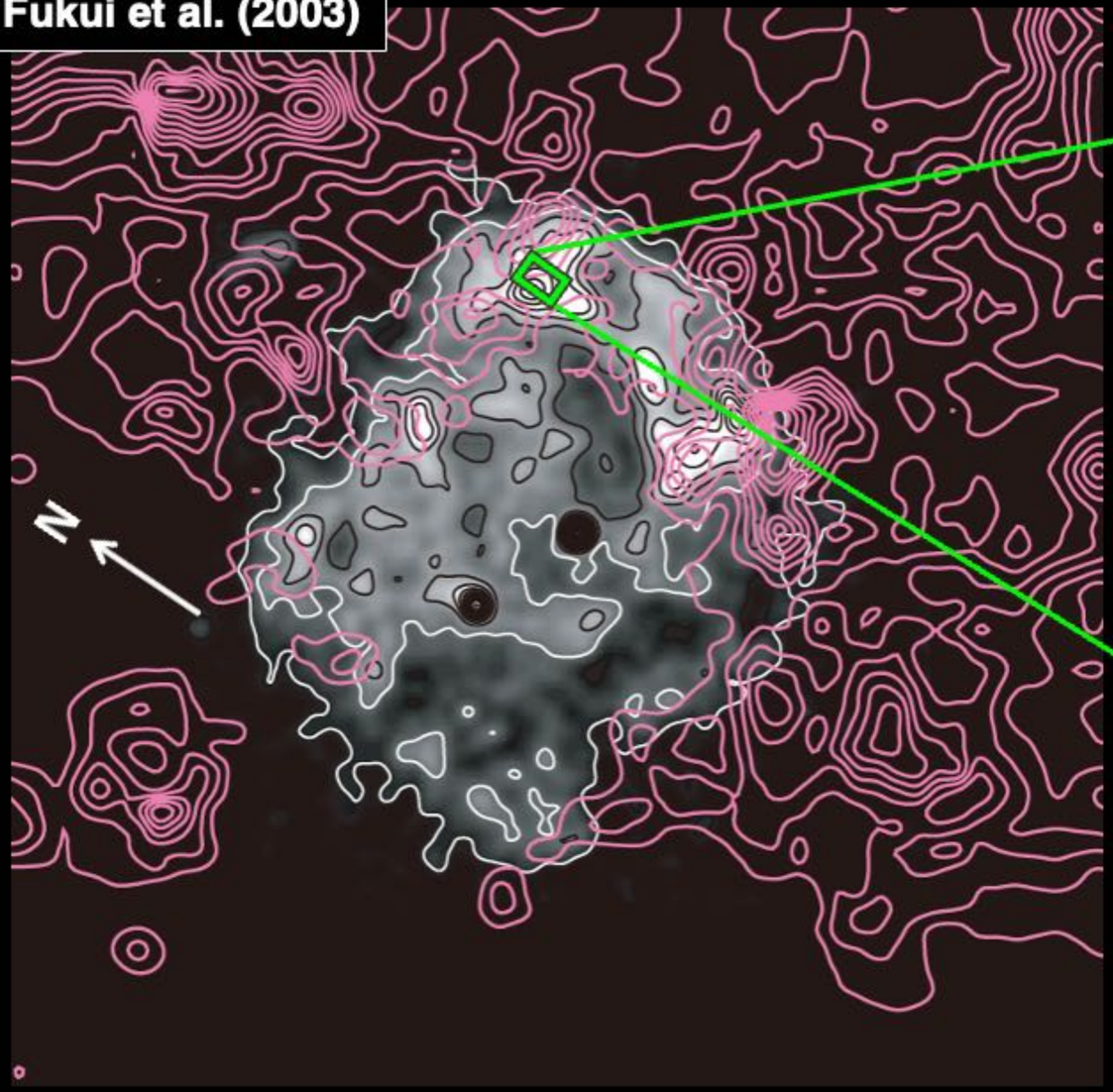

Image: *ROSAT* X-rays
Contours: NANTEN ^{12}CO(J = 1–0)

Uchiyama et al. (2007)

Images: Chandra X-rays

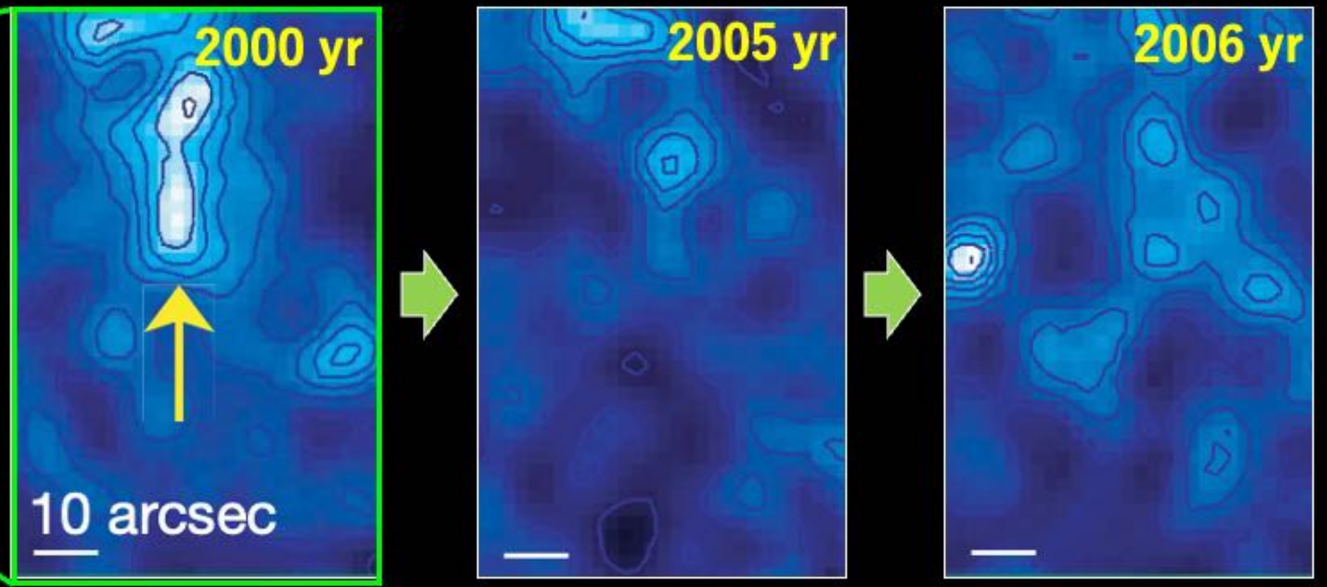

$$T_{\rm synch} \sim 1.5 \left(\frac{B}{1\ {\rm mG}}\right)^{-1.5} \left(\frac{\varepsilon}{1\ {\rm keV}}\right)^{-0.5} ({\rm yr})$$

$$T_{\rm acc} \sim 1\eta \left(\frac{B}{1\ {\rm mG}}\right)^{-1.5} \left(\frac{\varepsilon}{1\ {\rm keV}}\right)^{0.5} \left(\frac{V_{\rm s}}{3000\ {\rm km\ s^{-1}}}\right)^{-2} ({\rm yr})$$

X-ray hot spot shows B ~1 mG at 10 arcsec (~0.05 pc) scales

➡ Tiny clouds should be expected near the X-ray hot spots!?

ALMA CO observations toward the NW of RX J1713.7−3946

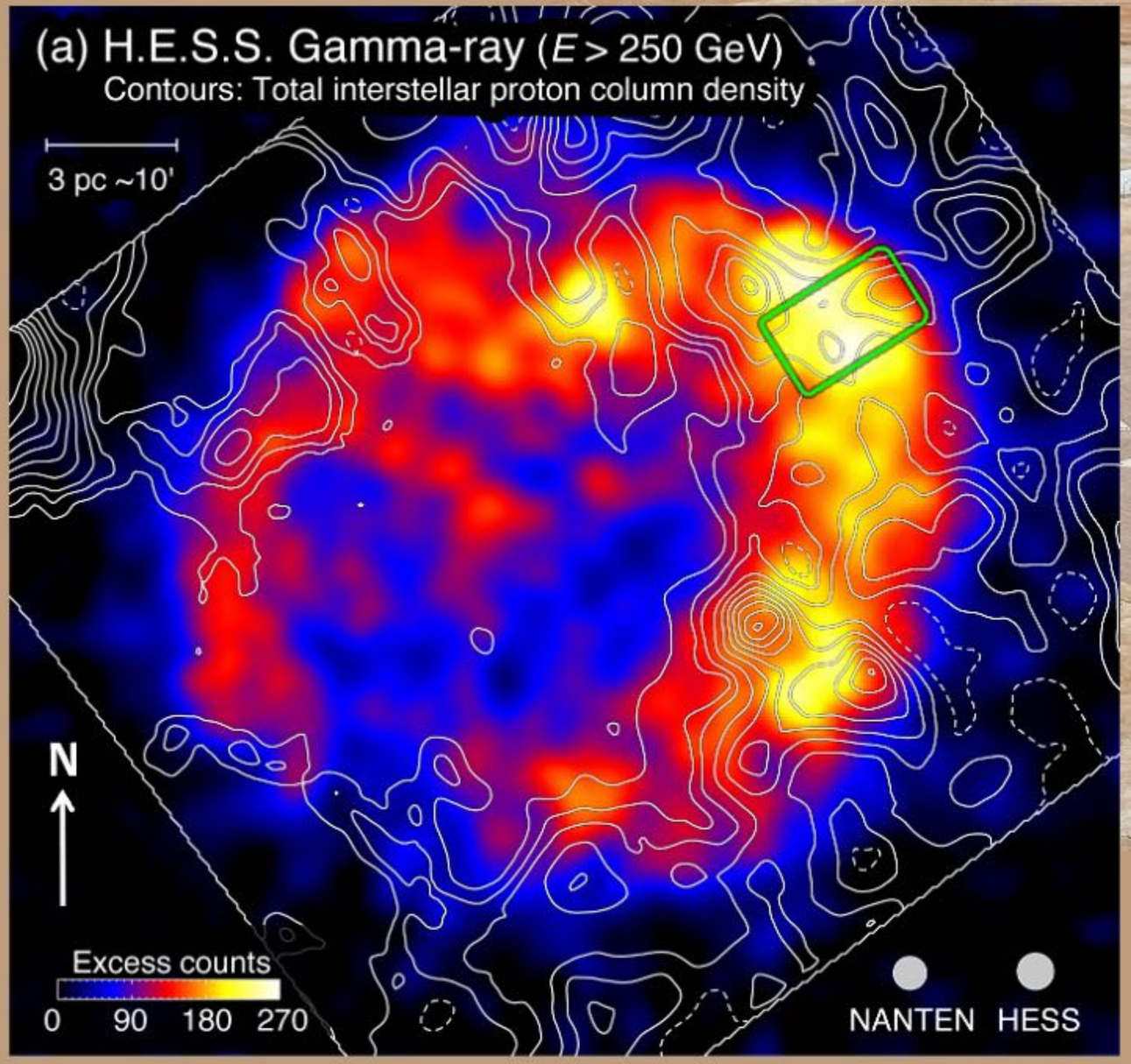

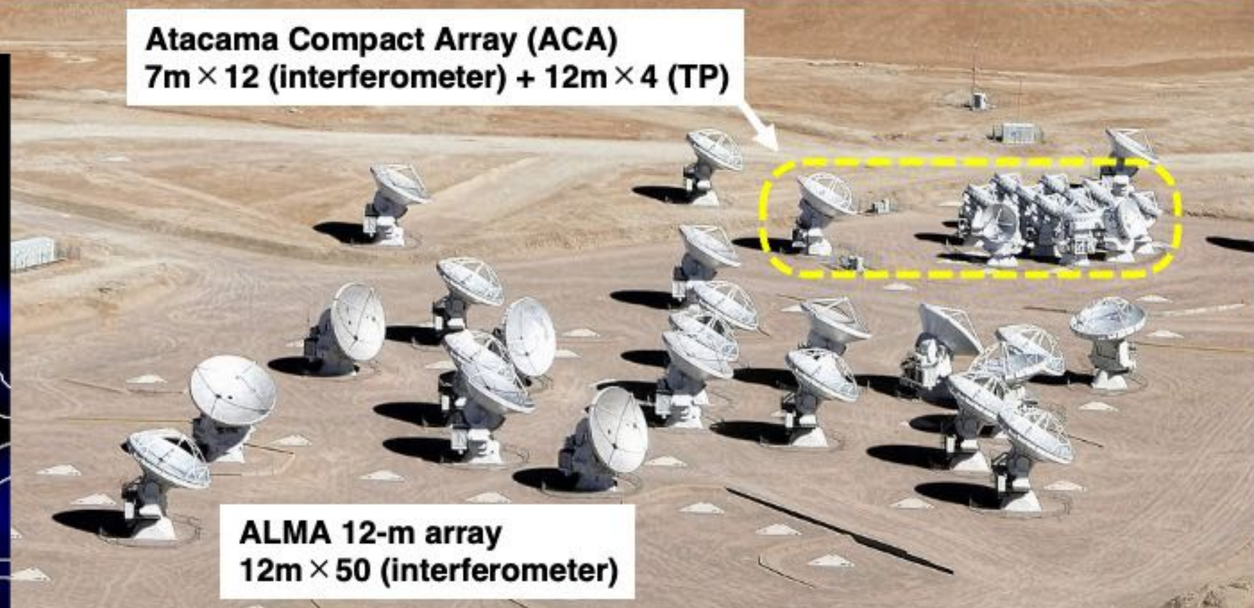

Project# (Cycle / PI)	2017.1.01406.S (Cycle 5 / H.Sano)
Target line	^{12}CO (J = 1–0)
Observed area	11.1' × 6.4' (mosaic mode)
Antennas	12-m array + ACA (7-m array + TP)
Observing time	**5.3 hrs (12-m) + 45.3 hrs (ACA)**
Baseline (u-v dist.)	8.9–313.7 m (3.4–120.6 $k\lambda$)
Beam size	**4.37" × 3.89" (~0.02 pc)**
RMS noise level	~ 0.13 K @ 0.4 km s^{-1}

Results 1: Overview of ALMA CO observations

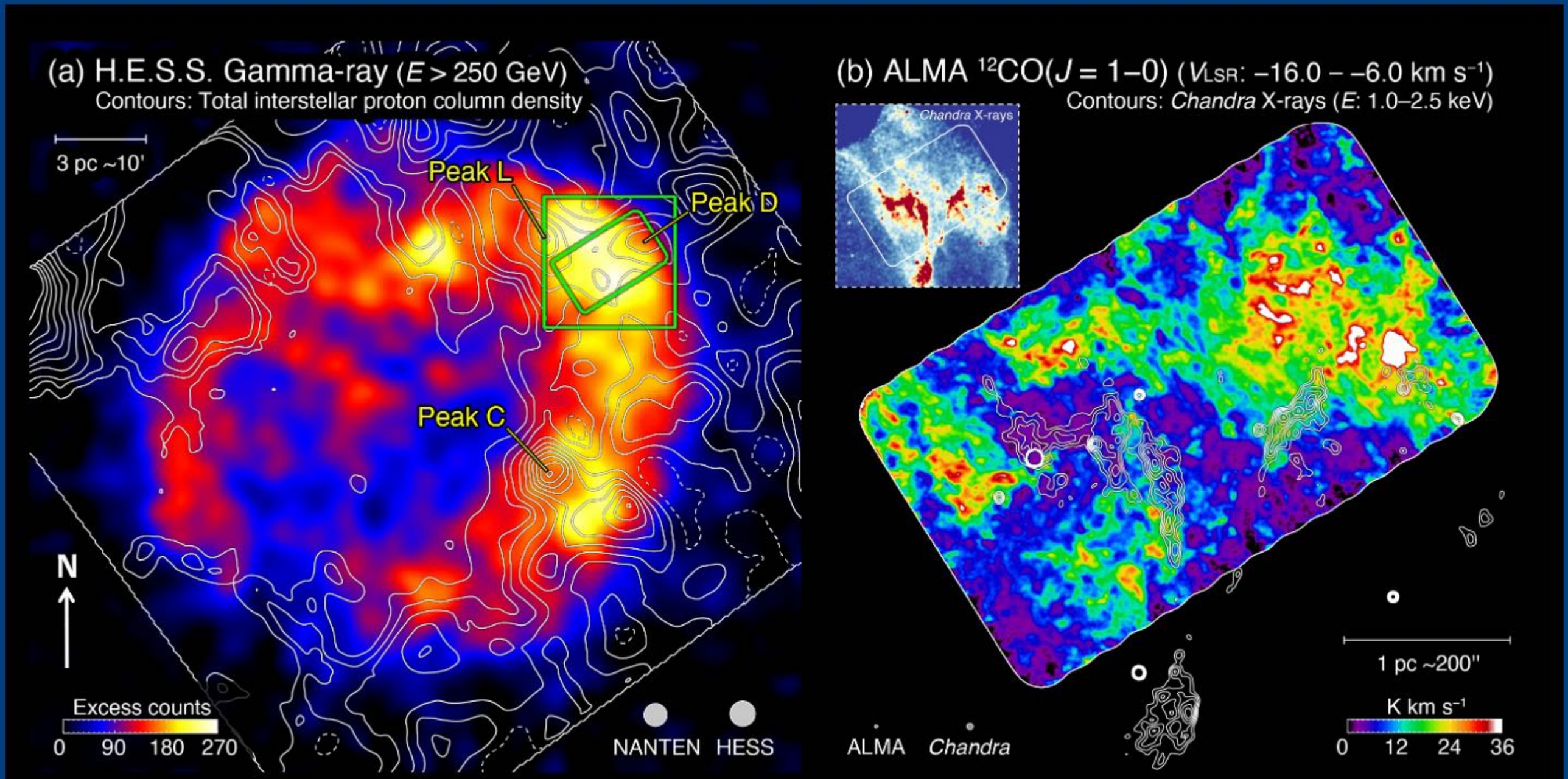

Sano et al. 2020c, ApJL, 904, L24

Results 2: Cloudlets survived from the wind/shock erosion

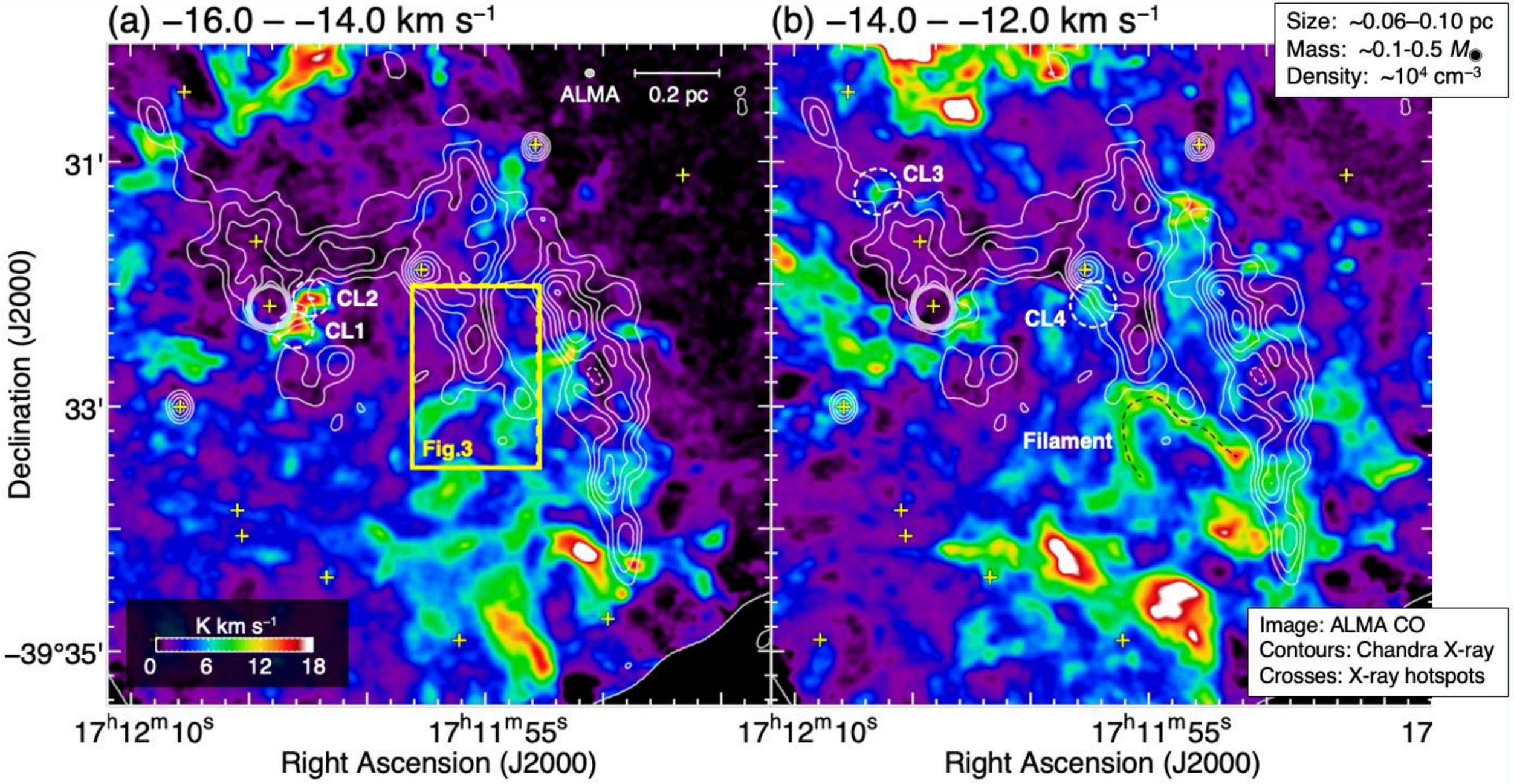

Results 3: Distributions of X-ray hot spots and cloudlets

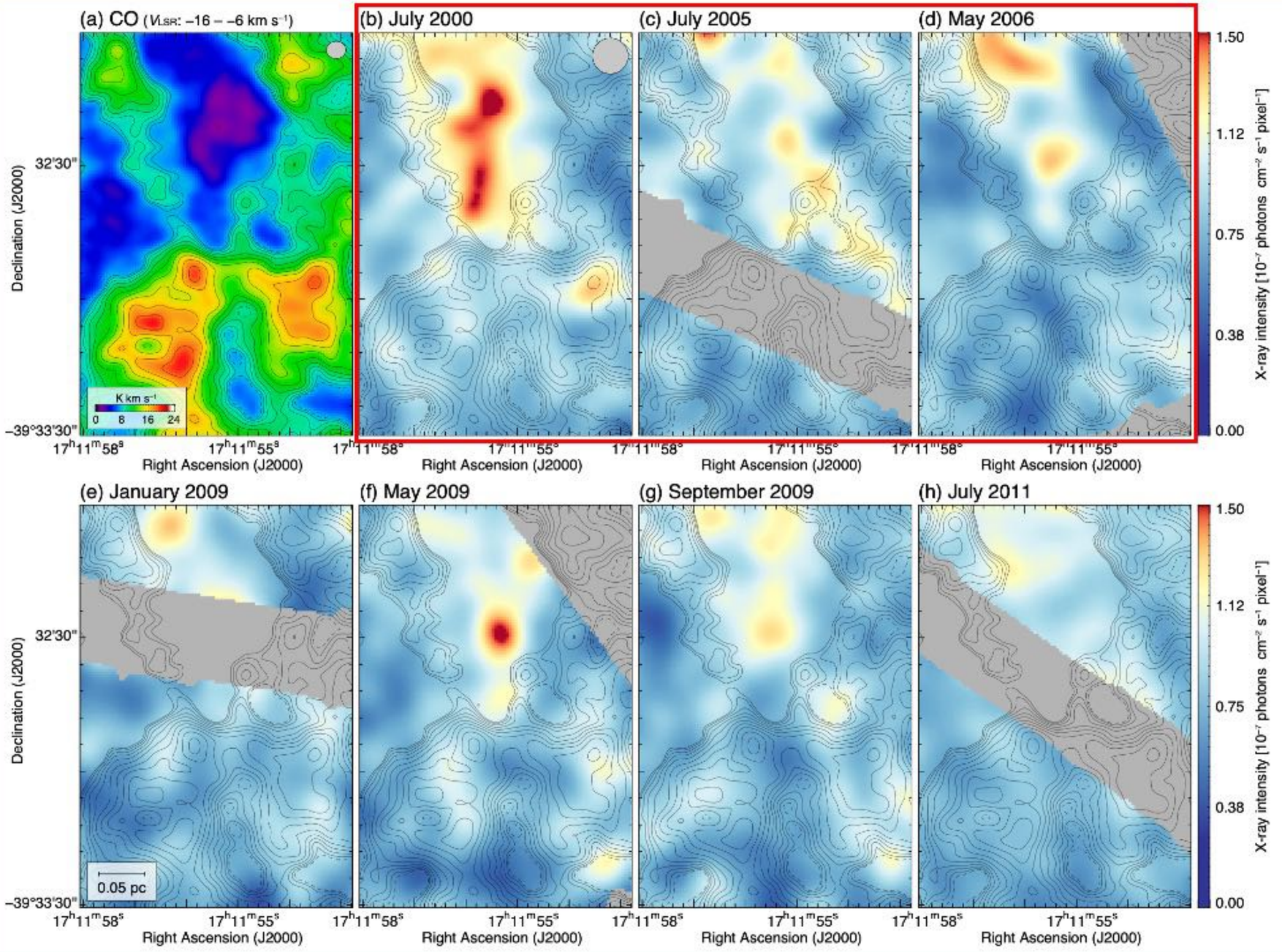

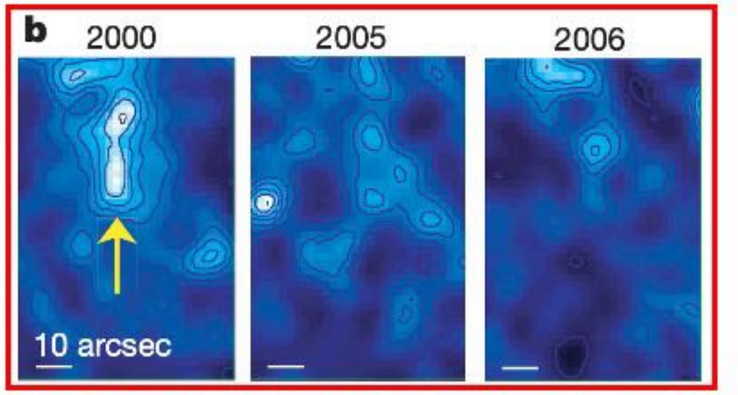

Almost the same area that presented in Uchiyama et al. (2007)

New hotspot on May 09 (~4σ)

➡ B ~0.3–3 mG

acceleration time < three years

cooling time < four months

Separation between clouds and hotspots: ~0.05–0.15 pc

Image: (a) ALMA CO (V_{LSR}: −16–6 km s^{-1})
(b–h) *Chandra* X-rays (E: 2–7 keV)
Contours: ALMA CO (V_{LSR}: −16–6 km s^{-1})

Sano et al. 2020c, ApJL, 904, L24

Discussion 1: *B* amplification via shock-cloudlet interactions

Spatial correspondence between X-ray hotspots and cloudlets cloud be understood as a result of the shock-cloud interaction

→ Celli et al. (2019) provides with us a numerical support!

	Celli+2019	This study
Cloud size [pc]	0.2	~0.06–0.10
Cloud density [cm^{-3}]	10^3	~10^4
Inter-cloud density [cm^{-3}]	0.01	~0.1
ISM density contrast	10^5	~10^5
B field or X-ray amplification	mainly cloud surroundings	cloudlets surroundings
Separation: cloud–B_{max} [pc]	~0.4	-------
Separation: cloud–hotspots [pc]	-------	~0.05–0.15

When we scaled the Celli's cloud to observed values ~0.06–0.10 pc, separation between the cloud and B_{max} to be ~0.12–0.20 pc, which is consistent with the observed values of ~0.05–0.15 pc.

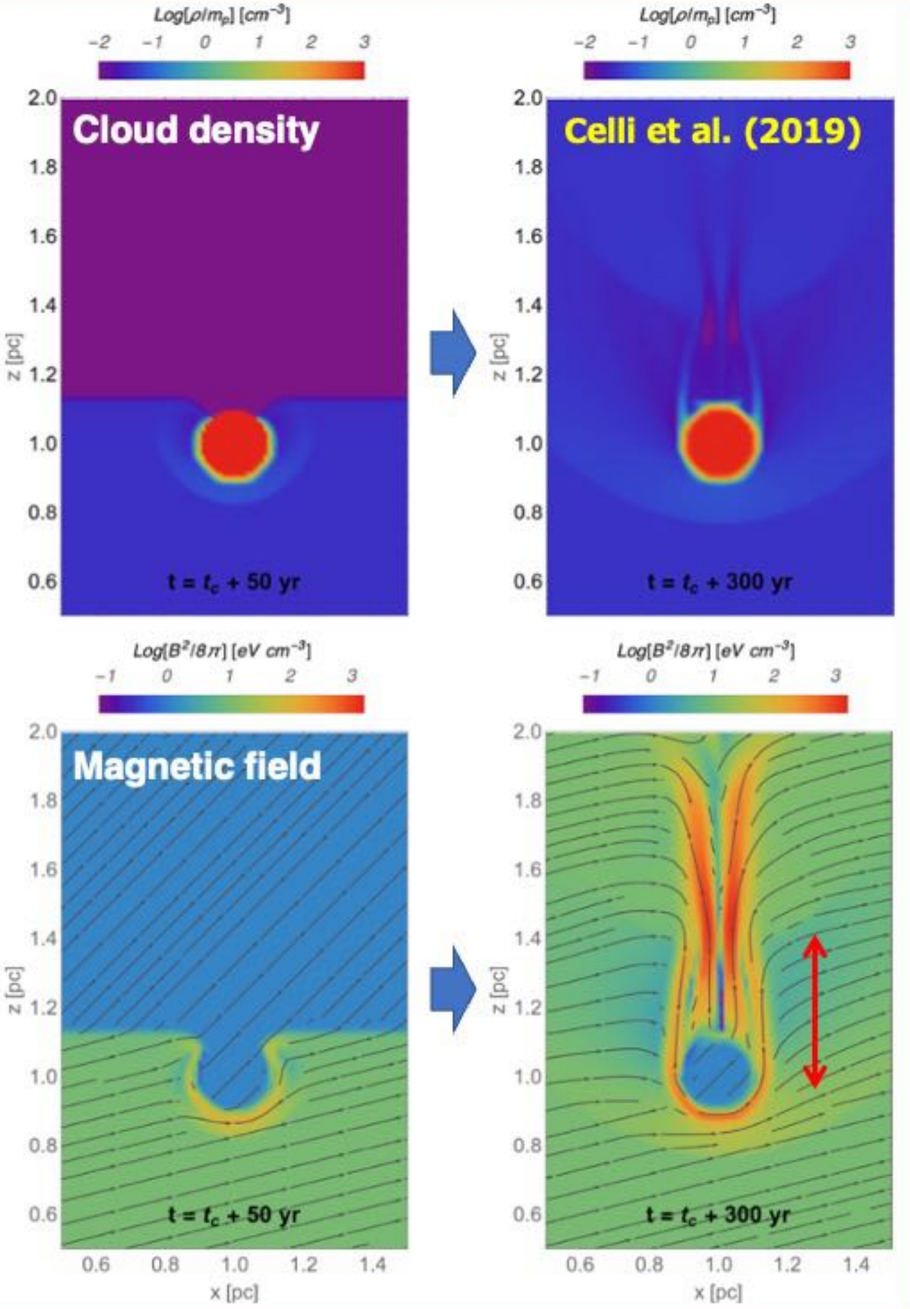

Discussion 2: Modulation of gamma-ray spectrum

$$l_{\rm pd} \simeq (\kappa_{\rm d}\, t)^{1/2} = 0.1\, \eta^{1/2} \left(\frac{E}{10\ {\rm TeV}}\right)^{1/2} \left(\frac{B}{100\ \mu{\rm G}}\right)^{-1/2} \left(\frac{t_{\rm age}}{10^3\ {\rm yr}}\right)^{1/2} {\rm pc},$$

Inoue et al. (2012)

$l_{\rm pd}$: penetration depth,
η: gyro factor,
E: CR proton energy,
B: magnetic field,
$t_{\rm age}$: SNR age

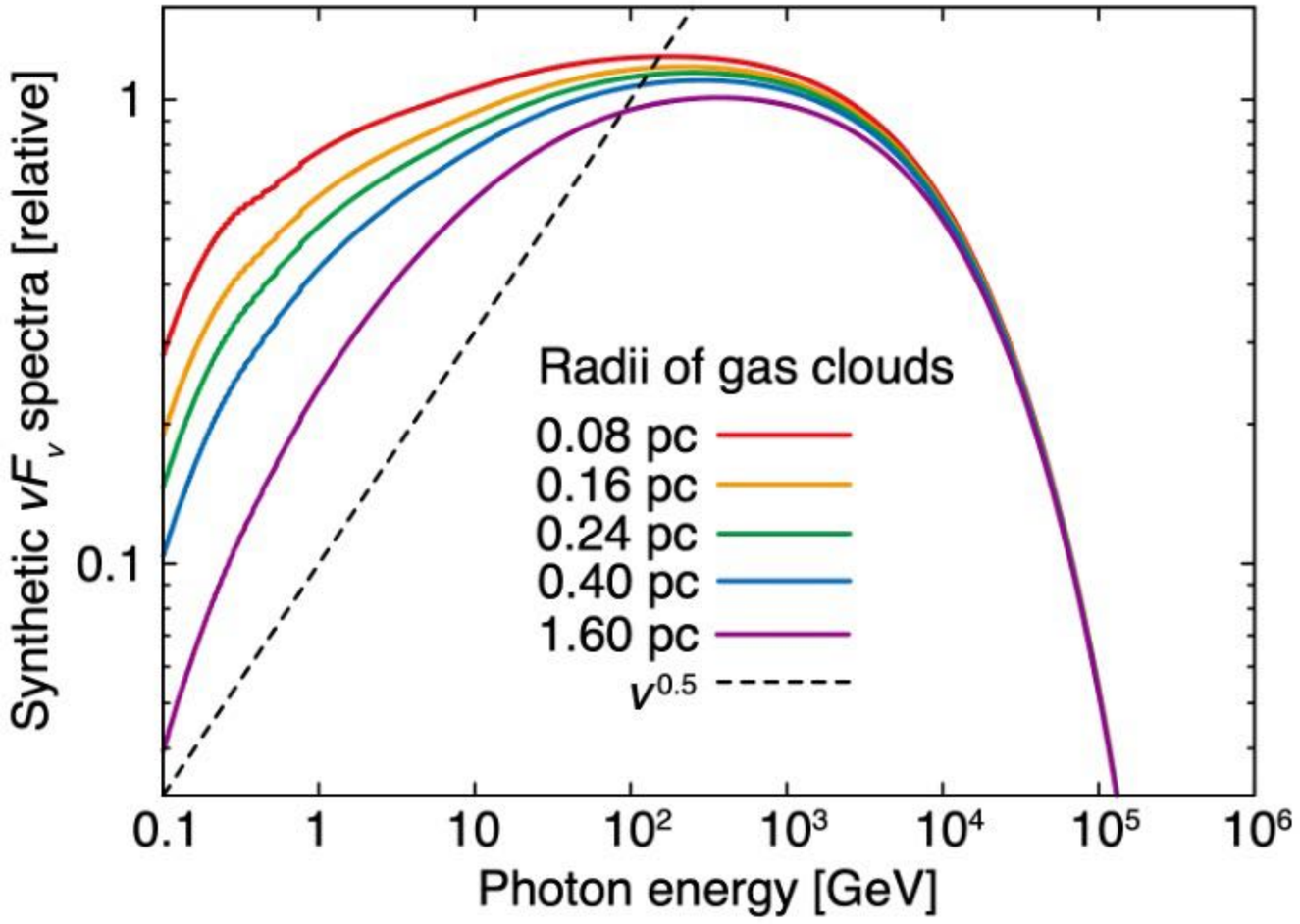

Flatter vF_v gamma-ray spectra will be expected toward the NW of RXJ1713

*Typical cloud radii are ~1–2 pc (Moriguchi+05)
e.g., CO cloud "peak C" (~1.5 pc) shows density concentration without small-scall structure

*Typical radii of cloudlets in the RXJ1713 NW are ~0.03–0.05 pc (this study)

Further gamma-ray observations with high-spatial resolution and sensitivity will reveal the gamma-ray spectral modulation...!!

Sano et al. 2020c, ApJL, 904, L24

ASTE & ALMA CO observations of the Magellanic SNRs

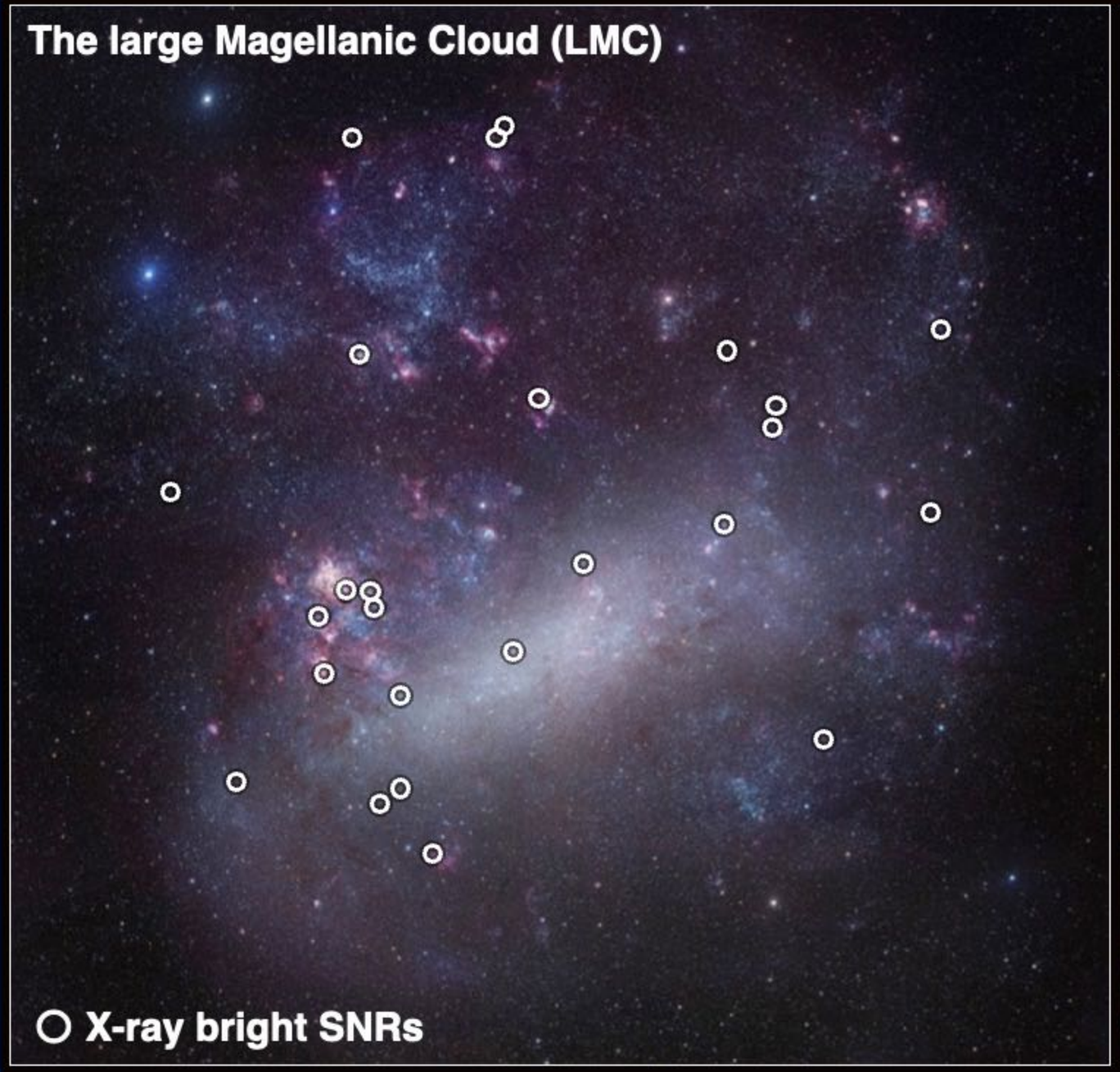

1. **Well-known distance**
   50 ± 1.3 kpc for the LMC (Pietrzyński et al. 2013)
   ~ 60 kpc for the SMC (Hilditch et al. 2005)

2. **Low ISM metallicity**
   ~0.3–0.5 $Z_\odot$ for the LMC (Westerlund 1997)
   ~0.05–0.2 $Z_\odot$ for the SMC, (Russell & Dopita 1992; Rolleston et al. 1999)

3. **Smaller contamination along the line of sight**

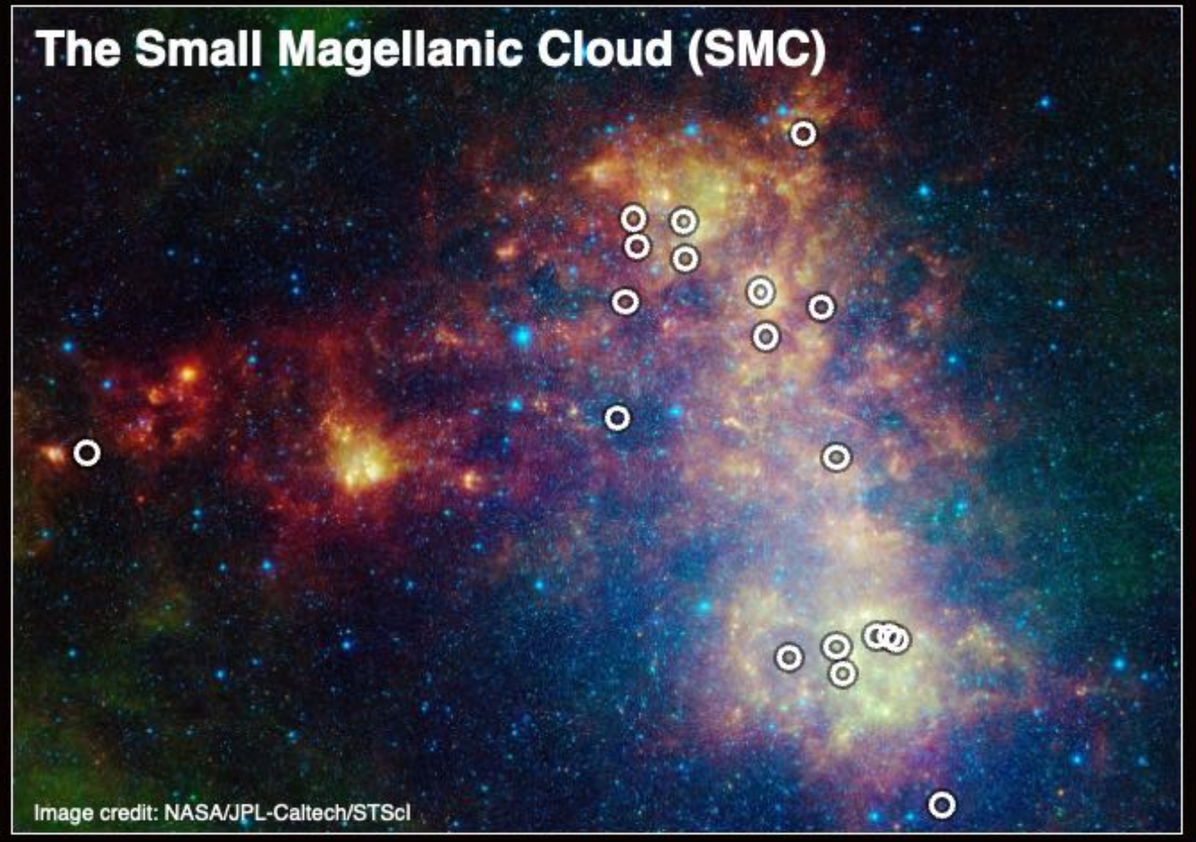

X-ray views of the Magellanic SNRs

Images: X-ray images obtained using Chandra or XMM-Newton

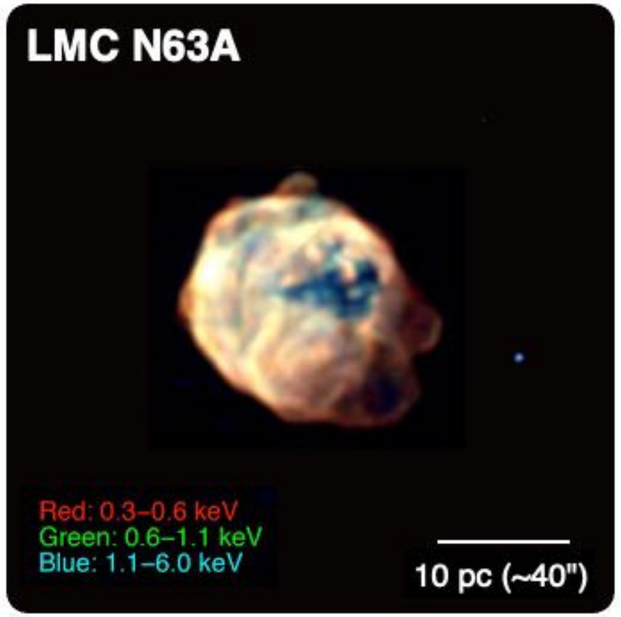

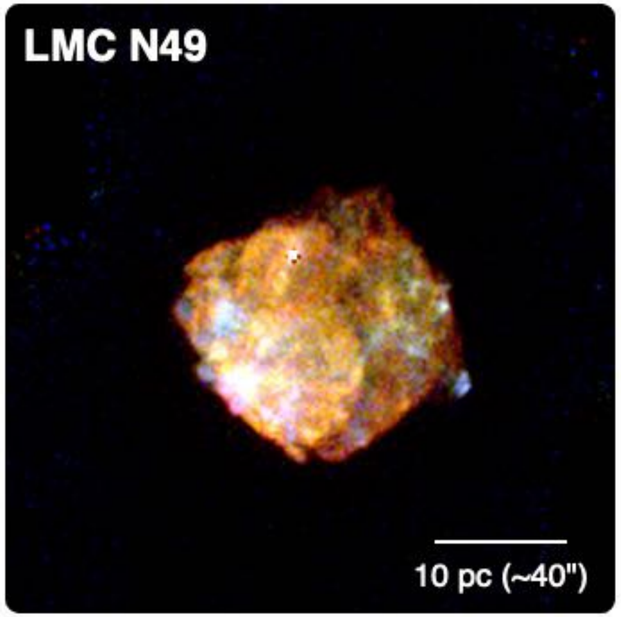

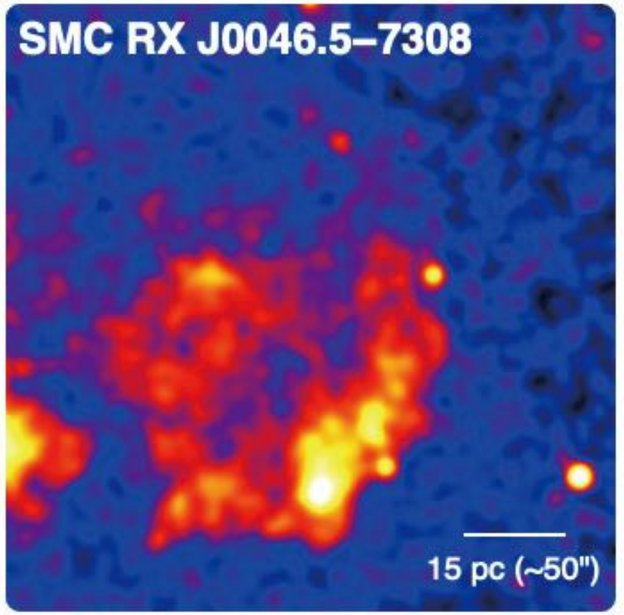

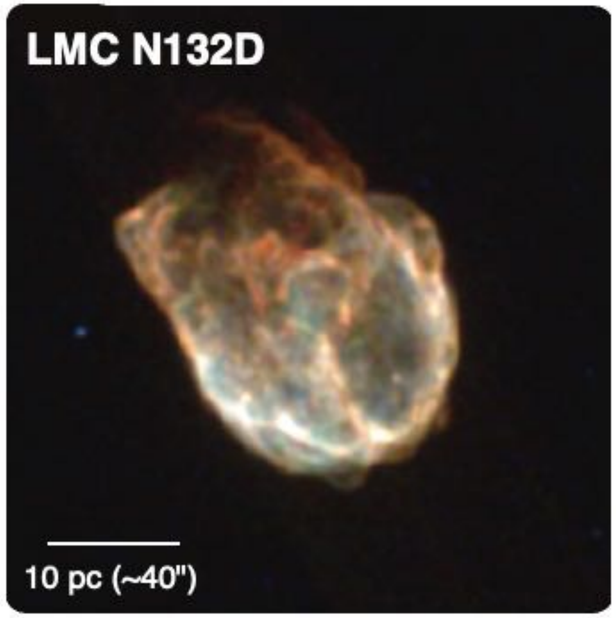

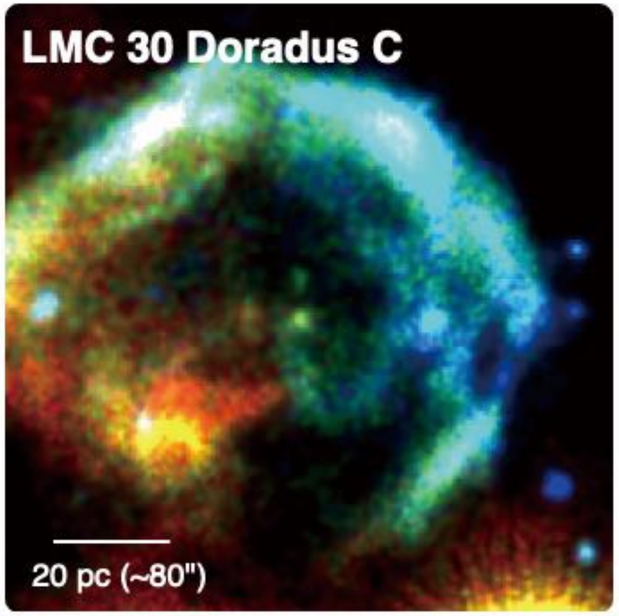

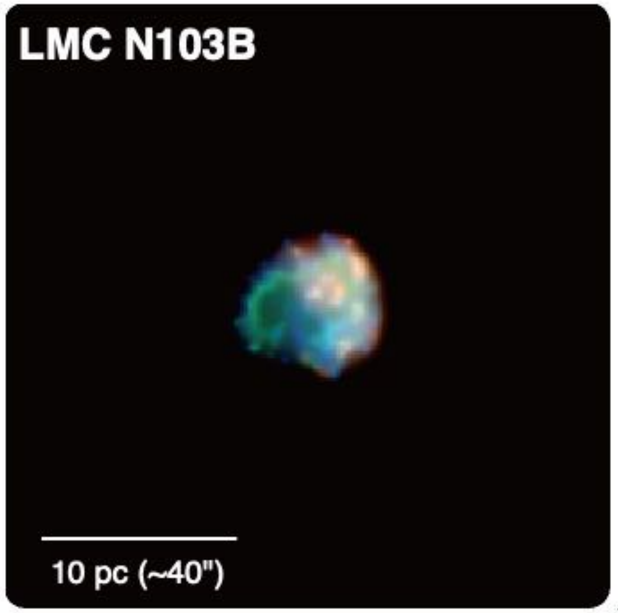

ASTE CO results toward the Magellanic SNRs

Image: ASTE ^{12}CO(J = 3–2)
Contours: *Chandra* X-rays

Sano et al. (2019a) ApJ, 873, 40

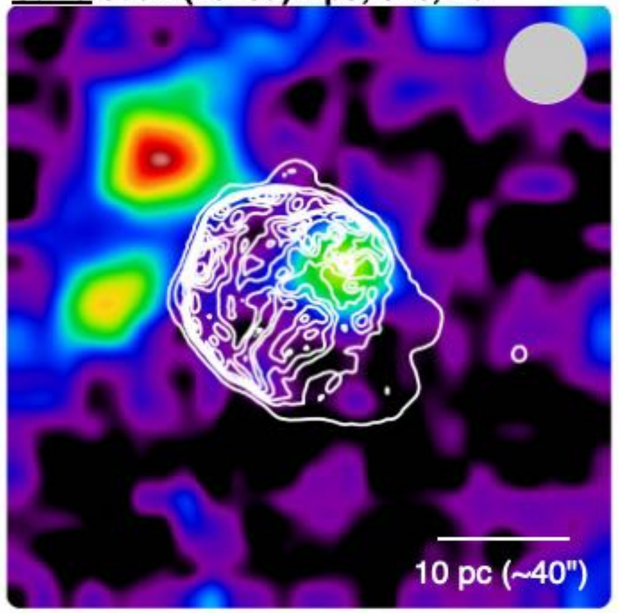

Yamane, Sano et al. (2018) ApJ, 864, 12

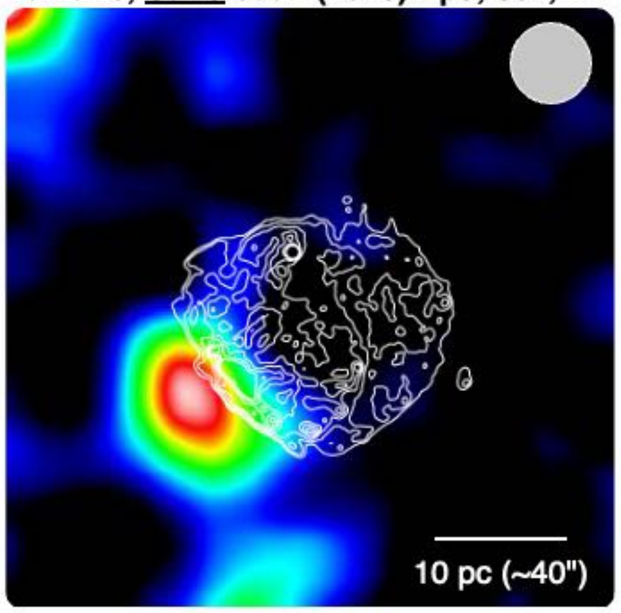

Sano et al. (2019b) ApJ, 881, 85

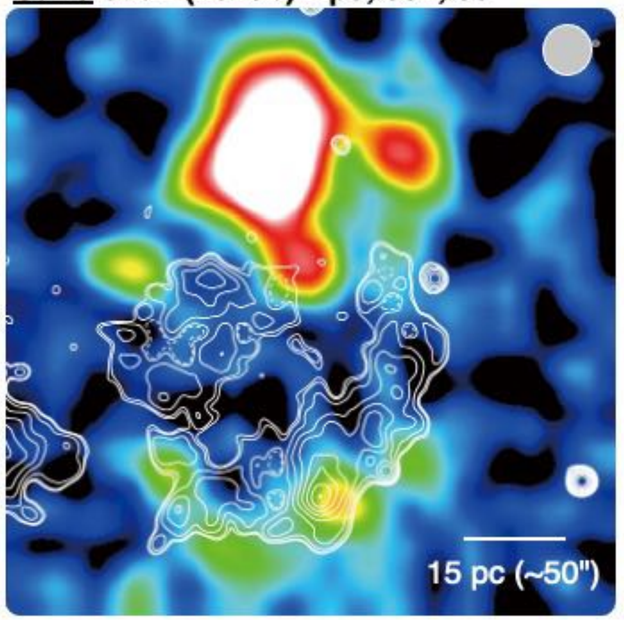

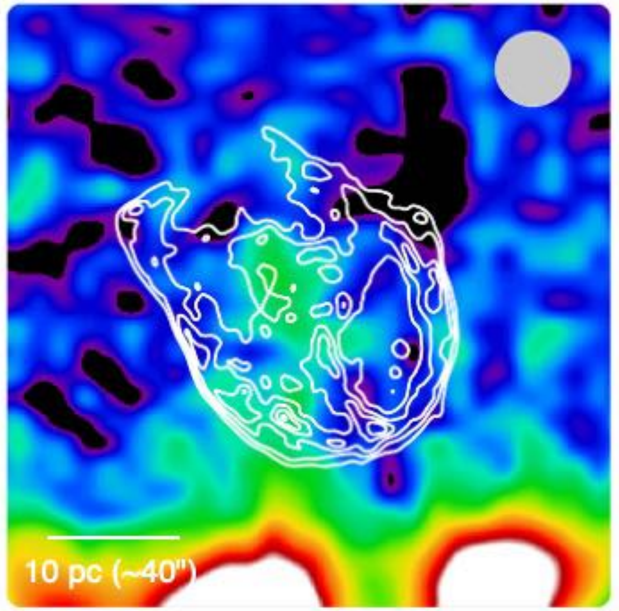

Sano et al. (2020) ApJ, 902, 53

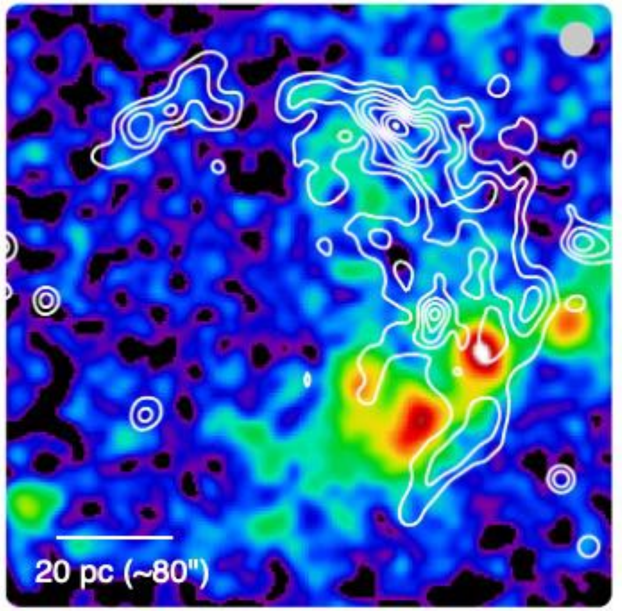

Yamane, Sano et al. (2021) ApJ, 916, 36

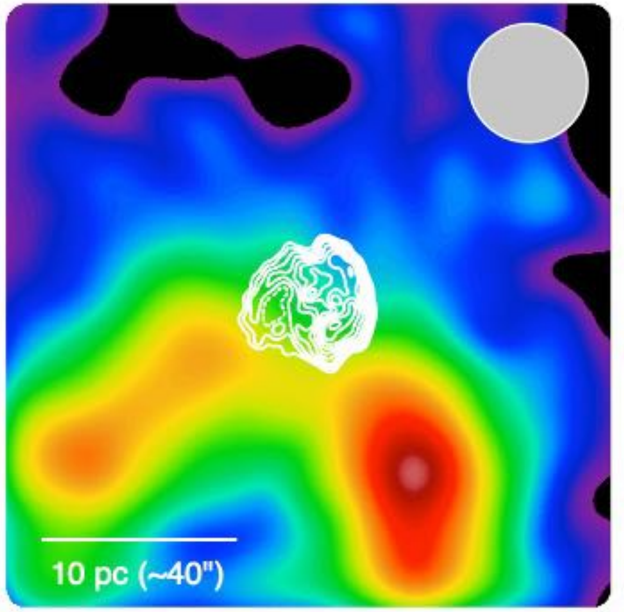

Sano et al. (2018) ApJ, 867, 7

ALMA CO results toward the Magellanic SNRs

Sano et al. (2019a) ApJ, 873, 40

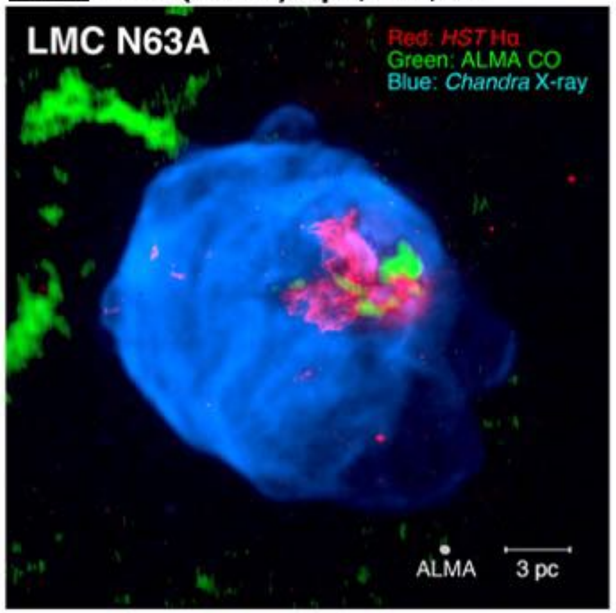

Yamane, Sano et al. (2018) ApJ, 864, 12

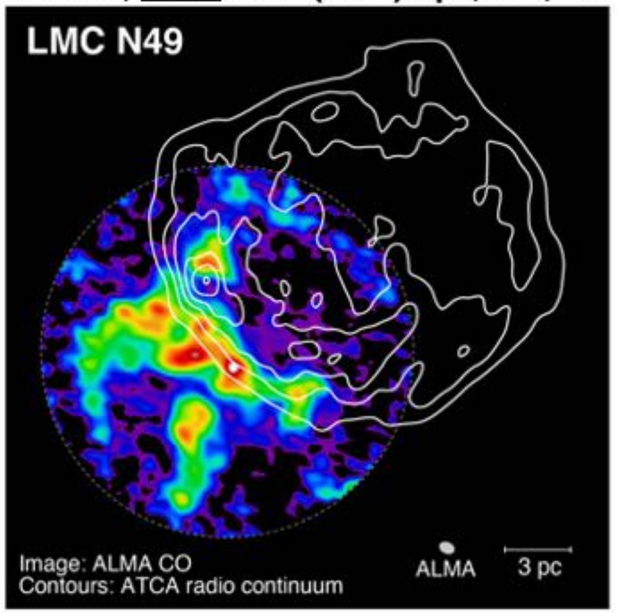

From archival data using ACA Band 6

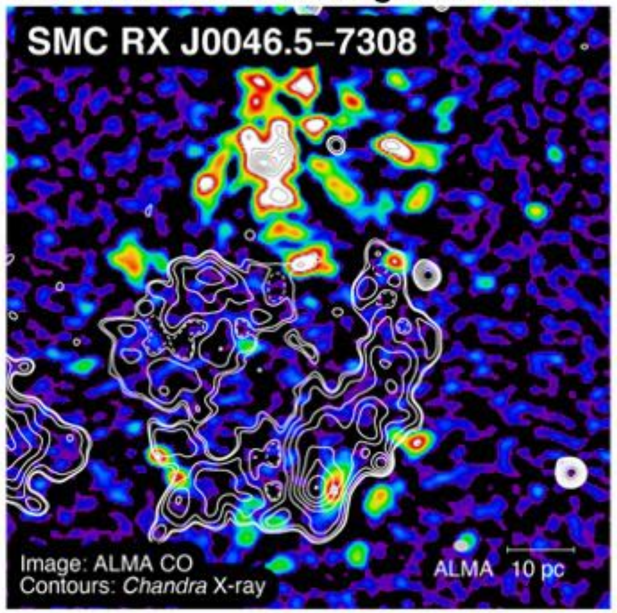

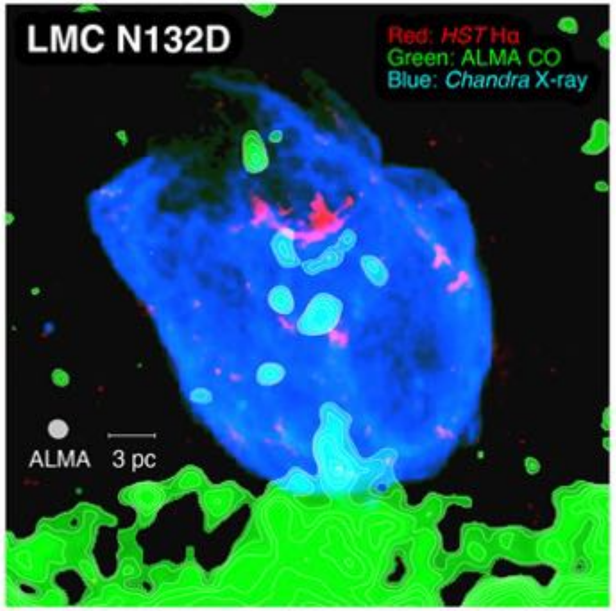

Sano et al. (2020) ApJ, 902, 53

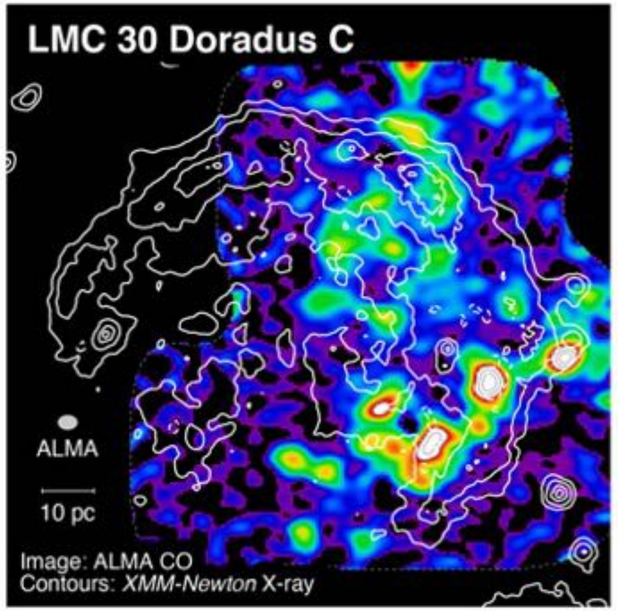

Yamane, Sano et al. (2021) ApJ, 916, 36

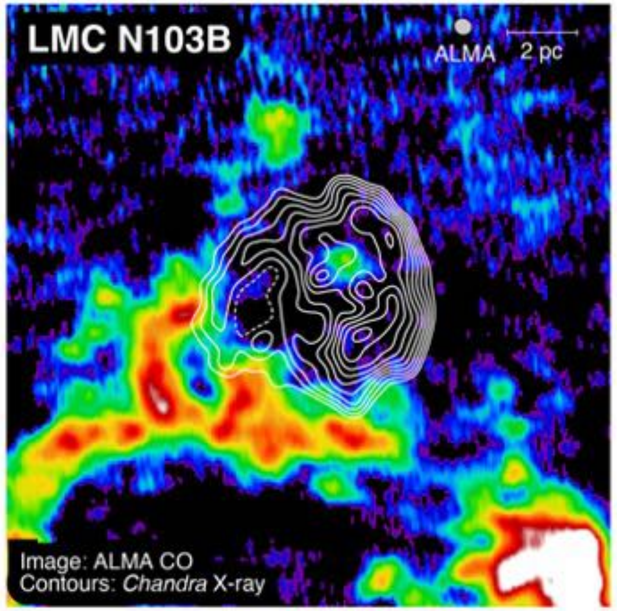

Sano et al. (2018) ApJ, 867, 7

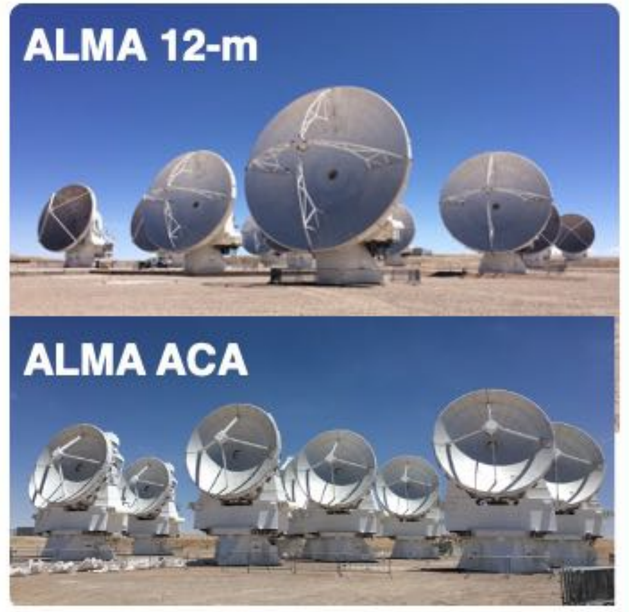

CO J = 3–2/1–0 ratio confirms physical association of clouds

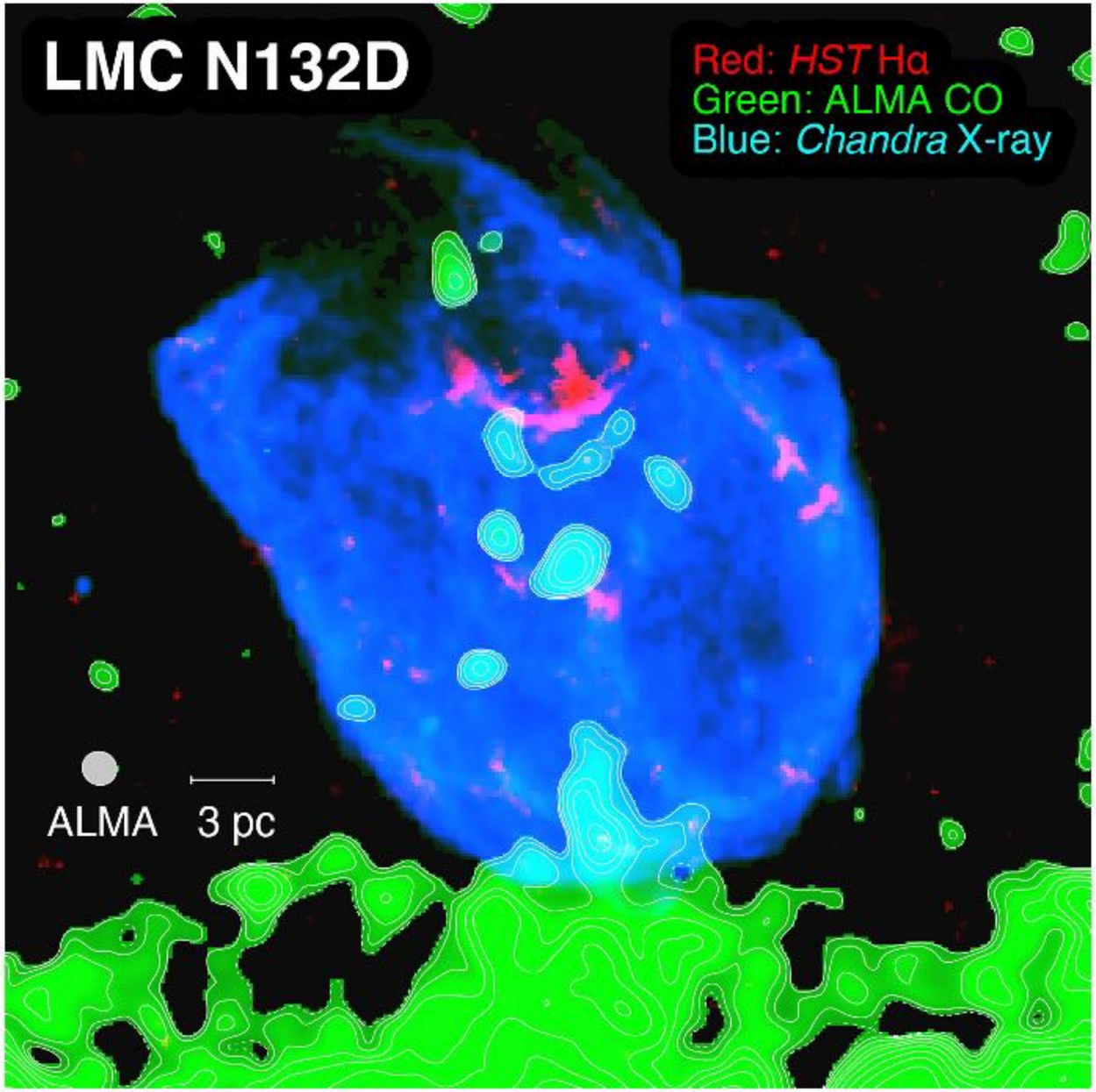

Sano et al. (2020) ApJ, 902, 53

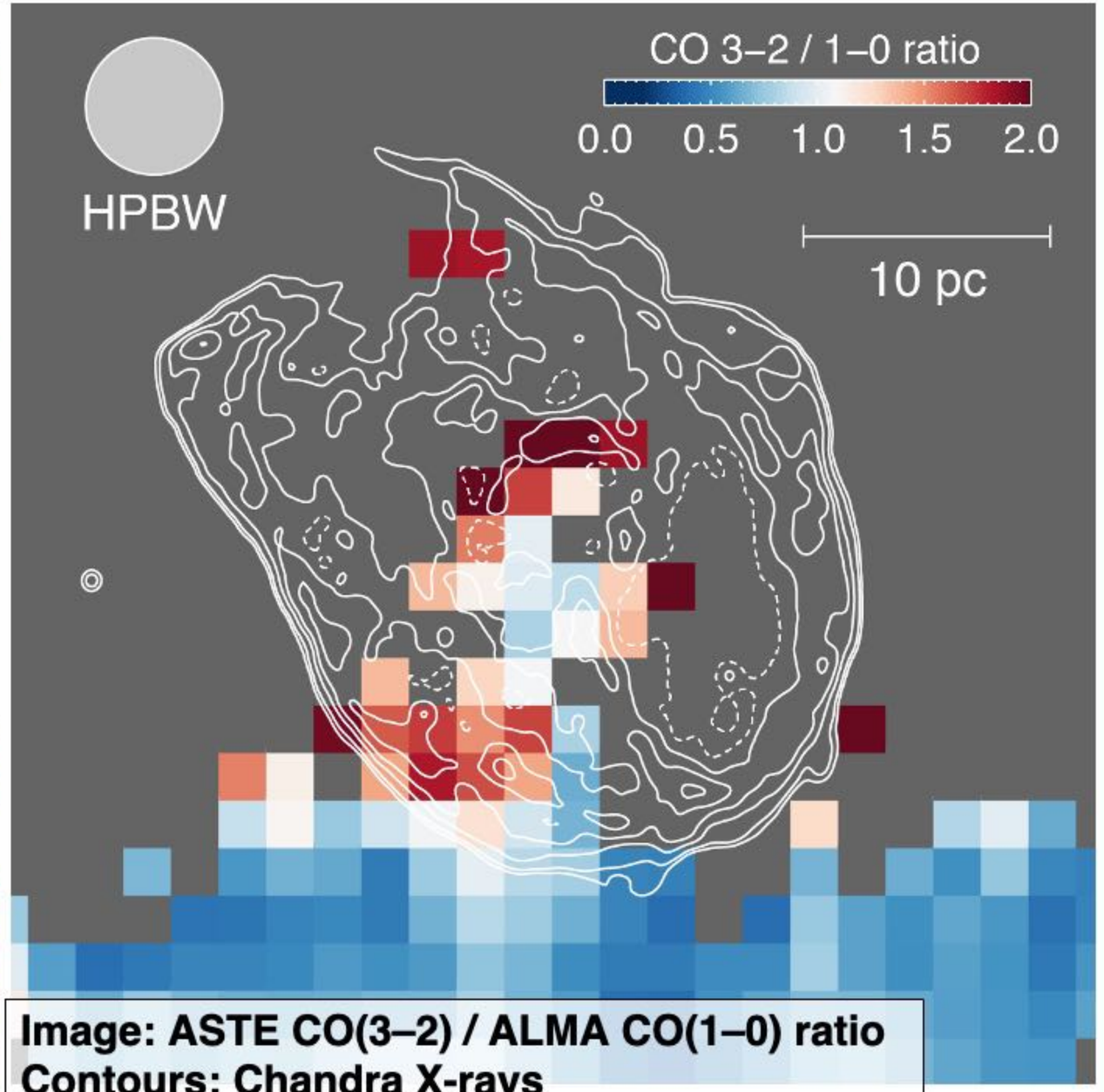

Image: ASTE CO(3–2) / ALMA CO(1–0) ratio
Contours: Chandra X-rays

X-ray spectroscopy toward the shocked cloud & intercloud region

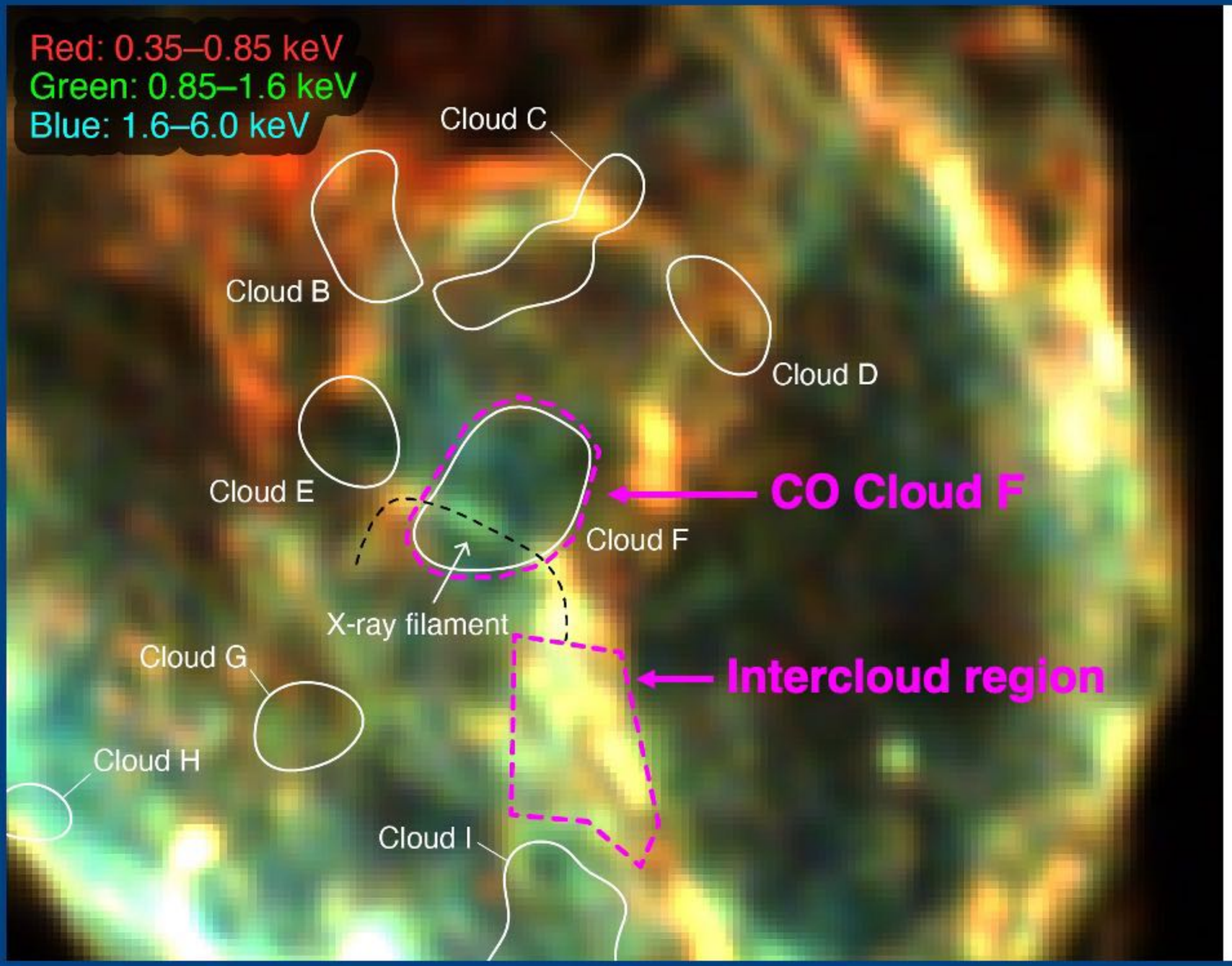

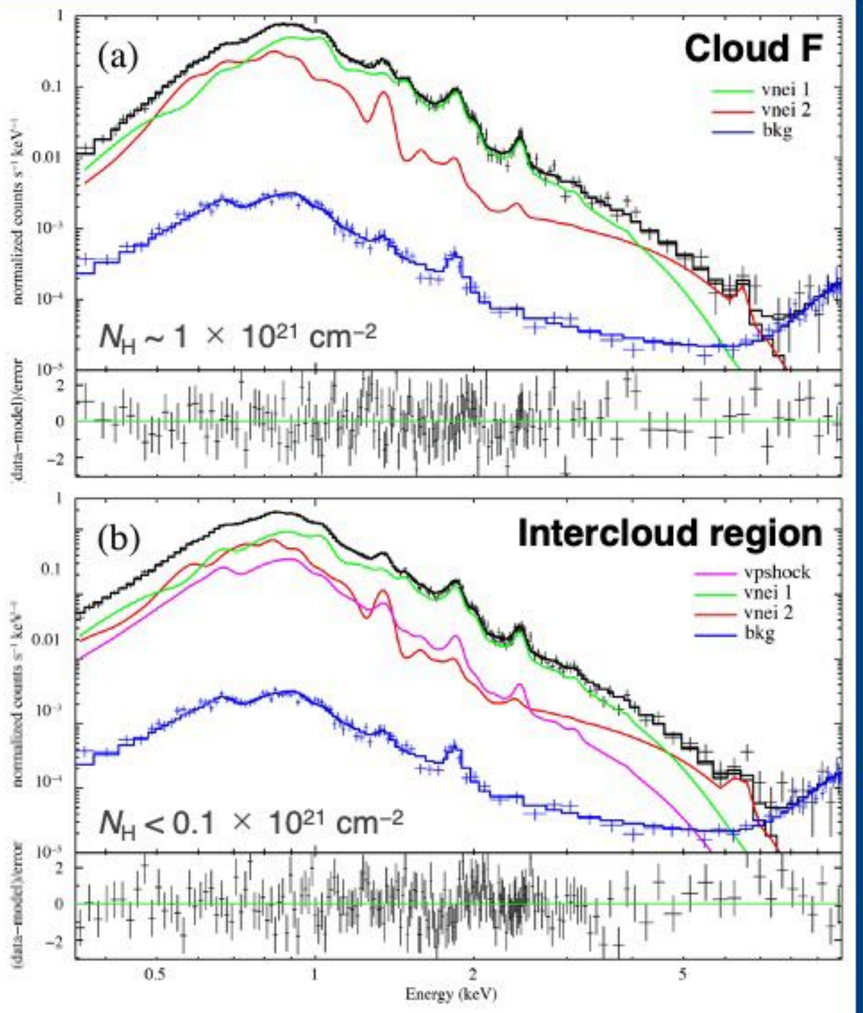

- Cloud F: CIE + NEI
- Intercloud: CIE + NEI + vpshock

Forward shock has been terminated in Cloud F
→ The ISM based X-ray spectroscopy is needed

[Japanese KAKENHI grant has been accepted (PI: Sano)]
[Chandra Large proposal has been accepted, (PI: Plucinsky, Co-I: Sano)]

Hard X-ray enhancement caused by shock-cloud interactions

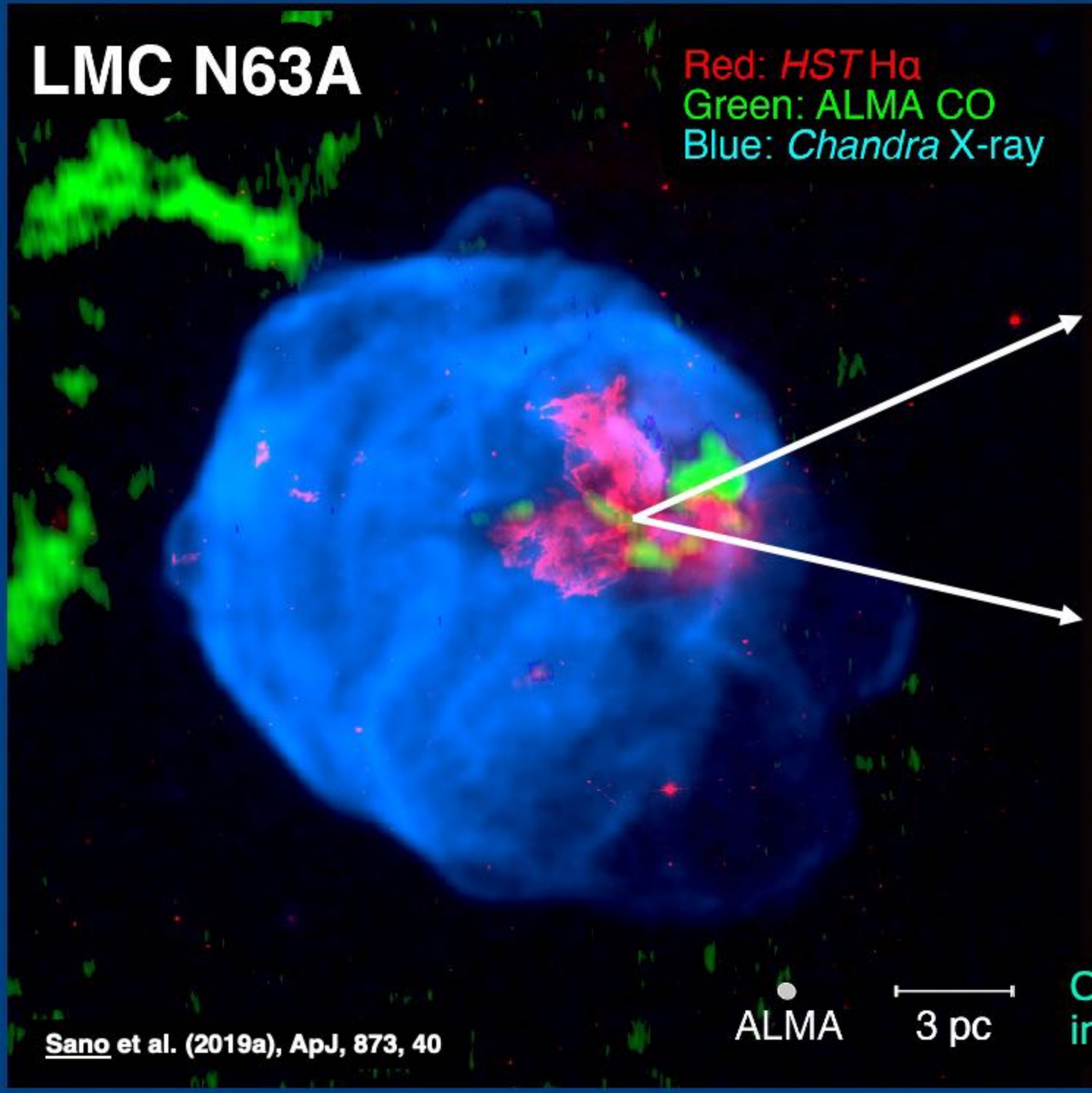

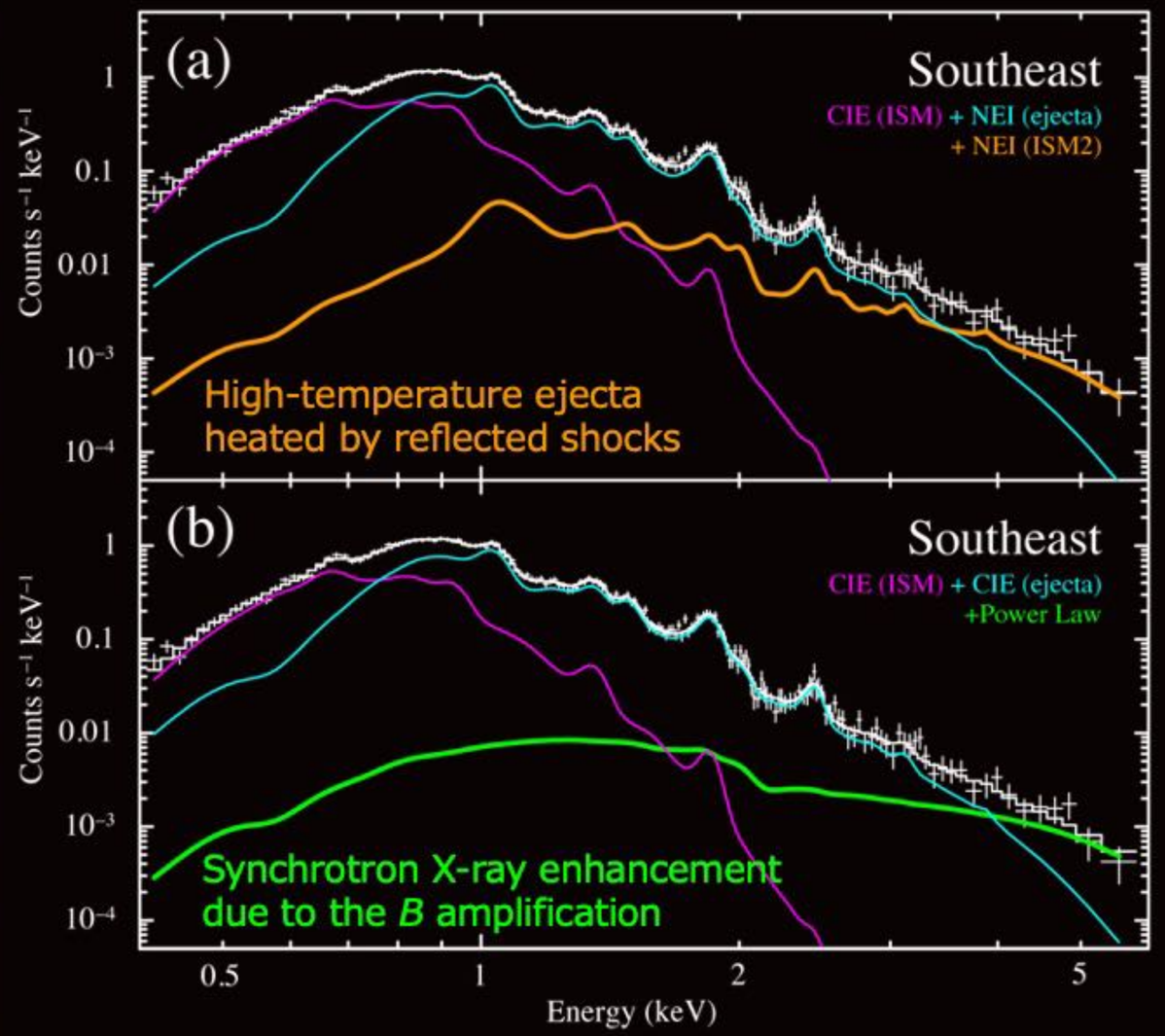

Sano et al. (2019a), ApJ, 873, 40

Combined analysis of Chandra & ALMA provides a new insight in understanding the X-ray spectra...!!

① Pursuit of the origin of Galactic cosmic-rays + ALMA results

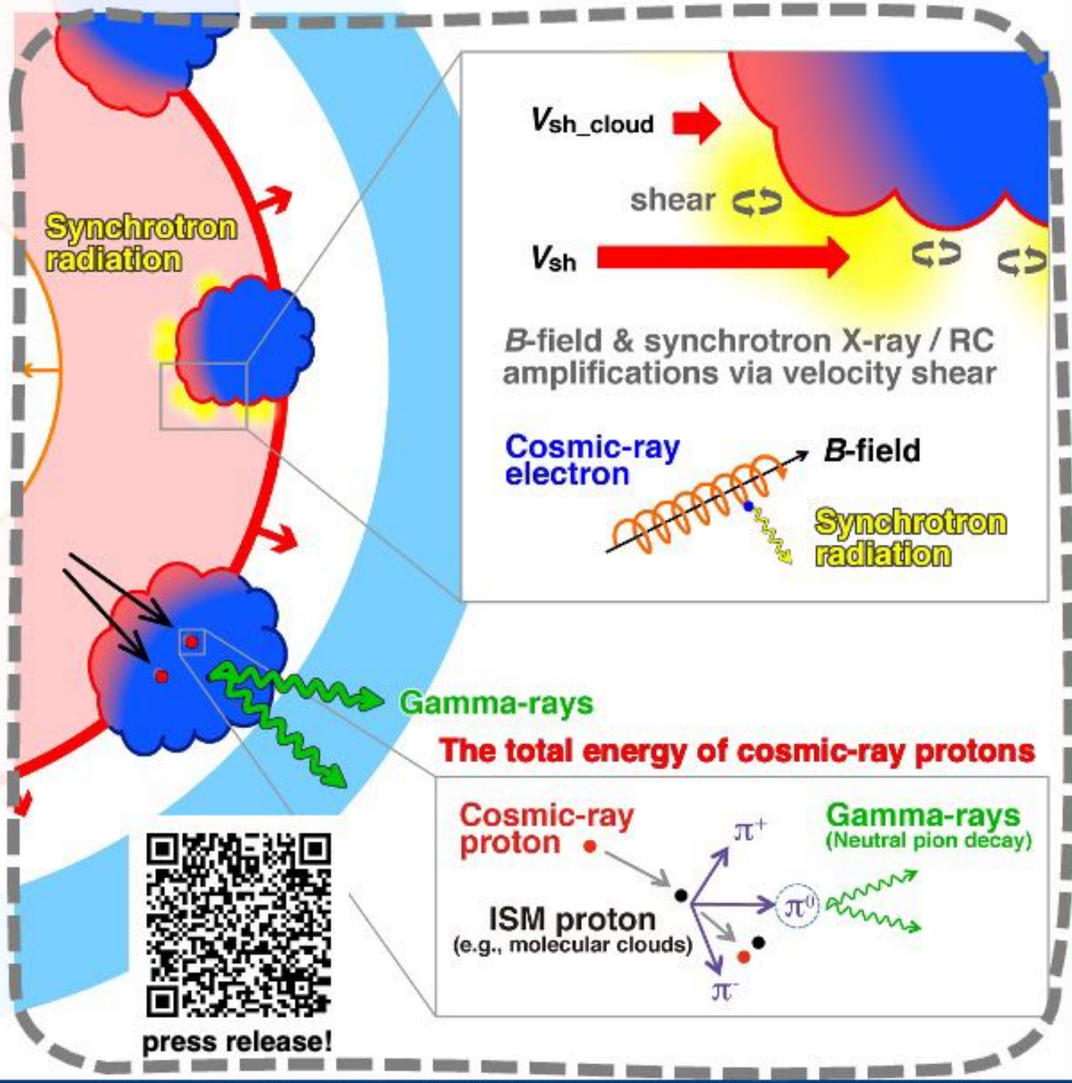

② The latest ALMA results of shocked filaments in SNRs

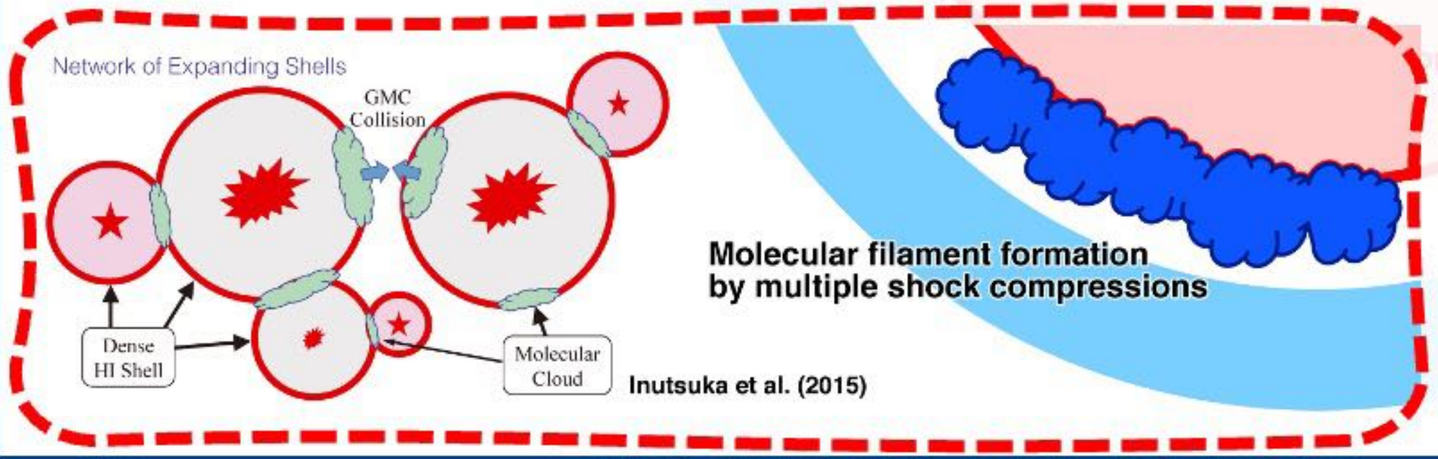

Filament paradigm for star formation

Herschel dust continuum

***Herschel* Gould Belt survey (André et al. 2010)**

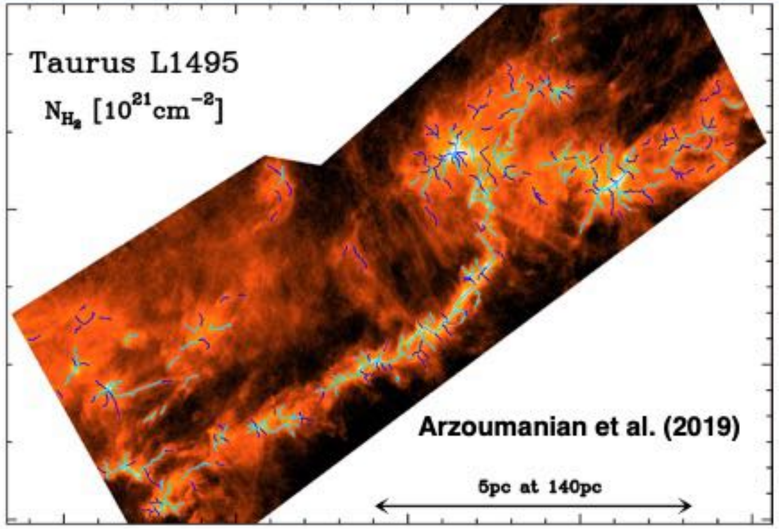

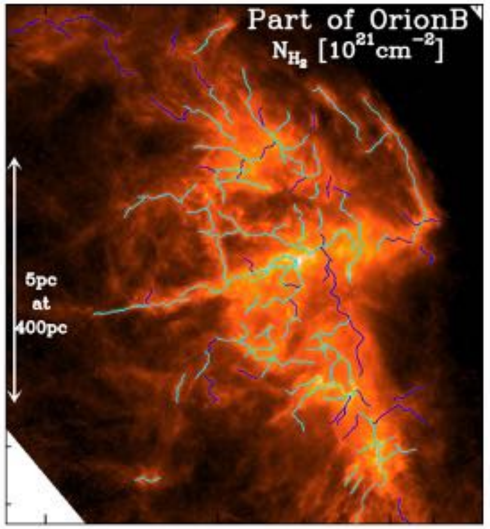

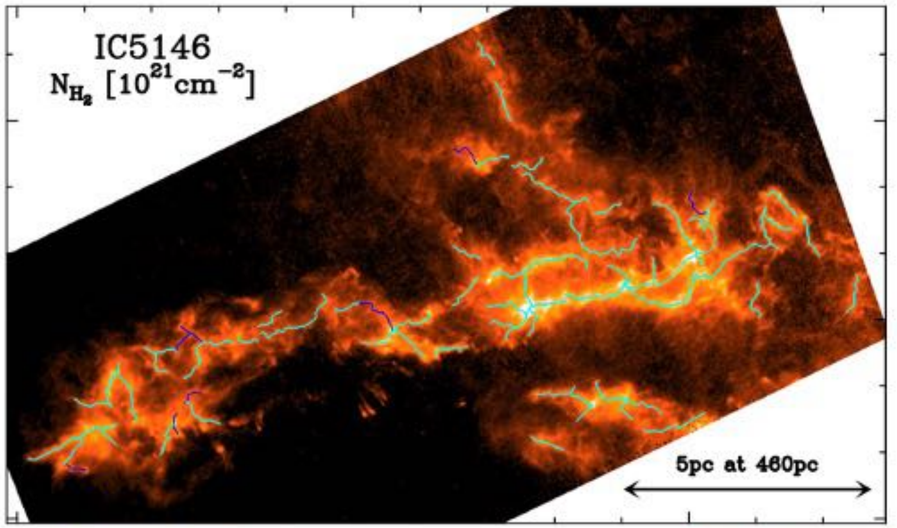

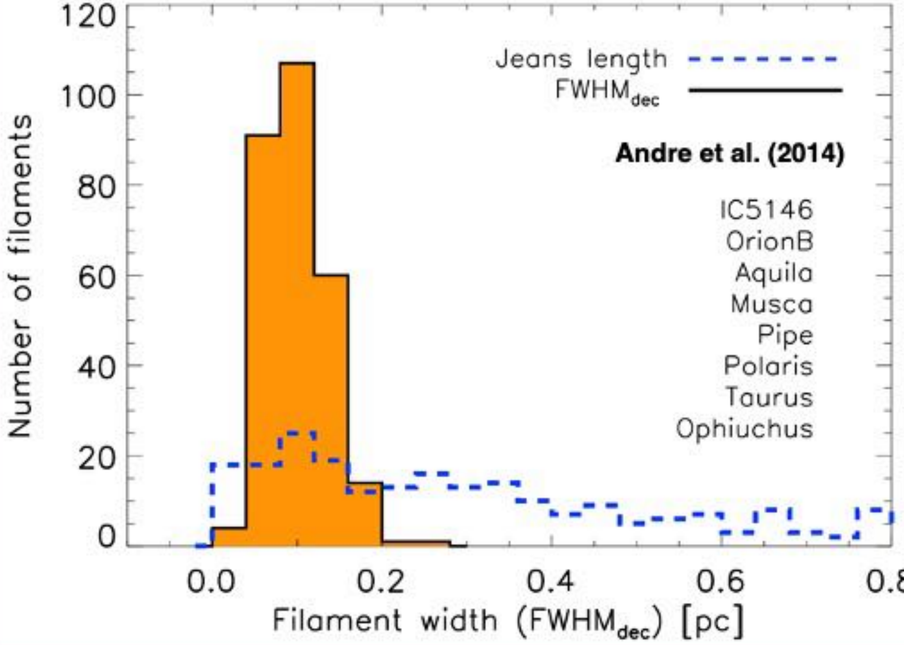

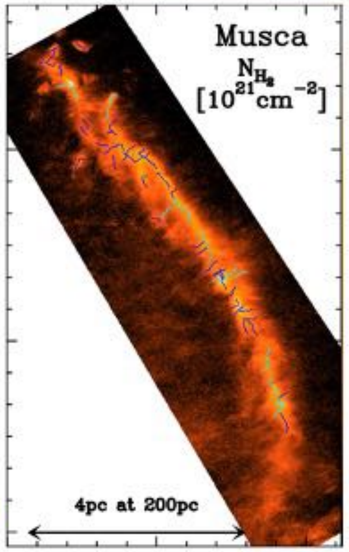

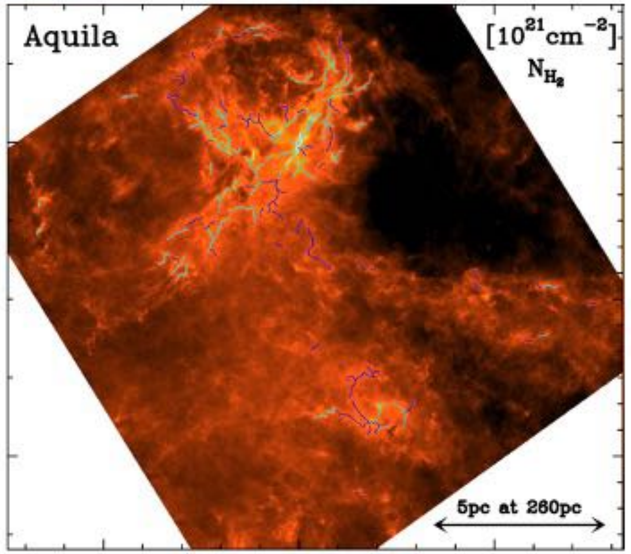

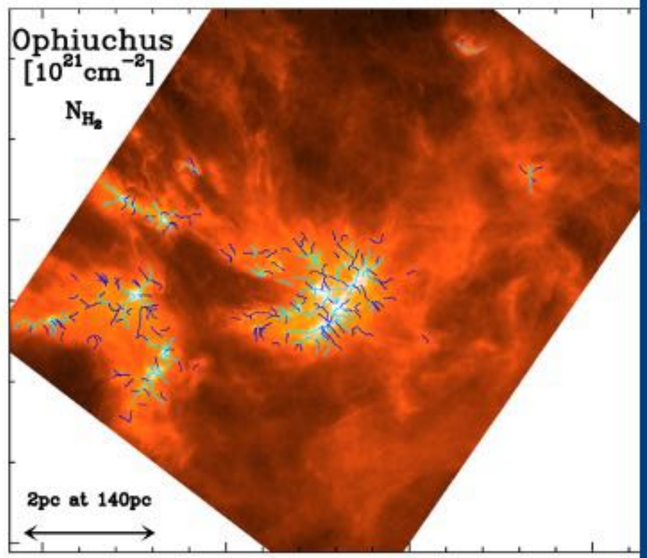

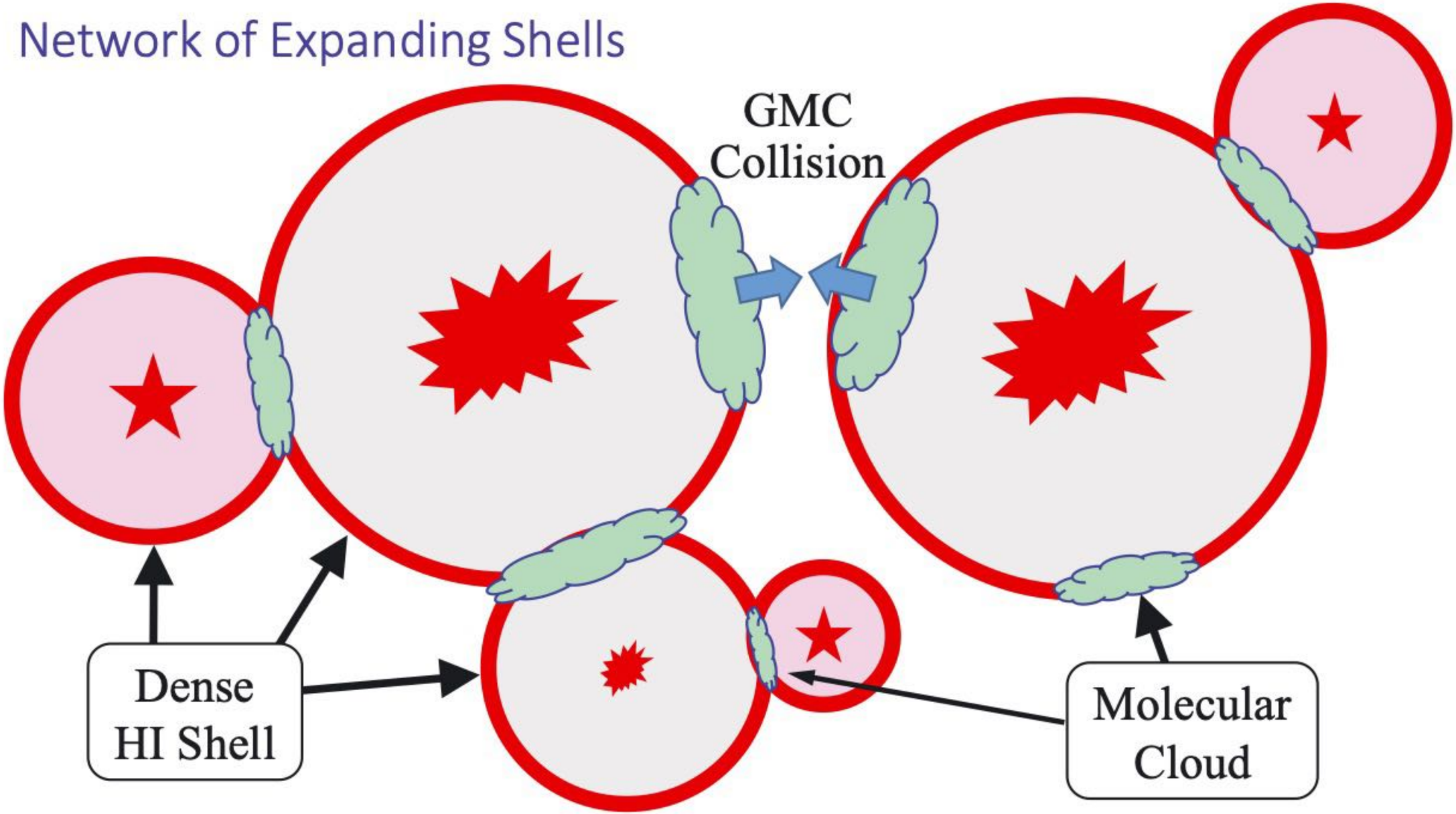

Inutsuka et al. (2015)

Filament paradigm for star formation: Multiple-shell compression model

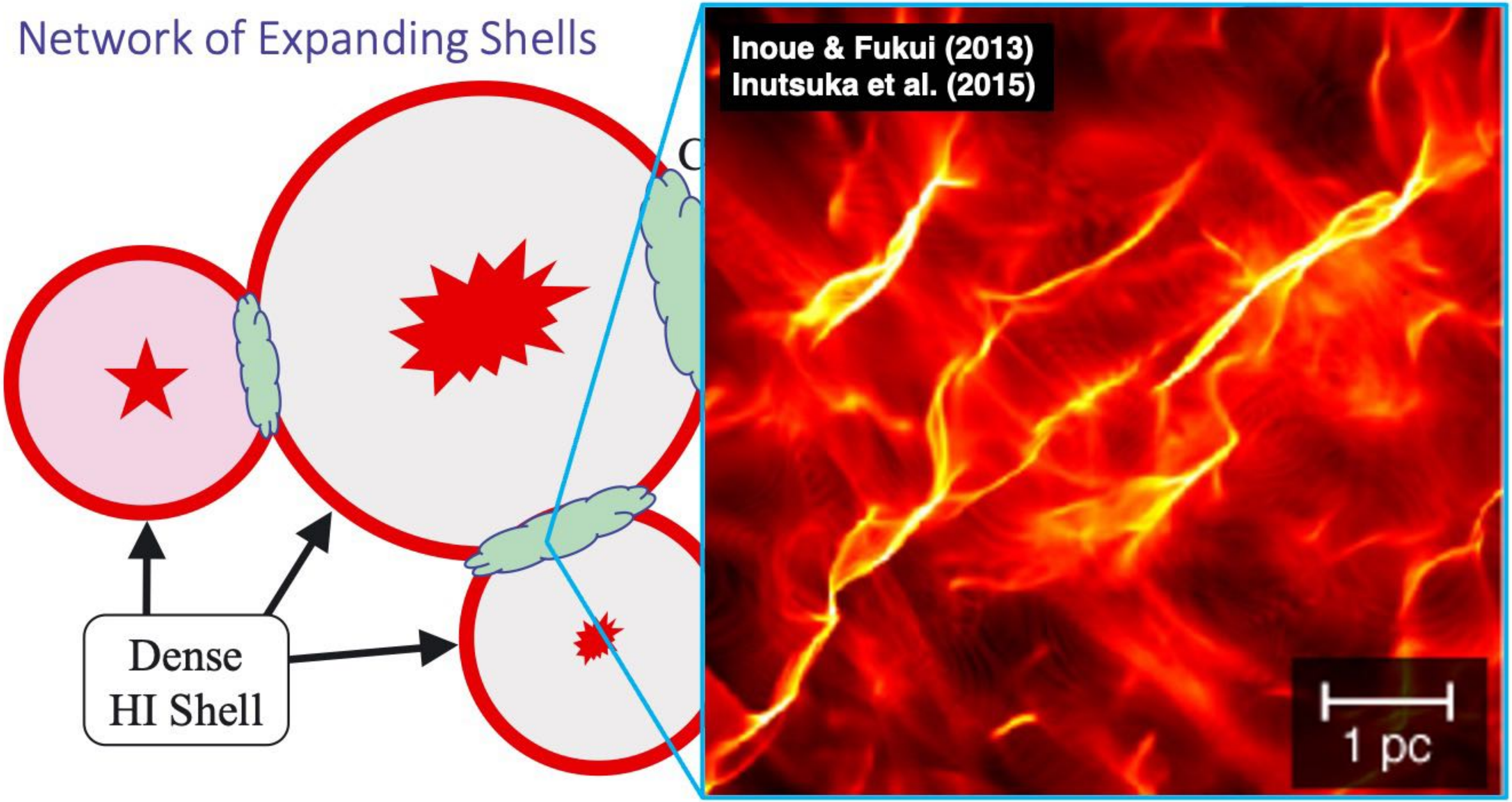

W28: An ideal site for testing the model

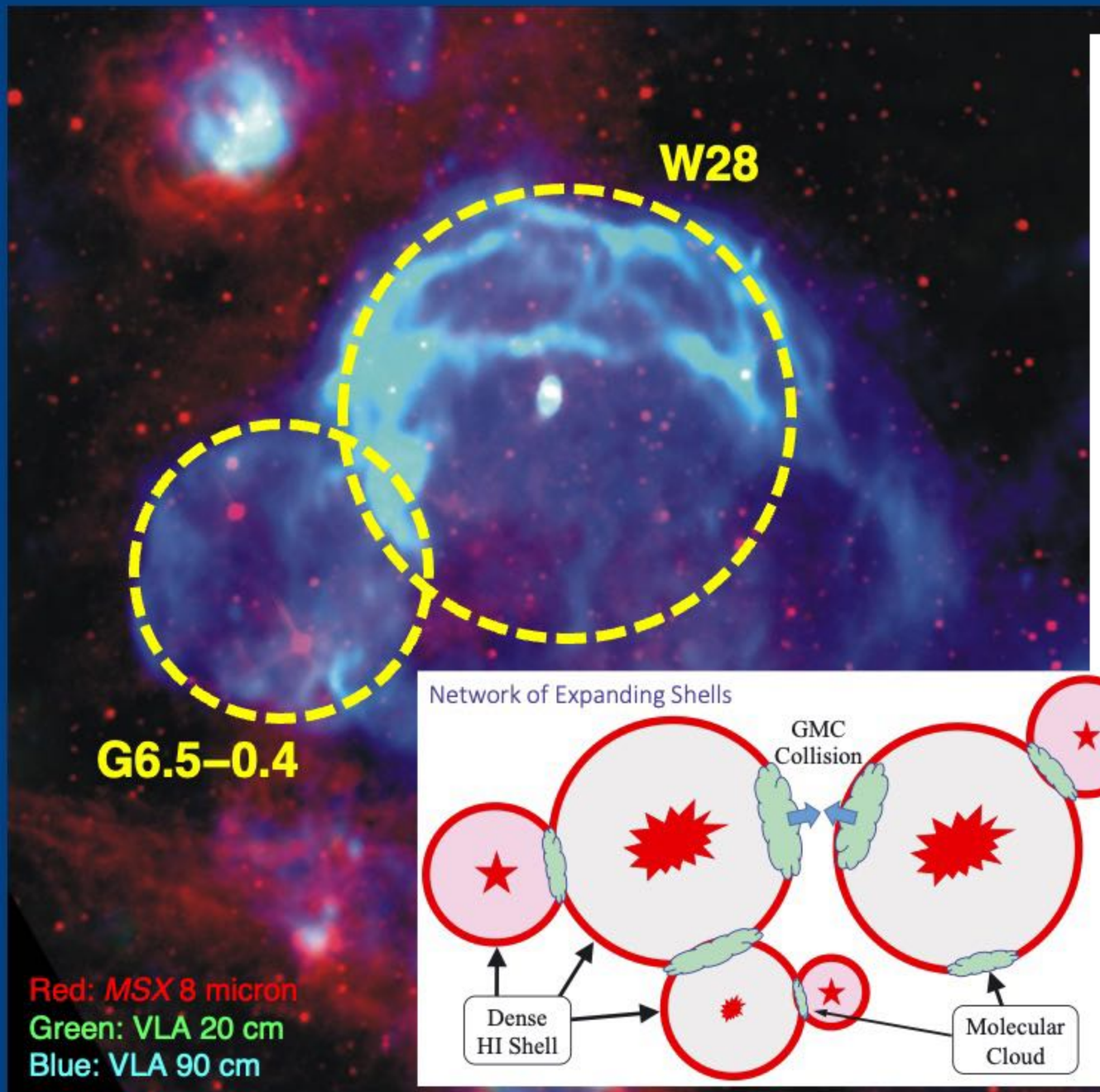

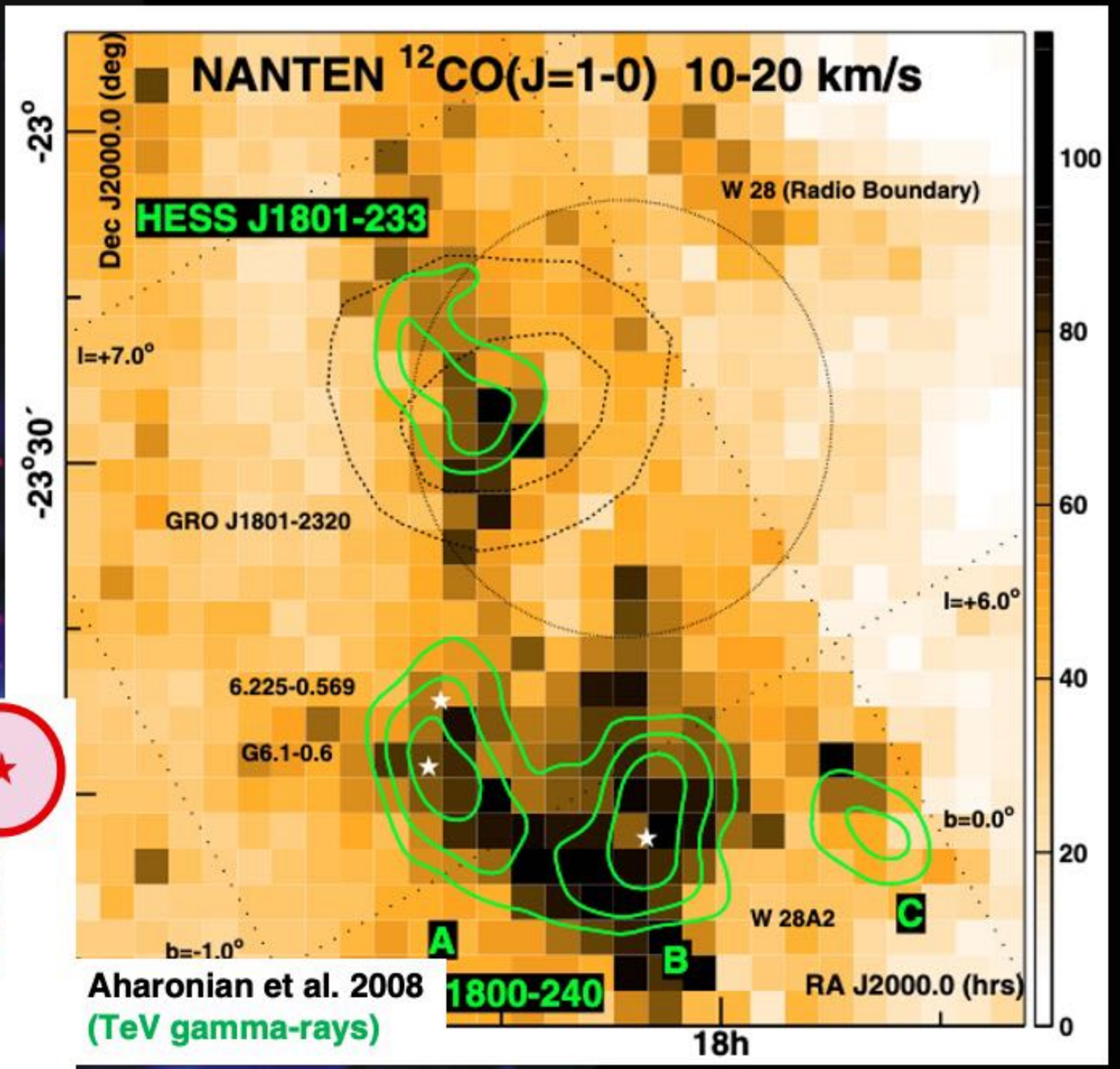

Aharonian et al. 2008
(TeV gamma-rays)

Molecular filaments revealed by JCMT

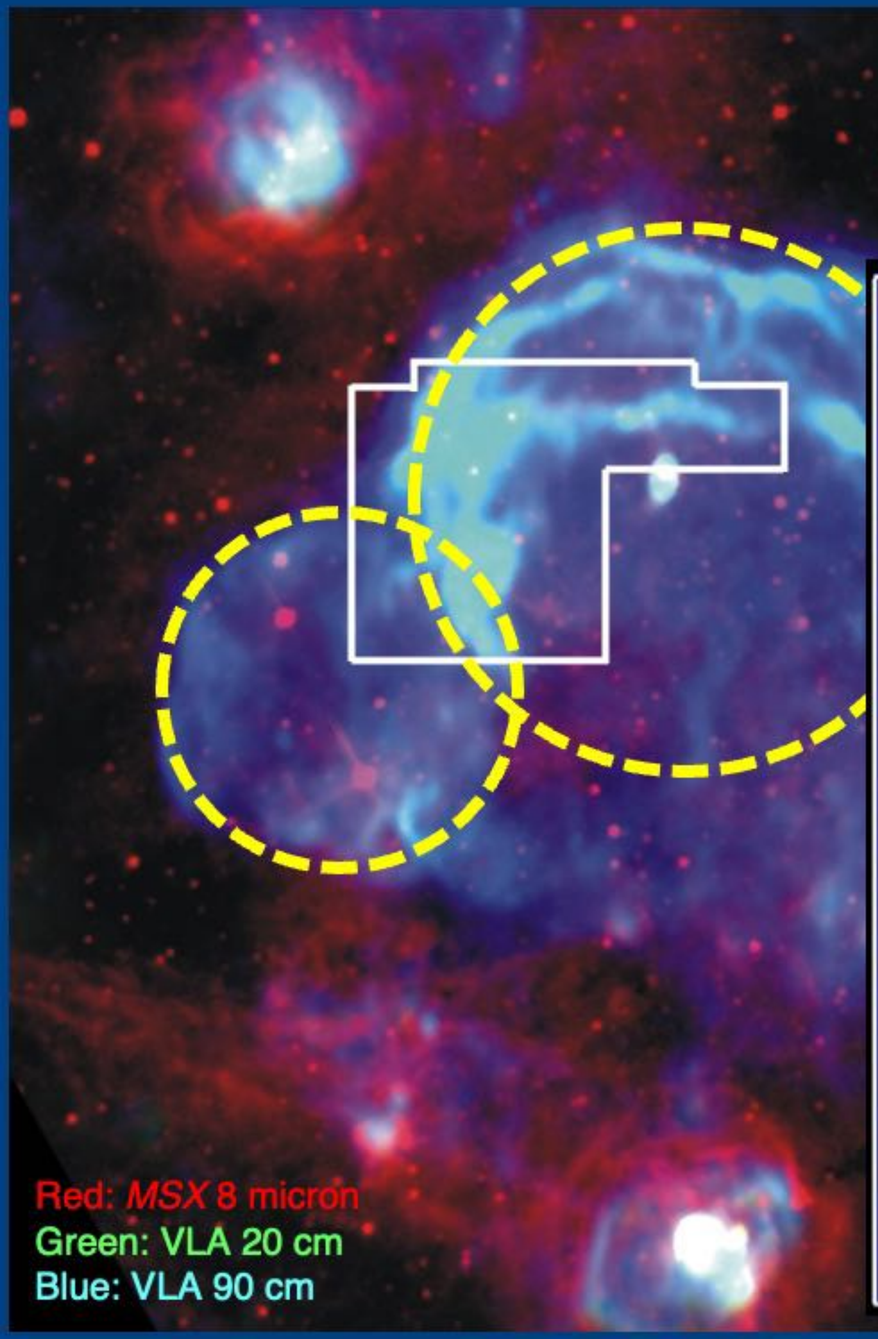

SNR W28

- Core-collapse / Mixed morphology
  (e.g., Manchester et al. 1985; Rho & Petre 1998)

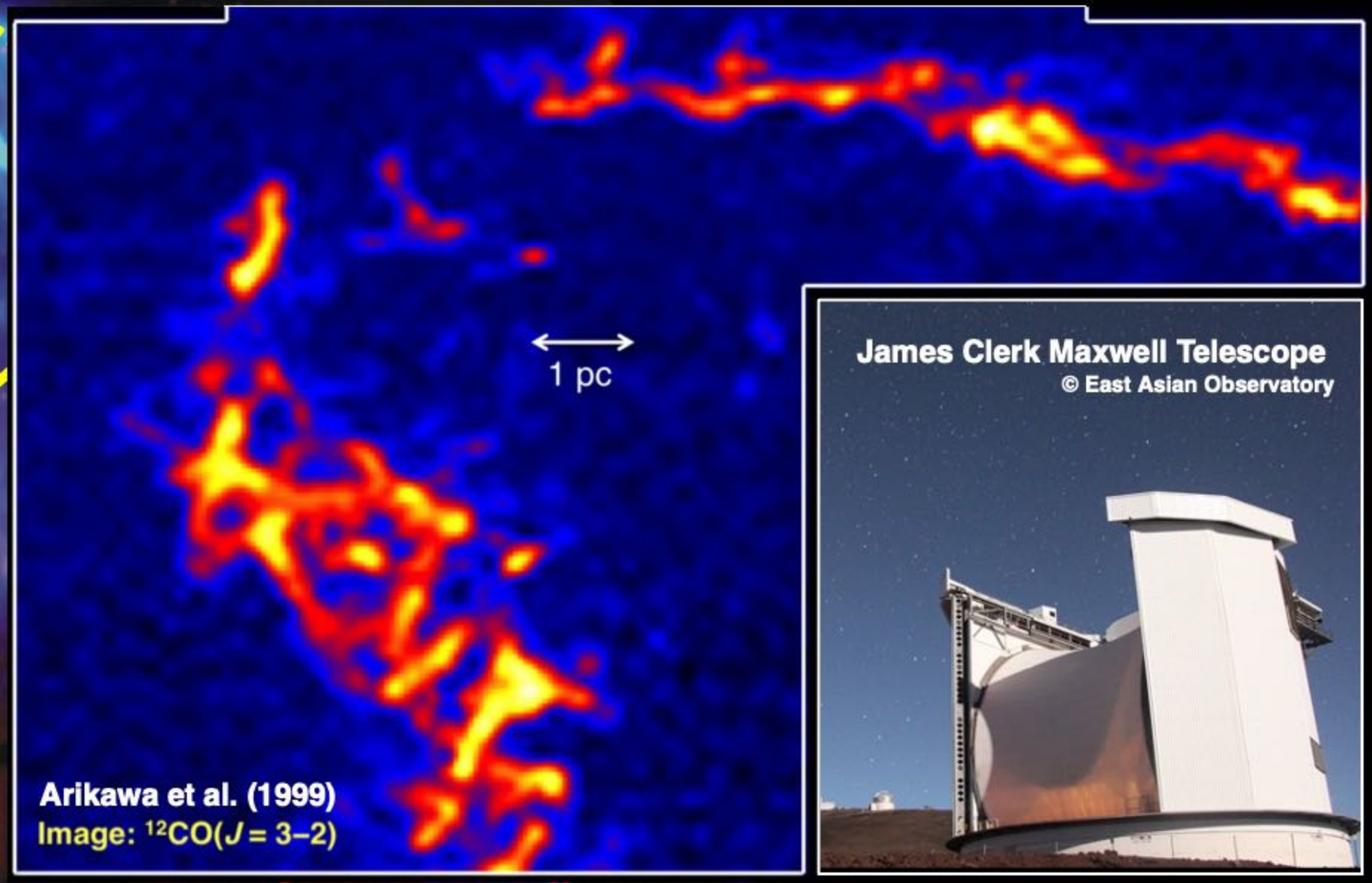

ALMA ACA observation (Cycle 7, Band 6, 1915 pointings, ~0.05 pc)

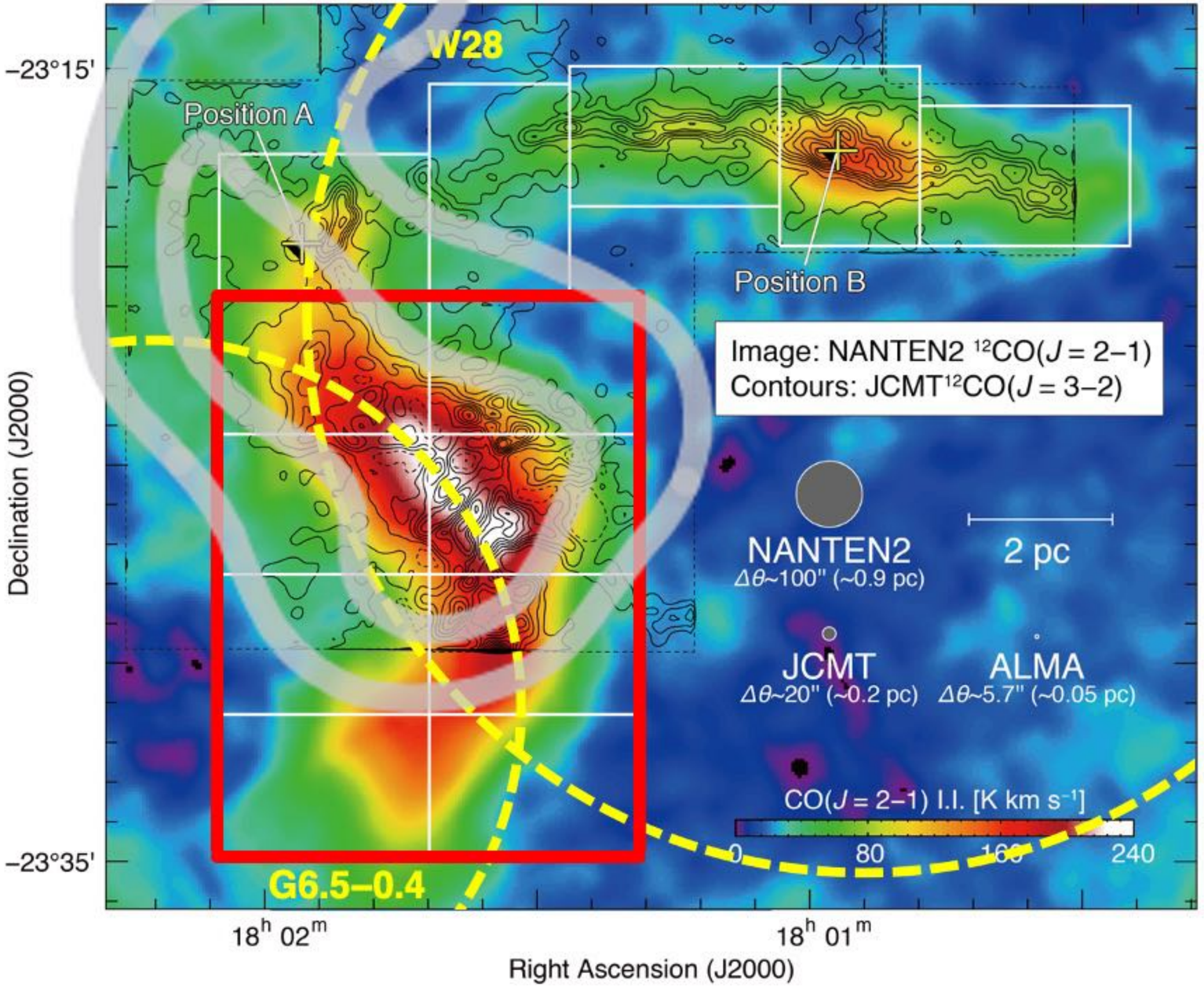

Project #	2019.1.01400.S (Cycle 7) 2021.2.00040.S (Cycle 8)
PI	Hidetoshi Sano
Band / line	Band 6 / CO (J = 2–1)
Observed area	5.3' × 3.5' (13 boxes)
Antennas	7 m + TP (ACA stand alone)
Beam size	**~9.46" × 4.51" (~0.06 pc)**
RMS noise	~ 0.11 K @ 0.3 km s^{-1}

Summary

1. **Interstellar gas associated with supernova remnants (SNRs)**

   Shock interaction with inhomogeneous and clumpy clouds is important in understanding the physical & chemical processes in interstellar space.

2. **Cosmic-ray acceleration in the SNR's shocks**

   Spatial comparison between the gamma-ray, ISM, and non-thermal X-rays provide an observational confirmation that supernova shocks can accelerate CR protons up to ~3 PeV (e.g., Fukui+12,17,21; Sano+19,21ab,22).

3. **Filament formation via multiple-shell compression**

   ALMA have spatially resolved filamentary molecular clouds associated with two SNRs as well as TeV/GeV gamma-rays (Sano et al. in prep.)

   ➡ Both the GeV and TeV CR protons can penetrate into the molecular filaments and producing hadronic gamma-rays..!